DOE/ET-53088-359 IFSR #359

New Developments in the Theory of Ion-Temperature-Gradient-Driven Turbulence in Tokamaks

NATHAN MATTOR

Institute for Fusion Studies
The University of Texas at Austin
Austin, Texas 78712

January 1989

NEW DEVELOPMENTS IN THE THEORY OF ION-TEMPERATURE-GRADIENT DRIVEN TURBULENCE IN TOKAMAKS

Publication No. _____

Nathan Mattor, Ph.D.

The University of Texas at Austin, 1989

Supervising Professor: Herbert L. Berk

This work considers three aspects of ion-temperature-gradient driven turbulence ("η_i-turbulence") in tokamaks, and the transport it causes.

Chapter I is a primer for those not familiar with the basics of this instability.

Chapter II presents a theory of weak η_i-turbulence near the threshold of instability. The model considers kinetic ions and adiabatic electrons in a sheared slab geometry. Linear theory shows that for $\eta_{th} < \eta_i \lesssim \eta_{th} + (1 + 1/\tau)L_n/L_s$ (where $\eta_{th} = 0.95$ is the instability threshold and $L_n/L_s \ll 1$) then $\gamma \ll \omega$ and a weak turbulence theory applies. The nonlinear wave kinetic equation indicates that ion Compton scattering is the dominant nonlinear saturation process. The wave kinetic equation is reduced to a differential equation for the spectrum, from which it is shown that the energy scatters to the linearly stable low k_y modes. The resulting spectrum of fluctuation levels (peaked about $k_\perp \rho_i \simeq 1$) is much

lower than that suggested by naïve extrapolation from the strong turbulence regime. The resulting ion thermal conductivity is also extremely low, so that strong ion heating can be expected to drive the ion temperature gradient to a level where this weakly turbulent threshold regime is surpassed.

Chapter III develops a theory of diffusive momentum transport driven by η_i-turbulence, in order to investigate the relation between momentum and thermal transport in neutral-beam-heated tokamaks with subsonic toroidal rotation velocity. The associated ion thermal diffusivity, χ_i, is identical to the kinematic ion shear viscosity:

$$\chi_\varphi = 1.3 \left[\frac{1+\eta_i}{\tau} + \left(\frac{L_n}{2c_s} \frac{dV_0}{dr} \right)^2 \right]^2 \frac{\rho_s^2 c_s}{L_s}.$$

In addition, the instability and level of η_i-turbulence is enhanced by radially sheared toroidal rotation. Thus, a scenario based on velocity shear enhanced η_i-turbulence is consistent with the experimentally observed relationship between thermal and momentum confinement.

Chapter IV is a study of η_i turbulence in the presence of flat density profiles, relevant to the high confinement discharges ("H-modes") on the D-III-D tokamak. Fluid theory predicts that as the density profile is flattened the ion thermal transport increases, reaching a plateau beyond the point $L_n > \sqrt{L_s L_T}$. From this, we conclude that straightforward application of the fluid theory is not suited to explain the observed improvement in energy confinement, and it may be necessary to invoke kinetic threshold effects as explored in Chapter II.

Chapter V is a summary of this work, and a list of suggestions for further investigation.

NEW DEVELOPMENTS IN THE THEORY OF ION-TEMPERATURE-GRADIENT DRIVEN TURBULENCE IN TOKAMAKS

by

NATHAN MATTOR, B.S.

DISSERTATION

Presented to the Faculty of the Graduate School of
The University of Texas at Austin
in Partial Fulfillment
of the Requirements
for the Degree of

DOCTOR OF PHILOSOPHY

THE UNIVERSITY OF TEXAS AT AUSTIN

May, 1989

To Rover

ACKNOWLEDGEMENTS

In addition to the fascination of Physics itself, one of the enjoyable things about this field is the remarkable people that one encounters. I am grateful to all those who have showed me the way over the years, and would like to thank the ones that come to mind.

I am extremely indebted to Professor Patrick H. Diamond, for starting me on some excellent problems, for showing me how to do research in Physics, and for deep insight and honest appraisal of my work and of others.

The influence of Professor Marshall N. Rosenbluth has been felt ever since his class convinced me to pursue theoretical Plasma Physics. The level of his research demonstrates to me that understanding the behaviour of plasmas is clearly on the forefront of modern Physics.

I am grateful to Dr. William L. Rowan, who got me off on the right foot in plasma physics, with a proper respect for the centrality of experiments.

I am honored that Professor H. L. Berk has kindly served as chairman for my thesis committee. I am also proud to have Professor D. E. Baldwin, Professor R. D. Hazeltine, Professor E. J. Powers, and Professor E. T. Vishniac offer the time to serve on my committee.

I am fortunate to have had some gifted teachers to bring Physics to life for me. Among these are Dr. William L. Allen, Professor R. Beringer, Professor R. Shankar, Professor M. E. Zeller, Professor A. Herzenburg, Dr. Steven Sanders, Professor W. L. Schieve, Professor W. Horsthemke, Professor J. A. Wheeler, Professor M. N. Rosenbluth, and Professor P. H. Diamond.

Encounters with Professor P. W. Terry, Professor E. T. Vishniac, Dr. T. S. Hahm, Dr. D. R. Thayer, Dr. B. D. Scott, Dr. H. Biglari, Professor T. M. O'Neil,

Dr. J. Malmberg, and Dr. A. J. Wootton have been illuminating.

I have learned as much from fellow students as I have from classes. Among those who stand out in my mind are F. L. Waelbroeck, X. Q. Xu, O. J. Kwon, F. Y. Gang, G. Craddock, G. S. Lee, T. Chieuh, M. A. Bryan, J. L. McDonald, M. J. Lebrun, S. Breed, N. Woodward, M. E. Glinsky, P. J. Hjorth, K. S. Fine, and T. Mitchell.

TABLE OF CONTENTS

CHAPTER I

INTRODUCTION

1.1 Overview

This thesis consists of three studies of ion temperature gradient driven turbulence ("η_i-turbulence" for short) in limits not considered previously. This work is part of a greater effort, ongoing since the early 1950's, to understand how plasmas transport across strong magnetic field lines as fast as they are observed to. The heat loss in fusion plasmas has generally been much faster than the traditional collisional (classical and neoclassical) theories predict, thus limiting the accessible temperature range to below that needed for energy breakeven. This is a major obstacle in the quest for economically feasible fusion energy.

Traditionally, attempts to explain anomalous thermal transport have focused on electron dynamics (with ion transport assumed neoclassical), owing in part to the fact that electron temperatures in a plasma are much more easily measured. However, beginning in the mid 1980's, direct measurement of *ion* temperatures has become possible (through active charge exchange spectroscopy), leading to the conclusion[1] (from measurements on D-III) that ion heat transport is often comparable to that from electrons, and a good deal larger than predicted by neaclassical models. The underlying mechanism of the anomalous transport was not well understood. At the same time, experiments on ALCATOR-C gave

the first indication that the η_i mode (which was developed theoretically in the 1960's) was linked to significant thermal transport in tokamaks.[2] This mode, described in further detail in Section 1.2, is basically a sound wave destabilized when the ion temperature gradient is steeper that the density gradient. Ion transport was suspected to underlie the degradation of energy confinement in ohmically heated plasmas at high densities, since in this regime the ohmically heated electrons transfer their energy to ions most rapidly. Following the suspicion that the anomalous ion channel was related to the η_i instability, hydrogen pellets were injected into the plasma, which tend to steepen the density gradient (which inhibits η_i transport). The experiment was a great success, with anomalous transport decreasing after the pellet injection, thus dramatically increasing the Lawson product $n\tau_E$ into the breakeven regime. This provided the first experimental evidence for the existence and importance of η_i modes.

More direct observation of η_i turbulence came on the TEXT experiment in 1986.[3] Laser scattering measurements indicated density fluctuations propagating in the direction of the *ion* diamagnetic drift (opposite to the more usually observed electron diamagnetic propagation), becoming large in the high density regime, just as predicted by the η_i theory. Furthermore, these fluctuations vanished after pellet injection, in accord with expectations based on experience from the ALCATOR-C experiments.

The above both concern ohmically heated plasmas. Evidence for the presence of η_i modes in beam heated tokamaks in low energy confinement ("L-

mode") regimes is given indirectly by the common observation that momentum and thermal confinement times tend to be the same, with similar scalings.[4,5] This suggests that a common mechanism underlies the transport of both, and a detailed analysis (which is the subject of Chapter III) shows that the η_i theory indeed predicts this result.

The above is rather compelling evidence for the presence of η_i modes in tokamaks. However, the existing theories are rather limited, neglecting a large number of effects which are potentially important in tokamak regimes. Thus, while the gross features of the theory have been more or less confirmed, more detailed issues remain to be addressed

1.2 Basic Description

Here, I outline the simplest possible scenario for transport from the η_i mode, from the local fluid instability to turbulent transport, with emphasis on the underlying physical picture.

In its most basic form, the η_i instability is a sound wave propagating parallel to the magnetic field, and destabilized by a radial ion temperature gradient. To demonstrate this, we consider an infinite, strongly magnetized plasma with magnetic field $\vec{B} = B_0\hat{z}$, and the density n_0 and ion temperature T_i varying in the x direction (representing the radial direction in a tokamak). We assume the usual scale separation in time and space dimensions, so that fluctuations may be described as evolving on a stationary background with constant gradi-

ents. Thus, the ion dynamics are described by the density, $n_i = n_0(x) + \tilde{n}_i(\vec{x})$, the parallel velocity, $v_\parallel = \tilde{v}_\parallel(\vec{x})$, and the pressure, $P_i = P_{0i}(x) + \tilde{p}_i(\vec{x})$. The perpendicular ion motion is given, to lowest order, by $\vec{v}_E \equiv \frac{c}{B}\hat{b} \times \nabla\tilde{\phi}$, where $\hat{b} = \vec{B}/B_0$ and $\tilde{\phi}$ is the electrostatic potential.

The ion dynamics can best be seen by retaining only a few terms in the linearized fluid equations. (These also emerge as the largest terms after a more careful ordering.[6]) Ion density evolves by parallel compression and perpendicular convection along the density gradient.

$$\frac{\partial\tilde{n}_i}{\partial t} + \frac{c}{B}(\hat{b} \times \nabla\tilde{\phi}) \cdot \nabla n_0 + n_0 \nabla_\parallel \tilde{v}_\parallel = 0. \tag{1.1}$$

The parallel ion motion is driven by pressure fluctuations:

$$\frac{\partial\tilde{v}_\parallel}{\partial t} = -\frac{\nabla_\parallel \tilde{p}_i}{\rho_0}. \tag{1.2}$$

Pressure fluctuations are caused by $\vec{E} \times \vec{B}$ convection along the equilibrium pressure gradient (where adiabatic corrections are negligible),

$$\frac{\partial\tilde{p}_i}{\partial t} + \frac{c}{B}(\hat{b} \times \nabla\tilde{\phi}) \cdot \nabla P_{0i} = 0. \tag{1.3}$$

Electron dynamics are relatively unimportant, and may be taken as adiabatic, along with the quasineutrality condition:

$$\tilde{n}_e = n_0 \frac{e\tilde{\phi}}{T_e} = \tilde{n}_i. \tag{1.4}$$

Taking the fluctuations to be of the form $\exp(i\vec{k}\cdot\vec{x} - i\omega t)$, then Eqs. (1.1)-(1.4) yield the following dispersion relation:

$$\omega^2 \left(1 - \frac{\omega}{\omega_{*e}}\right) = -k_\parallel^2 \frac{T_i}{m_i} \frac{n_0}{P_{0i}} \frac{dP_{0i}/dx}{dn_0/dx}, \tag{1.5}$$

where $\omega_{*e} = -\frac{k_y c T_e}{eBn_0}\frac{dn_0}{dx}$. When $|\omega| \ll |\omega_{*e}|$, this has the purely growing solution

$$\omega = ik_{\|}v_i(1+\eta_i)^{1/2}, \tag{1.6}$$

where $\eta_i \equiv d\ln T_i/d\ln n_0$, $p_i = n_i T_i$, and $v_i = T_i/m_i$. In this most basic form of the growth, it is evident that the η_i mode is a parallel sound wave (since $v_{\|}$ is driven by pressure fluctuations) and destabilized by the ion pressure gradient (since growth is proportional to dP_{0i}/dx).

To understand the instability physically, we consider Figure 1, with the geometry and gradients as given for Eqs. (1.1)-(1.3). A slight pressure fluctuation, arising spontaneously, will drive a parallel velocity fluctuation, by Eq. (1.2). The $\nabla_{\|}\tilde{v}_{\|}$ compression then gives rise to $\tilde{n}_i$ by the continuity equation, and thus $\tilde{\phi}$ from quasineutrality and adiabatic electron response. The $\tilde{\phi}$ then feeds back to the pressure equation, convecting higher pressure fluid down the gradient and reinforcing the initial perturbation. (For the low frequency regime that yields Eq. (1.6), the $\tilde{n}$ increase, produced by parallel compression (at a rate of ω), is quickly relaxed (at the rate of ω_{*e}) by the $\vec{E}\times\vec{B}$ convection along ∇n_0, although the small $\tilde{n}$ that remains is sufficient to produce a $\tilde{\phi}$ with significant effects).

It is interesting to note that compression, while generally considered to be a stabilizing effect, here exerts a purely destabilizing influence. This is because for the low frequency mode considered here, the sound wave produces *negative compressibility* relative to the radial density convection in Eq. (1.1), and the mode is effectively mass incompressible, $\nabla\cdot(n_i\vec{v}_i) \simeq 0$ This serves to maintain

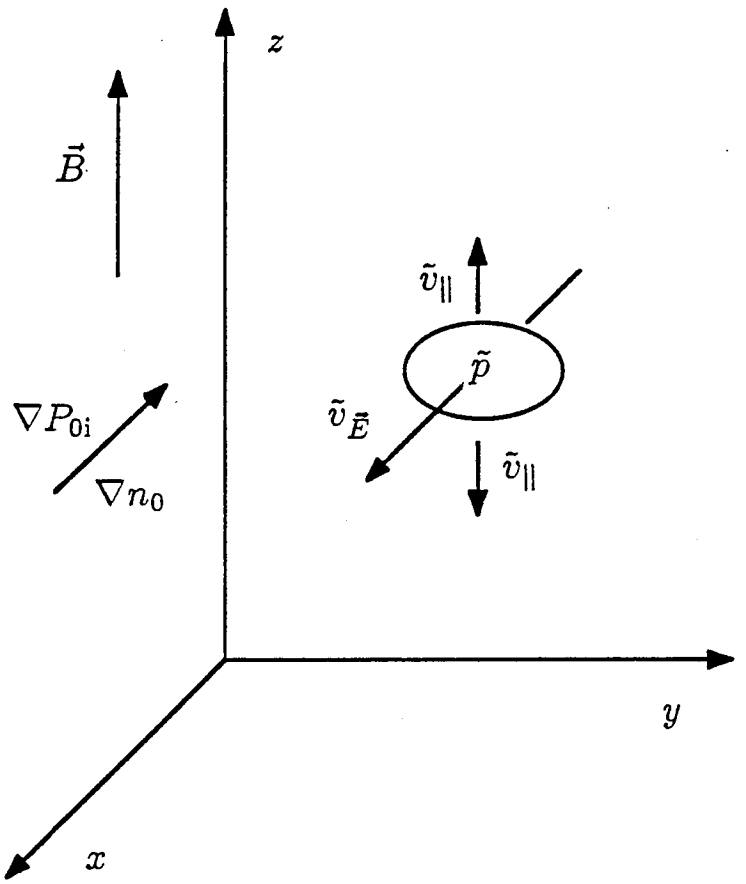

FIGURE 1.1: Physical picture of the local η_i instability mechanism.

the destabilizing dynamical effects of the parallel sound wave fluctuation, while minimizing the energetically stabilizing effects of compression.

This physical picture also illustrates how diffusive thermal transport arises from this instability, which comes from the convection of higher pressure fluid down the gradient. This transport is described by the ion heat flux,

$$q_i = \langle \tilde{v}_{E_x} \tilde{p}_i \rangle \,, \tag{1.7}$$

where $\langle \ldots \rangle$ represents an ensemble, time, or space average. Thus, the same phase relation between $\tilde{v}_{E_x}$ and $\tilde{p}_i$ that produces instability will also yield diffusive heat transport. For the simple picture given here, these two quantities are completely in phase, and heat transport is maximal. However, the other two fluid quantities, mass ($\tilde{n}$) and parallel momentum (proportional to $\tilde{v}_{\|}$) are 90° out of phase with $\tilde{v}_{E_r}$ and not transported. Phase shifts here can be provided by additional effects such as nonadiabatic electrons (transporting particles), or a velocity shear flow (which is the subject of Chapter III).

This linear picture implies that the instability simply grows until the free energy source is exhausted. In reality however, after sufficient growth, nonlinear terms become important, and the linearized equations are no longer valid. The nonlinear terms do a number of things to the exact dynamics of the modes, but considerable simplification can be gained from the fact that we are only interested in the effects which persist when averaged over the long time scale of transport. With the assumption that no long lasting phase relations build between different modes (the "random phase approximation"), then the dominant

contribution of the convective nonlinearities is diffusion of the phase coherent part of the fluctuations. Energetically, this nonlinear diffusion is a consequence of the transfer of excitation between different modes, but it can also alter the dynamical structure of the individual modes, although this latter effect has not been well explored. Linear growth shuts off as energy from the unstable modes couples to stable modes and is dissipated. In such a scenario (if it is dynamically allowable), the final outcome is a saturated spectrum of modes, all fluctuating in amplitude but remaining within a constant probability distribution (*i.e.*, the saturated turbulent spectrum). The aim of a nonlinear theory is to calculate the saturated spectrum, or at the very least estimate its amplitude, for use in the turbulent heat flux calculation, Eq. (1.7). Short of this, a "mixing length" estimate is commonly used,[7] which in the present case is given by $k_\perp \tilde{p} \simeq \nabla_\perp P_{0i}$. This is based on the argument that the growth shuts off when the gradient that feeds the instability is balanced by the gradient of the fluctuations. While this estimate often agrees with more detailed nonlinear calculations in cases where the mode structure is not significantly altered in the nonlinear stage, it does nothing to resolve the dynamics of the nonlinear evolution, which can be significantly different. In general, this kind of detailed question can be answered only by bypassing the mixing length assumption, and considering the nonlinear equations directly (through numerics or through closure schemes such as the DIA[8]). In the case of the fluid η_i mode, it has generally been found that the mixing length predictions persist in a more thorough analysis (except near threshold,

as in Chapter II), but one can never be confident of this a *priori*. In other cases (such as the nonlinear rippling mode[9]) the nonlinear dynamics have been found to be fundamentally changed.

Turbulence models like this give the local transport for a fixed set of profiles, but they are limited in two respects. First, experiments generally measure only *global* confinement parameters, which depend on a variety of transport mechanisms acting at different locations, and so only the crudest comparisons are possible analytically. Second, since the levels of transport contribute to determining the profiles, the model is not self consistent until the resulting profiles are known. To check both of these, it is necessary to use a transport code that combines this and other transport coefficients (assuming they are known!) with sources and sinks to predict the steady state profiles. Since this is the only method available for quantitative comparison of transport coefficients with experimental results, order of magnitude and qualitative comparisons (such as scalings, or relative levels of χ_i, χ_e, D, and χ_φ) tend to be more persuasive.

1.3 Additional Effects

Section 1.2 presented the most basic scenario of the fluid, unsheared, slab η_i mode dynamics and induced transport. Obviously, this is highly idealized, and the influences of a large number of other effects have been, and are being, considered. Here, I briefly review some of the more important effects.

Magnetic shear, whereby the poloidal component ($\sim y$ direction) of $\vec{B}$ varies radially, is a feature common to most magnetic fusion devices. This results in a $k_\parallel$ that varies with x, and since the dynamics are quite sensitive to $k_\parallel$, this serves to give the mode a radial structure.[10]

Perpendicular compression generally has a stabilizing influence, opposing $\nabla_\parallel \tilde{v}_\parallel$ and thereby shutting off the potential fluctuations that destabilize the mode. For the sheared slab modes (considered exclusively in the chapters that follow), perpendicular compression is provided by the polarization drift,[6] which acts to shield the potential fluctuations, and thus determines the radial mode width.

For toroidal geometry (with varying $|B|$ and curved field lines), perpendicular compression can come from the lower order curvature drift, which tends to obscure the sonic nature of the mode. However, the mode remains unstable from the concomitant introduction of bad curvature, but with a ballooning structure rather that the quasi-slab structure of the sound wave.[6,11] A tokamak will generally be somewhere between the slab and toroidal regimes, depending on the strength of the magnetic shear, $\hat{s}/q$, where $\hat{s} = d\ln q/d\ln r$

and $q = rB_\varphi/RB_\theta$ is the safety factor.

Landau damping is negligible so long as $|\omega| \gg k_\| v_i$, but for higher $k_\|$ or lower $|\omega|$ (which occurs as the mode approaches threshold) this condition no longer holds. As it turns out (for the slab-like modes) when $\eta_i \gg 1$, the mode is centered on a region of low $k_\|$, so that Landau damping is negligible (and the fluid picture is valid). However, as $\eta_i \to 1$, this is no longer the case, and the mode rapidly becomes stabilized.[12] Thus, while the fluid picture incorrectly suggests that the mode is stabilized at $\eta_i = -1$, the true threshold with Landau damping is $\eta_i \simeq 1$. One might note that the mechanism of Landau damping for η_i modes is different from the usual picture of flattening of the velocity space distribution. For η_i modes, the distribution of resonant particles changes through radial $\vec{E} \times \vec{B}$ convection along the *spatial* gradient of the distribution function. Resonant particles see a constant electric field, and hence are convected in one radial direction only, whereas nonresonant particles oscillate radially at various frequencies (and thus transport only statistically averaged, fluid quantities). Thus, Landau damping (or growth) comes from the response of $\tilde{\phi}$ to the changing number of resonant particles.

The eigenmodes with $l > 0$ (where l is the radial modenumber) are generally ignored in most studies. However, for sufficiently high η_i these modes are both more unstable and broader than the $l = 0$ mode, with both effects yielding a higher quasilinear diffusion rate. While this effect has been studied[13] for modes of a given l, a fully nonlinear theory which takes into account Landau

damping and nonlinear coupling of different radial eigenmodes has yet to be developed.

Magnetic field fluctuations ("finite β effects") do not have much influence on the η_i instability for $\beta \ll 1$, since in this limit $\tilde{B}$ is too feeble to alter the magnetic field lines enough to influence ion motion.[10] Electron transport, however, can be greatly influenced by much smaller $\tilde{B}$, and this effect in the strong turbulence regime is an area of current research.[14]

Near the threshold of the instability, the growth rate becomes less that the real part of the frequency, and the strong turbulence of the fluid regime changes to weak turbulence. Accompanying this transition, Compton scattering replaces triad resonances as the nonlinear saturation mechanism, resulting in much lower saturation and transport levels as the threshold is approached. This is the subject of Chapter II.

When a sheared velocity field parallel to the magnetic field is introduced (as when a tokamak is heated by tangential neutral beam injection), there are two important effects. First, the growth rate is enhanced from the effect of the shear flow as a free energy source. Second, a phase shift is introduced between the parallel the radial velocity fluctuations, allowing a radial flux of parallel momentum, which can be parametrized in terms of a positive definite turbulent viscosity or momentum diffusivity. This is the subject of Chapter III.

In the limit of no density gradient (as purported to be the case for H-modes on the D-III tokamak[15]) the nonlinear and linear theories must be revised

somewhat to account for mass compressibility entering the basic dynamics of the mode. This is the subject of Chapter IV.

CHAPTER II

ION TEMPERATURE GRADIENT DRIVEN TURBULENCE NEAR THE INSTABILITY THRESHOLD

2.1 Introduction

In recent years, ion temperature gradient driven turbulence[16] ("η_i turbulence") has become a promising explanation for the anomalous ion heat loss observed in tokamaks.[17] Most basically, the theory predicts that when the ion temperature gradient is steeper than some threshold value (parametrized by $\eta_i \equiv \frac{d \ln T_i}{d \ln n_0} > \eta_{th} \equiv 0.95$ in the simplest version of the theory[18]), the mode is destabilized and the resulting fluctuations cause ion heat conduction (parametrized by χ_i). This feature can qualitatively explain such experimental results as the improved energy confinement (τ_E) which accompanies pellet injection,[2] and the τ_E degradation that accompanies neutral beam heating of low confinement ("L-mode") plasmas.[19] Other successful qualitative predictions include the turbulent density fluctuations propagating in the ion drift direction observed in TEXT tokamak,[3] and also the equality of momentum and thermal confinement times for neutral beam heated tokamaks.[5,20,21] Quantitatively, strong turbulence theory predictions[16] of χ_i (valid in the "fluid limit" of $\eta_i \gg \eta_{th}$, where wave-particle interaction is negligible) are easily large enough to account for the anomalous heat loss observed.

With these strong indications of the relevance of the basic theory, the more detailed issue of self consistency arises. For the fluid regime, this requires that the predicted χ_i establishes an ion temperature profile consistent with the assumption that $\eta_i \gg \eta_{th}$. To examine this, a transport simulation has been performed,[22] which lets the profile evolve under the influence of the fluid regime χ_i, combined with other sources and sinks of ion heat. The vanishing of χ_i at the instability threshold (not accounted for by the fluid regime formula) is modelled by interpolating between the fluid regime (for $\eta_i \gg \eta_{th}$) and 0 for $\eta_i \leq \eta_{th}$. Results show that this χ_i is large enough that the ion temperature gradient cannot steepen significantly above threshold, and remains well below the fluid regime level (even with strong ion heating present). However, the validity of using the fluid χ_i for the threshold region is by no means clear, since the character of the instability changes quite a bit as threshold is approached. Thus, in order to determine whether the regime of fluid theory is accessible, a separate theory is required to resolve the transport in the threshold regime.

Previous linear studies[18,23,24,25] have determined the location of the threshold analytically, and investigated the growth rate near threshold numerically, but very little analytical theory valid *near* the threshold has been developed. Construction of a rigorous linear theory of these modes is complicated by the facts that stability comes from ion Landau damping (requiring kinetic theory), and that near threshold the last unstable modes have $k_\perp \rho_i \simeq 1$ (leading to nonlocal interaction). The nonlinear and transport behaviour of the η_i mode

near the threshold has naturally been even less well understood. There have been mixing length estimates of the quasilinear χ_i near threshold,[26] but this approach leads to spurious results (such as a fluctuation level of $\tilde{\phi} \sim 1/k_\perp L$, which does not vanish at threshold). A reliable prediction requires more careful consideration.

The difference between the fluid and threshold regimes, in addition to linear Landau damping, involves several important changes in the nonlinear behaviour. First, as the growth rate becomes less than the frequency, the strong turbulence approximations of the fluid regime become invalid, and a transition to weak turbulence ensues. Commonly used estimates such as $e\tilde{\phi}/T \sim 1/k_\perp L$ to find saturation levels, and $D \sim \gamma/k_\perp^2$ for transport, apply only for strong turbulence, where the nonlinearities are large enough to balance the linear terms. For weak turbulence (where the nonlinearities are small), a calculation based on the wave kinetic equation is necessary to obtain reliable predictions. Second, the frequency broadening of strong turbulence becomes negligible, and the triad resonances that are automatically allowed in strong turbulence for matching wavevectors ($\vec{k} = \vec{k}' + \vec{k}''$) must satisfy the additional constraint of linear frequency matching ($\omega_{\vec{k}} = \omega_{\vec{k}'} + \omega_{\vec{k}''}$). Finally as linear wave particle resonances grow more important, nonlinear wave-particle interaction becomes a more effective saturation mechanism. A weak turbulence expansion is appropriate for considering these changes.

This chapter presents a theory of η_i transport near the threshold of in-

stability, with an emphasis on weak turbulence theory. We consider the usual paradigm model of sheared slab geometry with gyrokinetic ions and adiabatic electrons. The linear theory uses an eigenmode analysis for the real part of the frequency (for $\gamma \simeq 0$), and a local approximation to find the growth rate. This technique retains the essential features and orderings of the threshold regime, but is also simple enough for construction of a tractable nonlinear theory. The nonlinear theory follows the weak turbulence expansion, whereby the linear modes are substituted iteratively into the nonlinearity (which is smaller by an approximate factor of γ/ω). This leads to a wave kinetic equation, describing the evolution of the spectrum as a balance of linear growth and nonlinear scattering and damping. This is solved for the saturated spectrum, which is used to calculate the turbulent ion thermal flux.

The principal results of this chapter are the following:

1. When $\eta_{th} \leq \eta_i < \eta_{th} + (1 + 1/\tau)\frac{L_n}{L_s}$, (where $\eta_{th} = 0.95$ and $L_n/L_s \ll 1$), then $\gamma \ll \omega$ and a weak turbulence expansion applies.
2. Linear theory shows that near threshold, the modes that are unstable have frequency $\omega \sim (L_n/L_s)^2\omega_{*i}$, linear growth rate $\gamma \sim (L_n/L_s)(\eta_i - \eta_c)\omega_{*i}$, and width $\Delta_x \sim \rho_i$, where η_c is the $k_\perp$ dependent threshold. Furthermore, only the $l = 0$ radial eigenmode mode is unstable at threshold.

3. The frequency is very dispersive, $\frac{d\ln\omega}{d\ln k_y} \neq 1$, and therefore wave-wave interactions and turbulent shielding are negligible in this regime.

4. Nonlinear saturation of the instability occurs through ion Compton scattering to the lower k_y modes, which are stable. The resulting spectrum is given by

$$\left(\frac{e\tilde{\phi}}{T_i}\right)^2 = \sqrt{\frac{2}{\pi}}\left(\frac{q\rho_i}{r\hat{s}}\right)\frac{(1+1/\tau)^2}{\eta_i^2}\left(\frac{L_n}{L_s}\right)^2\left(\frac{\rho_i}{L_s}\right)^2 I(b),$$

where $I(b)$ is a spectral intensity function of $b = k_y^2\rho_i^2$, which vanishes at threshold and is concentrated about $b = 1$ (Fig. 2.2 and after Eq. (2.29)). The coefficient of $I(b)$ is smaller that that for $\eta_i \gg \eta_{th}$ by a factor on the order of $(L_n/L_s)^2 \ll 1$.

5. The ion thermal conductivity from turbulent $\vec{E}\times\vec{B}$ convection is given by

$$\chi_i = N_{th}\frac{(1+1/\tau)^2}{2\sqrt{\pi}}\left(\frac{L_T}{L_s}\right)^2\frac{\rho_i^2 v_i}{L_s}$$

where N_{th} is a threshold dependent function of η_i given by Eq. (2.35) and shown in Figure 2.3. The magnitude of χ_i is less than an extrapolation from the $\eta_i \gg \eta_{th}$ regime by a factor on the order of $(L_T/L_s)^2 \ll 1$.

The remainder of this chapter is organized as follows. Section 2.2 presents the basic model and equations used in the theory. Section 2.3 de-

velops a simple semi-local linear theory (frequency, growth rate, and basic mode structure) valid in the neighborhood of the threshold. Section 2.4 develops the nonlinear theory, including derivation of the wave kinetic equation, which is an integral equation for the spectrum. This equation is solved approximately for the saturated spectrum. Section 2.5 outlines the derivation of the ion thermal conductivity, χ_i. Section 2.6 contains a short summary and conclusions. Also of interest are Appendix A, which addresses the stability and growth of the $l > 0$ radial eigenmodes, and Appendix B, which addresses the stability of the flat density modes ($L_n/L_s \to \infty$).

2.2 Basic Model

The goal of this work is to develop only the framework of an analytical theory of the η_i instability near the threshold. The essential features of the η_i instability are the drive from the ion temperature gradient, ion Landau damping (from magnetic shear) and the nonlinear $\vec{E} \times \vec{B}$ drift, which determines mode coupling and transport. These are described in our model by the nonlinear electrostatic ion gyrokinetic equation[27] with adiabatic electrons, in a sheared slab geometry, with all inhomogeneities (density, ion temperature, and magnetic shear) in the radial (x) direction.

In a sheared slab model, the magnetic field is $\vec{B} = B_0 (\hat{z} + (x/L_s)\, \hat{y})$. There are density and ion temperature gradients in the x direction, characterized by L_n and L_T, where $-dn_0/dr = n_0/L_n$ and $-dT_i/dr = T_i/L_T$. In general,

we consider the regime $L_T \sim L_n \ll L_s$, usually true for tokamaks. (We also consider, in Appendix B, the stability of the $L_n > L_s$ "flat density" case, which may be relevant to H-mode discharges.) Since all inhomogeneities are radial, then linear perturbations have the form $\tilde{f}(x)\exp(-i\omega t + ik_y y + ik_z z)$. The modes are centered about the point where $\vec{k}\cdot\vec{B} = 0$, which in the closed field line configuration of the tokamak is allowable only on rational surfaces, $x_s(\vec{k})$. The point $x = 0$ is chosen at the rational surface of the "test mode", so that $k_\parallel = k_y x/L_s$, and for the "background modes" (which are nonlinearly coupled to the test mode) $k_\parallel{}' = k_y'(x - x_s(\vec{k}'))/L_s \equiv k_y' x'/L_s$. The mode has low frequency, $\omega \lesssim \omega_{*i}$, radial width on the order of ρ_i (since the broader modes are stabilized by Landau damping), and has phase velocity $\omega/k_\parallel \lesssim v_i$ over most of the mode.

In the gyrokinetic model, electrostatic ion dynamics are described by the phase space distribution function $F(\vec{r},\vec{v},t) = F_0(x,v) + \tilde{f}(\vec{r},\vec{v},t)$, where F_0 is a local maxwellian (*i.e.*, with $n_0(x)$ and $T_i(x)$), and $\tilde{f}$ is the rapidly varying part of the distribution function. The nonadiabatic part of $\tilde{f}$ evolves according to the nonlinear gyrokinetic equation[27] in the electrostatic limit:

$$\left(\frac{\partial}{\partial t} + ik_\parallel v_\parallel\right)\tilde{h}_{\vec{k}} - \left(\frac{\partial}{\partial t} + i\omega_{*i}\left(1 + \eta_i\left(\frac{mv^2}{2T_i} - \frac{3}{2}\right)\right)\right)F_0 J_0\left(\frac{k_\perp v_\perp}{\Omega_i}\right)\frac{e\tilde{\phi}_{\vec{k}}}{T_i} = \frac{e}{m_i\Omega_i}\sum_{\vec{k}'+\vec{k}''=\vec{k}}\hat{b}\cdot\left(\vec{k}'\times\vec{k}''\right)J_0\left(\frac{k_\perp{}' v_\perp}{\Omega_i}\right)\tilde{\phi}_{\vec{k}'}\tilde{h}_{\vec{k}''}, \qquad (2.1)$$

where,

$$\omega_{*i} = \frac{cT_i}{eB}\frac{d\ln n_0}{dx}, \qquad \eta_i = \frac{d\ln T_i}{d\ln n_0}, \qquad F_0 = n_0\left(\frac{m}{2\pi T_i}\right)^{3/2} e^{-mv^2/2T_i},$$

J_0 is the zeroth Bessel function, and $\|$ and $\perp$ refer to the magnetic field direction, $\hat{b} = \vec{B}/|B|$. The right hand side of this equation describes mode coupling due to the $\vec{E} \times \vec{B}$ nonlinearity.

Electrons are taken as adiabatic ($\tilde{n}_e = n_0 e\tilde{\phi}/T_e$), and Eq. (2.1) is closed with the quasineutrality equation, $\tilde{n}_e = \tilde{n}_i$, or

$$(1 + 1/\tau)\, n_0 \frac{e\tilde{\phi}_{\vec{k}}}{T_i} = \int d^3v J_0 \left(\frac{k_\perp v_\perp}{\Omega_i} \right) \tilde{h}_{\vec{k}}, \tag{2.2}$$

where $\tau = T_e/T_i$.

Equations (2.1) and (2.2) describe the η_i instability in both the fluid ($\eta_i \gg 1$) and kinetic ($\eta_i \sim 1$) regimes. The fluid equations that describe the η_i instability are reproduced by the velocity moments of Eq. (2.1), in the $\omega/k_\| > v_i$ limit. Close to marginal stability, Landau damping becomes important ($\omega/k_\| > v_i$) and a weak turbulence expansion is applicable (valid in the $\gamma \ll \omega$ regime[28]). The latter is the limit examined in the remainder of this chapter.

2.3 Linear Theory

The focus of this chapter is nonlinear dynamics and transport, so what we require from the linear theory is a simple model that describes the most basic properties of the frequency, growth rate, and structure of the modes. Several authors have discussed the linear behaviour of the η_i mode near threshold, but none completely enough for our purposes. Coppi *et al.*[10] derived an integral equation which reduces to a differential equation when $k_\perp^2 \rho_i^2 \ll 1$; near threshold, however, the dominant modes have $k_\perp^2 \rho_i^2 \simeq 1$, described by the fully nonlocal integral equation. The physical reason for this radially nonlocal interaction is that the mode is both narrow ($\Delta_x \sim \rho_i$) and slow ($\omega/\omega_{*i} \ll L_n/L_s \ll 1$). Thus, correlation across the width of the mode (on an ion transit time scale of $\Delta_x/v_i \sim \Omega_i^{-1}$), dominates decorrelation over this distance (which occurs, through shear, on the slower time scale of $\Delta_x/\Delta\left(\omega/k_\parallel\right) \gg \Omega_i^{-1}$), resulting in strong nonlocal interaction. However, such integral equations are notoriously difficult to solve, and so threshold behaviour is generally analyzed with a gyrokinetic equation, which lends itself to two routes of approximation. First, a local approximation[18,23,24] has the advantage of allowing simple algebraic solution for $\omega(\vec{k})$, however it does nothing to resolve the mode structure, which is important for the nonlinear theory. The second method is to expand to order $(k_x\rho_i)^2 = \rho_i^2 \frac{\partial^2}{\partial x^2}$, and solve the resulting differential equation either analytically (directly or with a WKB approximation) or with a shooting code.[25] While this method does resolve the mode structure, for the present case it becomes overly

complicated when carried out to the order necessary to resolve the weak growth rate, and furthermore, since it relies on a $(k_x\rho_i)^2$ expansion for modes which have width $k_x\rho_i \simeq 1$, it is not clear that this complication leads to a more reliable result than the method described below.

The present analysis calculates for the lowest order mode structure and frequency (real part only, with $|\gamma| \ll |\omega|$) by an expansion in $(k_x\rho_i)^2$, and finds the growth rate using local theory. The growth rate of the modes is then calculated by summing the local growth of the individual parts of the mode, which corresponds mathematically to $\frac{\partial}{\partial t}\int|\tilde{\phi}_{\vec{k}}|^2dx = \int\frac{\partial}{\partial t}|\tilde{\phi}_{\vec{k}}|^2dx$. Associating the former with the growth rate of the mode, and the latter with the local growth rate, we obtain the formula:

$$\gamma_{\vec{k}} = \frac{\int_{-\infty}^{\infty}\gamma_{\vec{k}}\left(k_{\|}\right)\left|\tilde{\phi}_{\vec{k}}\right|^2 dx}{\int_{-\infty}^{\infty}\left|\tilde{\phi}_{\vec{k}}\right|^2 dx}. \tag{2.3}$$

This semi-local mode analysis offers a tractable formulation of the linear dynamics, consistent with the ordering of this regime. The main approximation is the neglect of detailed nonlocal effects, and it is doubtful that anything short of solving the full integral equation could account for these properly.

Linearizing Eq. (2.1), Fourier transforming in t, solving for $\tilde{h}$, and substituting into Eq. (2.2) produces the following mode equation:

$$\epsilon_{\vec{k}}\left(\omega_{\vec{k}} + i\gamma_{\vec{k}}\right)\tilde{\phi}_{\vec{k}} = 0, \tag{2.4}$$

where the linear dielectric function is given by:

$$\epsilon_{\vec{k}}\left(\omega\right) = 1 + 1/\tau - \frac{\omega_{*i}}{\omega}\eta_i\Gamma_0\zeta^2 + \frac{\omega_{*i}}{\omega}\left(\frac{\eta_i}{\eta_c} - 1 - \zeta^2\eta_i + \frac{\omega}{\omega_{*i}}\right)\Gamma_0\zeta Z\left(\zeta\right). \tag{2.5}$$

Here Z is the plasma dispersion function, and

$$\zeta = \omega/\sqrt{2}v_i k_\parallel, \qquad v_i^2 = T_i/m_i, \qquad \Gamma_n = e^{-b_\perp} I_n(b_\perp), \qquad b_\perp = k_x^2\rho_i^2 + b,$$
$$b = k_y^2\rho_i^2, \qquad \rho_i = \tfrac{v_i}{\Omega_i}, \qquad \omega = \omega_{\vec{k}} + i\gamma_{\vec{k}},$$

I_n is a modified Bessel function, and $\eta_c^{-1} \equiv \frac{1}{2} + b_\perp\left(1 - \frac{\Gamma_1}{\Gamma_0}\right)$ is the $k_\perp$ dependent critical value[18] of η_i. It is useful to note here that the ordering in the threshold regime, which can be verified *a posteriori*, is

$$\omega/\omega_{*i} \sim s^2, \quad \zeta \sim s, \quad \eta_i - \eta_c < s,$$

where $s = L_n/L_s \ll 1$ is used as a small parameter.

a. *Local Analysis*

In the local approximation, Eq. (2.4) is solved treating k_x algebraicly. Assuming that $|\gamma_{\vec{k}}| \ll |\omega_{\vec{k}}|$, we can make the approximation

$$\epsilon_{\vec{k}}(\omega_{\vec{k}} + i\gamma_{\vec{k}}) = \epsilon'_{\vec{k}}(\omega_{\vec{k}}) + i\epsilon''_{\vec{k}}(\omega_{\vec{k}}) + i\gamma_{\vec{k}}\partial\epsilon'_{\vec{k}}/\partial\omega_{\vec{k}}$$

(where $\epsilon = \epsilon' + i\epsilon''$). With this, and noting that $\epsilon''_{\vec{k}}(\omega_{\vec{k}})$ comes only from the resonant part of $Z(\zeta)$, Eq. (2.4) may be manipulated into the form:

$$\epsilon'_{\vec{k}}(\omega_{\vec{k}}) = p - \frac{\omega_{*i}}{\omega}\eta_i\zeta^2 + \epsilon''_{\vec{k}}\frac{ReZ}{ImZ} = 0, \tag{2.6}$$

and after some straightforward manipulation,

$$\epsilon''_{\vec{k}}(\omega_{\vec{k}}) = \frac{\omega_{*i}}{\omega}\left(\frac{\eta_i}{\eta_c} - 1 - \frac{p-1}{p}\eta_i\zeta^2\right)\frac{p\zeta ImZ(\zeta)}{p + \zeta ReZ(\zeta)}, \tag{2.7}$$

where $p \equiv (1 + 1/\tau)/\Gamma_0$.

Expanding $Z(\zeta)$ for $\zeta \ll 1$ (*i.e.*, strong ion resonance), then solving Eq. (2.6) yields

$$\begin{aligned} \omega_{\vec{k}}(k_\parallel) &= \frac{pv_i^2 k_\parallel^2}{\omega_{*i}} \left(\frac{\eta_i}{2} + \frac{\eta_i}{\eta_c} - 1 \right)^{-1} \\ &\simeq \frac{2pv_i^2 k_\parallel^2}{\eta_i \omega_{*i}}, \end{aligned} \tag{2.8}$$

where the latter equality comes from the ordering $|\eta_i - \eta_c| < s$ (derived later in this section from the $|\gamma| \ll |\omega|$ requirement) . From the above, it is easy to show that $\partial\epsilon'/\partial\omega_{\vec{k}} \simeq -p/\omega_{\vec{k}}$ and $\zeta = \sqrt{2}pv_i k_\parallel/\eta_i\omega_{*i}$, and then using $\gamma = \frac{-\epsilon''}{\partial\epsilon'/\partial\omega}$, we obtain the local growth rate:

$$\gamma_{\vec{k}}(k_\parallel) = \sqrt{2\pi}\frac{v_i|k_\parallel|}{\eta_i}\left[\frac{\eta_i}{\eta_c} - 1 - \frac{2p(p-1)v_i^2}{\eta_i\omega_{*i}^2}k_\parallel^2\right]\exp\left[-2\left(\frac{pv_i k_\parallel}{\eta_i\omega_{*i}}\right)^2\right]. \tag{2.9}$$

Equations (2.8) and (2.9) agree well with the numerical solutions of Eqs. (2.4) and (4), treated locally.[23] We briefly review their analytical stability criterion, here exhibited in Eq. (2.9) by the terms in the first set of brackets, which determine the sign of $\gamma_{\vec{k}}(k_\parallel)$. Since the coefficient of $k_\parallel^2$ is positive, then if $\eta_i > \eta_c$, there is a band of $k_\parallel$ (centered about $k_\parallel = 0$) for which $\gamma_{\vec{k}}(k_\parallel) > 0$. This corresponds nonlocally to an unstable fluctuation centered on the mode rational surface, and stabilized on the edges by Landau damping. If $\eta_i \leq \eta_c$, then $\gamma_{\vec{k}}(k_\parallel) \leq 0$ for all $k_\parallel$, and no instability exists. Figure 2.1 shows $\eta_c(b)$. From this plot, it is clear that as η_i decreases from the fluid regime, the low $k_\perp$ modes (broader in x, thus more heavily Landau damped) are stabilized. Threshold occurs when the last mode is stabilized, which occurs for $b_{th} \simeq 1$ and $\eta_c(b_{th}) \equiv \eta_{th} \simeq 0.95$.

b. Mode Analysis

The most straightforward way to examine the mode structure is to expand every $\Gamma_n(b_\perp)$ in Eq. (2.5) to order $k_x^2\rho_i^2$, and treat the resulting differential equation with a WKB approximation. However, this analysis is rather complicated, and defeats the purpose of finding a *simple* formulation of the linear theory. A method to circumvent this complication comes from the insight gained from local theory that the dominant imaginary terms in the mode equation balance on the average (*i.e.*, the terms which vary as γ and as $\frac{\eta_i}{\eta_c(b_\perp)} - 1$, with *all* of $b_\perp$, before any expansion). While radial variation of k_x leads to *some* nonvanishing imaginary part of the potential function, shooting code analysis confirms that the effects of this may be neglected to lowest order. Furthermore, it is not clear that this complication leads to a more reliable result than the present method, for the $k_x\rho_i \simeq 1$ modes. In the spirit of a semi-local theory, we shall neglect the imaginary part of the mode equation entirely.

Keeping only the dominant (real) part of Eq. (2.5) with the ordering of the local theory, taking $k_\parallel = k_y x/L_s$, and expanding in k_x yields:

$$\rho_i^2 \frac{d^2\tilde{\phi}_{\vec{k}}}{dx^2} + \frac{1}{1-\Gamma_1/\Gamma_0}\left(1 - \frac{ps^2\omega_{*i}}{\eta_i\omega_{\vec{k}}}\frac{x^2}{\rho_i^2}\right)\tilde{\phi}_{\vec{k}} = 0, \tag{2.10}$$

where $s = L_n/L_s$, and the argument of Γ_n is b $(= k_y^2\rho_i^2)$ instead of $b_\perp$ as before. This is a Weber's equation, and the general solution is given by the Hermite functions:

$$\tilde{\phi}_{\vec{k}} = H_l\left(x/\Delta_x\right)\exp\left[-x^2/2\Delta_x^2\right] \tag{2.11}$$

where $\Delta_x^2 = \eta_i \omega_{\vec{k}} / p s^2 \omega_{*i}$. Combining this with the dispersion relation, we find:

$$\omega_{\vec{k}} = \omega_{*i} \frac{p s^2}{\eta_i} \frac{\Delta_x^2}{\rho_i^2}, \tag{2.12}$$

and

$$\frac{\Delta_x^2}{\rho_i^2} = (2l+1)^2 \left(1 - \frac{\Gamma_1}{\Gamma_0}\right). \tag{2.13}$$

This we regard as the lowest order structure of the mode, and may be modified by outward propagation (from ϵ'', ignored here) or other effects.

The growth of the $l = 0$ mode is calculated using Eq. (2.3) with $\gamma_{\vec{k}}(x)$ given by Eq. (2.9) (assuming $L_n/L_s \ll 1$), yielding

$$\gamma_{\vec{k}} = \sqrt{2}\omega_{*i} \frac{L_n}{L_s} \frac{\Delta_x}{\eta_i \rho_i} \left[\frac{\eta_i}{\eta_c} - 1 - \frac{2p\,(p-1)}{\eta_i} \left(\frac{L_n}{L_s}\right)^2 \frac{\Delta_x^2}{\rho_i^2}\right]. \tag{2.14}$$

The stability and growth of the $l > 0$ modes is derived in Appendix A. The stability threshold in the $L_n/L_s \to \infty$ (flat density) regime is derived in Appendix B.

We now discuss the main features of the linear theory. First, it may seem surprising that Δ_x is independent of L_s, since $k_\parallel$ sets the radial scale. However, this is also true in the $\eta_i \gg 1$ fluid limit, where Δ_x is determined by shielding from the polarization drift, and apparently the present case is similar. Furthermore, Eq. (2.13) is consistent with the kinetic shooting code results of Ref. 13, which found that Δ_x depends primarily on l, and not L_s/L_T or η_i. Second, the frequency of these modes, given by Eq. (2.12), is just the local

frequency evaluated at the mode edge (where $k_\parallel = k_y \Delta_x / L_s$). Third, the instability threshold of the modes is essentially the same as that of the local theory, but with a small correction from the last term in the brackets of Eq. (2.14) ($\sim (L_n/L_s)^2$) coming from the fact that modes of finite width cover both unstable and stable regions at threshold. We shall ignore it for the $l = 0$ mode, but for the broader $l > 0$ modes this correction becomes larger, so that these modes are not unstable in the $\eta_i \simeq \eta_c$ regime considered here (Appendix A). Finally, in comparison with the $\eta_i \gg \eta_{th}$ and $\gamma \gg \omega$ fluid regime, the real part of the frequency remains on the same order of magnitude in both regimes, $\omega \sim s^2 \omega_{*i}$ (the frequency in the fluid limit may be checked from the dispersion relation in, *e.g.*, Ref. 16), while the growth rate changes from $\gamma \sim (1 + \eta_i) s \omega_{*i}$ in the fluid regime to $\gamma \sim (\eta_i - \eta_c) s \omega_{*i}$ here. That the basic ordering is the same in both threshold and fluid regimes (except for the η_i dependence) implies that this is in fact a continuation of the same root.

We have checked the analytical results with a shooting code, which retains all the imaginary parts of Eqs. (2.4) and (2.5) and expands in $k_x^2 \rho_i^2$ (although this is not necessarily more reliable than the present analysis for the $k_x \rho_i \simeq 1$ regime). Results confirm that the mode is basically gaussian in structure with width as predicted, albeit a small degree of propagation past the turning points occurs, typically resulting in $\Delta_x \propto (L_s/L_n)^\alpha$ with $\alpha \lesssim 1/4$. In view of this kind of uncertainty, in the remainder of the chapter we shall take $\tilde{\phi} \sim e^{-x^2/2\Delta_x^2}$, (with Δ_x unspecified and possibly complex), to allow for

the possibility of unresolved broadening through propagation. (The method of calculating frequency and growth rate allows for this uncertainty.) When quantitative estimates require a mode width, Eq. (2.13) will be used.

The exactness of this mode analysis is somewhat uncertain (since we have relied on an expansion for $k_x^2\rho_i^2 \ll 1$), but several qualitative features may be expected to persist in a more detailed solution. First, the turning points in Eq. (2.10) would be the same even without expansion in k_x, since at these points, $k_x \to 0$. The existence of these fixed turning points indicates that even in a more exact theory there will be a normal mode (as opposed to a convective mode) whose width is on the order of ρ_i (*i.e.*, the separation of the turning points). Second, the radial quantization (parametrized by l) may be regarded as a real physical effect, since the modes are radial bound states. Finally, it is reasonable that only the $l = 0$ mode is unstable at the threshold, since the higher modes are broader, and hence more heavily Landau damped.

The validity of this theory depends on the $|\gamma| \ll |\omega|$ and $|\omega| \ll |k_\parallel v_i|$ assumptions. The former of these gives the strongest restriction. Either by comparing the $\gamma_{\vec{k}}$ and $\omega_{\vec{k}}$ of the normal mode, or by requiring in the local theory that the region where $\gamma\left(k_\parallel\right) > \omega\left(k_\parallel\right)$ (which will always occur at the mode center, since $\omega \propto k_\parallel^2$ while $\gamma \propto k_\parallel$ near the rational surface) occupy a negligible part of the mode, we obtain the restriction:

$$|\eta_i - \eta_c| < \frac{1 + 1/\tau}{\sqrt{2}\Gamma_0}\frac{\Delta_x}{\rho_i}\frac{L_n}{L_s} \simeq (1 + 1/\tau)\frac{L_n}{L_s}. \tag{2.15}$$

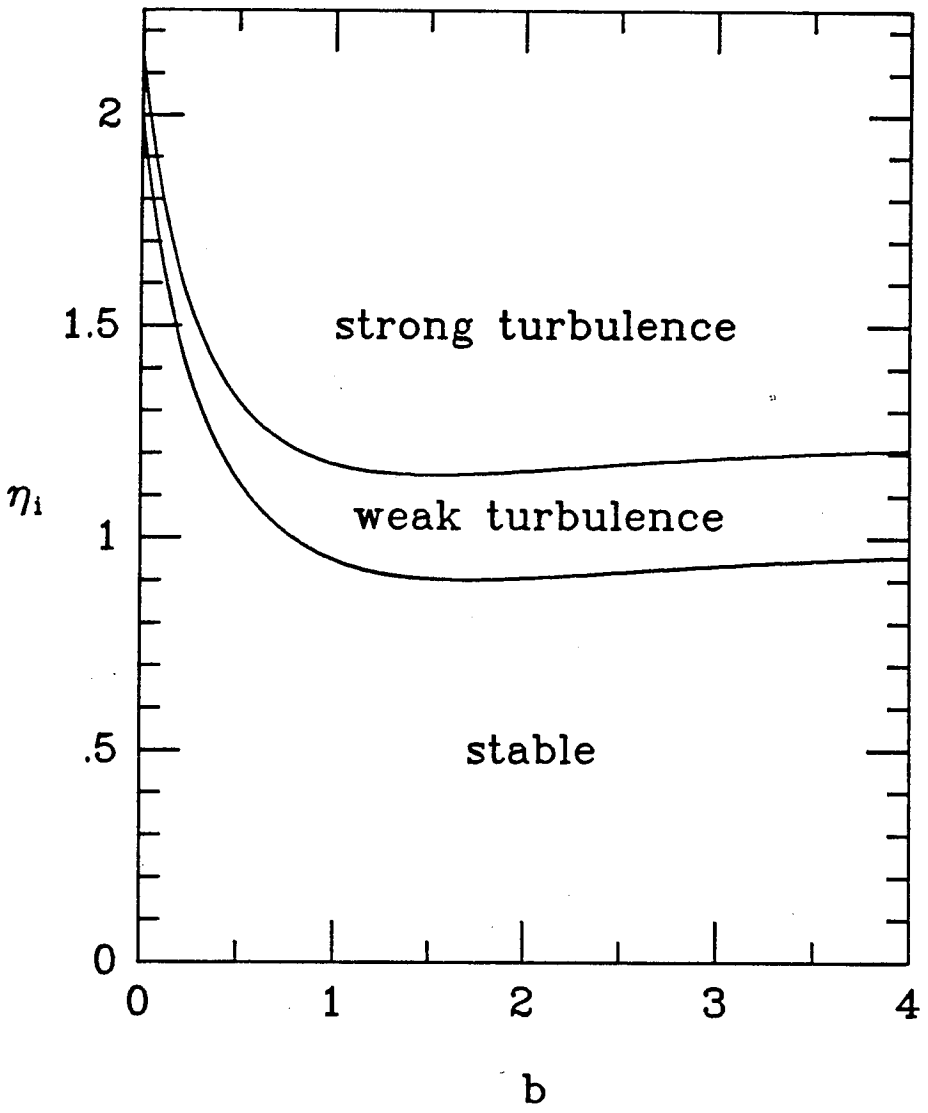

FIGURE 2.1: Stability threshold and weak turbulence regime, where $\gamma \ll \omega$, for $L_n/L_s = 0.1$, $\tau = 1$.

This range is plotted in Fig. 2.1. Since $L_n/L_s \ll 1$, Eq. (2.15) means that the range of η_i covered by this theory is rather narrow. It appears that $|\omega| \ll |k_\parallel v_i|$ remains true well above this threshold regime, meaning that between the fluid and threshold regimes there exists a third regime, characterized by $\gamma \gtrsim \omega$ (invalidating the present expansion) and $|\omega| \ll |k_\parallel v_i|$ (ion resonances). This regime is discussed further in Section 2.6.

For a fixed value of η_i, Eq. (2.15) limits the range of validity in k_y space. Letting $k_y = k_{y,crit} + \delta k_y$ (where $k_{y,crit}$ is the marginally stable k_y for fixed η_i), then Eq. (2.15) yields:

$$|\delta k| \lesssim \left(\sqrt{2}\frac{1+1/\tau}{\Gamma_0}\frac{L_n}{\eta_i L_s}\frac{\Delta_x}{\rho_i}\Big/\frac{\partial^2\eta_c}{\partial k_y^2}\right)^{1/2} \simeq k_{y,crit}\left(\frac{L_n}{L_s}\right)^{1/2}$$

In other words, as $k_y \to 0$ past $k_{y,crit} - \delta k$, the mode becomes *strongly* stabilized, so that $|\gamma| > |\omega|$ (Fig. 2.1). Hence these low k_y modes are not described by our theory, but they are probably not important in the spectrum energy balance. This is discussed further in the next section.

Finally, we note that our theory seems to predict instability for the $k_y\rho_i \to \infty$ modes. However, this result is probably unphysical, since at shorter wavelength, certain stabilizing effects appear which are ignored in this theory, such as collisional viscosity or electron dissipation.

2.4 Nonlinear Theory

This section examines the transfer of fluctuation energy from unstable to stable linear modes, in order to determine the turbulent spectrum. The weak turbulence expansion is used to derive the wave kinetic equation, which is solved to yield the fluctuation level and spectrum at saturation.

The weak turbulence expansion[28] proceeds as follows. Noting that the linear part of Eq. (2.1) is of order $\omega\tilde{h}$, while the nonlinearity is of order $\gamma\tilde{h}$ (Eq. (2.21) verifies *a posteriori* that the saturation amplitude of the fluctuations is of order γ), then for $\gamma < \omega$ the equation can be solved by perturbing about the linear solution as follows. For simplicity of notation, we write Eq. (2.1) as

$$L_{1,\vec{k}}\tilde{h}_{\vec{k}} + L_{2,\vec{k}}\tilde{\phi}_{\vec{k}} = \sum_{\vec{k}'} C_{\vec{k}',\vec{k}''}\tilde{\phi}_{\vec{k}'}\tilde{h}_{\vec{k}''} \tag{2.16}$$

with $L_{1,\vec{k}}, L_{2,\vec{k}}$, and $C_{\vec{k}',\vec{k}''}$ defined from the corresponding terms in Eq. (2.1). Letting $\tilde{h}_{\vec{k}} = \tilde{h}^{(1)}_{\vec{k}} + \tilde{h}^{(2)}_{\vec{k}} + \ldots$, we have, to lowest order, the linear equation:

$$L_{1,\vec{k}}\tilde{h}^{(1)}_{\vec{k}} + L_{2,\vec{k}}\tilde{\phi}_{\vec{k}} = 0, \tag{2.17}$$

and to n^{th} order,

$$L_{1,\vec{k}}\tilde{h}^{(n)}_{\vec{k}} = \sum_{\vec{k}'} C_{\vec{k}',\vec{k}''}\tilde{\phi}_{\vec{k}'}\tilde{h}^{(n-1)}_{\vec{k}''}. \tag{2.18}$$

Equations (2.17) and (2.18) are solved by iteratively substituting $\tilde{h}^{(1)}_{\vec{k}}$ into the nonlinearity of the second order equation, and repeating to n^{th} order. Substituting $\tilde{h}^{(1)}_{\vec{k}} + \tilde{h}^{(2)}_{\vec{k}} + \tilde{h}^{(3)}_{\vec{k}}$ into Eq. (2.2) produces

$$\epsilon^{(1)}_{\vec{k}}(\omega)\,\tilde{\phi}_{\vec{k}} + \sum_{\substack{\vec{k}'+\vec{k}''=\vec{k} \\ \omega'+\omega''=\omega}} \epsilon^{(2)}_{\vec{k}',\vec{k}''}(\omega',\omega'')\tilde{\phi}_{\vec{k}'}\tilde{\phi}_{\vec{k}''}$$

$$+ \sum_{\substack{\vec{k}'+\vec{k}''+\vec{k}'''=\vec{k} \\ \omega'+\omega''+\omega'''=\omega}} \sum \epsilon^{(3)}_{\vec{k}',\vec{k}'',\vec{k}'''}(\omega',\omega'',\omega''')\tilde{\phi}_{\vec{k}'}\tilde{\phi}_{\vec{k}''}\tilde{\phi}_{\vec{k}'''} = 0 \quad (2.19)$$

where the symmetrized dielectric functions are given by

$$\epsilon^{(1)}_{\vec{k}}(\omega) = (1+1/\tau)\frac{n_0 e}{T_i} + \int d^3v \frac{J_0 L_{2,\vec{k}}}{L_{1,\vec{k}}}$$

$$\epsilon^{(2)}_{\vec{k}',\vec{k}''}(\omega',\omega'') = \frac{1}{2}\int d^3v \frac{J_0 L_{2,\vec{k}''}}{L_{1,\vec{k}'+\vec{k}''}L_{1,\vec{k}''}} C_{\vec{k}'\vec{k}''} \quad + \quad \left(\vec{k}' \leftrightarrow \vec{k}''\right)$$

$$\epsilon^{(3)}_{\vec{k}',\vec{k}'',\vec{k}'''}(\omega',\omega'',\omega''') = \frac{1}{2}\int d^3v \frac{J_0 L_{2,\vec{k}'''}}{L_{1,\vec{k}}L_{1,\vec{k}''+\vec{k}'''}L_{1,\vec{k}'''}} C_{\vec{k}',\vec{k}''+\vec{k}'''}C_{\vec{k}'',\vec{k}'''}$$
$$+ \left(\vec{k}'' \leftrightarrow \vec{k}'''\right),$$

where $J_0 = J_0\left(\frac{k_\perp v_\perp}{\Omega_i}\right)$. Following Ref. 28, Eq. (2.19) may be divided into two equations. The real part becomes an equation for the frequency and linear structure of the mode,

$$\epsilon'_{\vec{k}}\left(\omega_{\vec{k}}\right)\tilde{\phi}_{\vec{k}} = 0, \quad (2.20)$$

as examined in Section 2.3. The imaginary part of Eq. (2.19), after some manipulation, becomes the wave kinetic equation, which describes linear instability and nonlinear evolution of the spectrum

$$\frac{1}{2}\frac{\partial \epsilon'}{\partial \omega_{\vec{k}}}\frac{\partial}{\partial t}\left|\tilde{\phi}_{\vec{k}}\right|^2 = -\epsilon''_{\vec{k}}\left(\omega_{\vec{k}}\right)\left|\tilde{\phi}_{\vec{k}}\right|^2 + Im \sum_{\substack{\vec{k}'+\vec{k}''=\vec{k} \\ \omega'+\omega''=\omega}} \frac{2\left|\epsilon^{(2)}_{\vec{k}',\vec{k}''}\left(\omega_{\vec{k}'},\omega_{\vec{k}''}\right)\right|^2}{\epsilon^{(1)}_{\vec{k}'+\vec{k}''}\left(\omega_{\vec{k}'}+\omega_{\vec{k}''}\right)}\left|\tilde{\phi}_{\vec{k}'}\right|^2\left|\tilde{\phi}_{\vec{k}''}\right|^2$$

$$+ Im \sum_{\substack{\vec{k}'+\vec{k}''=\vec{k} \\ \omega'+\omega''=\omega}} \frac{4\epsilon^{(2)}_{\vec{k}',\vec{k}''}\left(\omega_{\vec{k}'},\omega_{\vec{k}''}\right)\epsilon^{(2)}_{\vec{k},-\vec{k}'}\left(\omega_{\vec{k}},-\omega_{\vec{k}'}\right)}{\epsilon^{(1)}_{\vec{k}''}\left(\omega_{\vec{k}''}\right)}\left|\tilde{\phi}_{\vec{k}'}\right|^2\left|\tilde{\phi}_{\vec{k}}\right|^2$$

$$- Im \sum_{\vec{k}'+\vec{k}''=\vec{k}} \epsilon^{(3)}_{\vec{k}',-\vec{k}',\vec{k}}\left(\omega_{\vec{k}'},-\omega_{\vec{k}'},\omega_{\vec{k}}\right)\left|\tilde{\phi}_{\vec{k}'}\right|^2\left|\tilde{\phi}_{\vec{k}}\right|^2, \quad (2.21)$$

where $\epsilon^{(1)}_{\vec{k}} = \epsilon'_{\vec{k}} + i\epsilon''_{\vec{k}}$, and $\omega_{\vec{k}}$ refers to only the real part of the frequency.

Physically, nonlinear transfer is the result of two processes. First are three-wave resonances, described by the second and third terms on the right hand side of Eq. (2.21). This is a transfer of energy between the test mode $\vec{k},\omega$ and background modes $\vec{k}',\omega'$ and $\vec{k}'',\omega''$, and requires a match of both wavenumber ($\vec{k} = \vec{k}' + \vec{k}''$) and frequency ($\omega = \omega' + \omega''$). Although this process dominates when $\eta_i \gg \eta_{th}$ (in strong turbulence[16]), in the present case it is much less important. This is because triads of waves which satisfy both $\vec{k}$ and $\omega_{\vec{k}}$ matching are rare, since $\omega_{\vec{k}}$, given by Eq. (2.12), is strongly dispersive ($\frac{d\ln\omega}{d\ln k_y} \neq 1$), and frequency broadening is negligible for weak turbulence ($\Delta\omega \simeq \gamma \ll \omega$). The second nonlinear coupling process is ion Compton scattering (also known as nonlinear Landau damping), described by the last term on the right hand side of Eq. (2.21). This is a transfer of energy between two modes $\vec{k},\omega$ and $\vec{k}',\omega'$ which occurs when an ion resonates with their beat wave, *i.e.* $v_{\|i} = (\omega - \omega')/(k_\| - k'_\|)$. Compton scattering dominates energy transfer in the threshold regime, accompanying the presence of significant *linear* wave-ion resonances.

Neglecting the three-wave resonance terms, (as well as turbulent shielding, for the same reason) we can write the wave kinetic equation as:

$$\frac{1}{2}\frac{\partial}{\partial t}\left|\phi_{\vec{k}}\right|^2 = \gamma^l_{\vec{k}}\left|\phi_{\vec{k}}\right|^2 + \gamma^c_{\vec{k}}\left|\phi_{\vec{k}}\right|^2, \tag{2.22}$$

where $\gamma^l_{\vec{k}}$ is the local linear growth rate, Eq. (2.9), and $\gamma^c_{\vec{k}}$ is the nonlinear

Compton scattering term:

$$\gamma_{\vec{k}}^{c} = \frac{\Omega_i^2}{\omega_{\vec{k}}^2} Im \sum_{\vec{k}'} \rho_i^4 (\vec{k} \times \vec{k}')_{\parallel}^2 \int d^3v J_0^2 J_0'^2 \left(R_{\vec{k}'} \left(\omega_{\vec{k}'} \right) + R_{\vec{k}-\vec{k}'} \left(\omega_{\vec{k}} - \omega_{\vec{k}'} \right) \right) \left| \frac{e\tilde{\phi}_{\vec{k}'}}{T_i} \right|^2 \cdot \div \frac{\partial \epsilon'_{\vec{k}}}{\partial \omega_{\vec{k}}}, \tag{2.23}$$

where,

$$J_0 = J_0 \left(\frac{k_\perp v_\perp}{\Omega_i} \right), \qquad J_0' = J_0 \left(\frac{k'_\perp v_\perp}{\Omega_i} \right),$$

$$R_{\vec{k}} (\omega) = -\frac{eF_0}{T_i} \quad \frac{\omega - \omega_{*i} \left(1 + \eta_i (\frac{mv^2}{2T_i} - \frac{3}{2}) \right)}{\omega - k_\parallel v_\parallel}.$$

In deriving Eq. (2.23), the test mode has been assumed situated at $x = 0$, so that $k'_\parallel > k_\parallel \to 0$. None of the linear theory has been used in deriving Eq. (2.23).

Equation (2.22) suggests that a possible saturation mechanism for the linear instability is Compton scattering to the lower k_y damped modes, which can dissipate energy. We now discuss several details of this mechanism. First, the tendency for Compton scattering to transfer energy to lower wavenumbers will be demonstrated from the form of $\gamma_{\vec{k}}^{c}$ after it has been further refined. Second, although we speak informally of Compton scattering only in terms of energy transfer between modes, this is not strictly the case. In the scattering process, some energy is lost to the scattering ion (in the form of nonlinear Landau damping), so that the true saturation mechanism is some combination of scattering and nonlinear damping. However, in either case, the ultimate sink of wave energy is heating of ions, leading to a net ion thermal diffusion as

calculated in Section 2.5. Third, Compton scattering is a binary process, and transfer from $\vec{k}$ to $\vec{k}'$ requires that the product $\tilde{\phi}_{\vec{k}}(x)\tilde{\phi}_{\vec{k}'}(x)$ be nonzero, which in turn requires finite levels of excitation for both modes (as well as mode overlap). The finite excitation level for linearly stable modes can be provided by nonlinear destabilization (*i.e.*, when $\gamma_{\vec{k}}^l + \gamma_{\vec{k}}^c > 0$), as described by Eq. (2.22). Finally, we note that that there must be enough modes to cover a given radial interval, *i.e.*, $\sum_{k'} \Delta_x' > \Delta r$. Estimating the mode width as ρ_i, and noting that the number of modes between r and $r + \Delta r$ with poloidal modenumber m is, on the average, $m/q(r) - m/q(r + \Delta r)$ (where q is the safety factor and $\hat{s} = d\ln q/d\ln r$), we find the condition

$$m_{max} \gtrsim \sqrt{qr/\rho_i \hat{s}} \sim 30$$

(estimated for $r \sim 1\text{m}, \rho_i \sim 1\text{mm}$, and $q \sim \hat{s} \sim 1$). Typically this condition is easily met.

Several simplifications render Eq. (2.22) more tractable. First, we convert the discrete spectral sum (which involves complicated information about the rational surface of each mode) into an integral over the distribution of modes, with a density of states. Smoothing the mode distribution in x' (to avoid rational surface information), and k_y' (to avoid discrete m information) results in

$$\sum_{k_y'} \longrightarrow \frac{r\hat{s}}{q} \int dk_y' \, |k_y'| \int dx'.$$

Second, it is useful to decompose the spectrum as

$$\left|\frac{e\tilde{\phi}_{\vec{k}'}}{T_i}\right|^2 = S\left(k'_y\right)\exp(-x'^2/\Delta_{x'}^2),$$

where $S(k_y)$ is the spectral amplitude and $\exp(-x'^2/\Delta_{x'}^2)$ accounts for the linear mode structure, Eq. (2.11). Finally, by averaging Eq. (2.22) over the width of the test mode (*i.e.*, in x), the local linear growth rate becomes the modal one (following the method of the linear theory), and the odd term of $(\vec{k}\times\vec{k}')_\parallel^2$ in $\gamma_{\vec{k}}^c$ vanishes from the antisymmetry of k_x ($\sim x/\Delta_x^2$ for the $l=0$ mode). After some tedious algebra, this produces

$$\gamma_{\vec{k}}^c = -\sqrt{\frac{\pi}{2}}\frac{r\hat{s}}{q\rho_i}\frac{\Omega_i L_s \Gamma_0}{(1+1/\tau)\,\omega_{\vec{k}}}\int_{-\infty}^{\infty}\frac{dx'}{|x'|}\int_{-\infty}^{\infty}dk'_y K(k_y,k'_y)\exp\left(-\frac{x'^2}{\Delta_{x'}^2}\right)S\left(k'_y\right), \tag{2.24}$$

where the kernel of the integral is given by

$$\begin{aligned}K(k_y,k'_y) =& \rho_i^4\left(k_x^2 k'^2_y + k_y^2 k'^2_x\right)G(b,b')\exp\left[-\frac{\left(\omega_{\vec{k}}-\omega_{\vec{k}'}\right)^2}{2s^2{\omega'_{*i}}^2}\frac{\rho_i^2}{x'^2}\right]\\ &\times\left\{\left(\omega_{*i}-\omega'_{*i}\right)\left[\left(\frac{1}{2}+\frac{G'(b,b')}{G(b,b')}\right)\eta_i - 1 - \frac{\eta_i}{2}\frac{\left(\omega_{\vec{k}}-\omega_{\vec{k}'}\right)^2}{s^2{\omega'_{*i}}^2}\frac{\rho_i^2}{x'^2}\right]\right.\\ &\left.+\omega_{\vec{k}}-\omega_{\vec{k}'}\right\}\end{aligned}$$

The contribution from $R_{\vec{k}'}$ in Eq. (2.23) has vanished from symmetry in k'_y (*i.e.* $S\left(k'_y\right) = S\left(-k'_y\right)$, following from symmetry of the equations), and

$$G(b,b') = \int_0^\infty d(v_\perp^2)J_0^2\left(\sqrt{2b}v_\perp\right)J_0^2\left(\sqrt{2b'}v_\perp\right)e^{-v_\perp^2},$$

$$G'(b,b') = \frac{\partial}{\partial\alpha}G\left(\frac{b}{\alpha},\frac{b'}{\alpha}\right)\Big|_{\alpha=1}.$$

With $\gamma_{\vec{k}}^c$ in the form of Eq. (2.24), the wave kinetic equation (Eq. (2.22) with Eq. (2.14) for $\gamma_{\vec{k}}^l$) becomes an integral equation for $S(k_y)$. The integral operator in $\gamma_{\vec{k}}^c$ closely resembles that in the integral equation that formally describes the linear η_i instability.[10] The primary difference is that the x' integral in the present case, representing spatial overlap of different modes, is replaced with a time integral in the linear case, representing self interaction within one mode.

In both the linear and nonlinear cases, few methods are available for direct solution of the full integral equation. One numerical approach to the solution might be to let a test spectrum evolve via the wave kinetic equation, until a steady state spectrum is attained (which avoids the numerical instability associated with direct inversion of the integral operator). However, numerical solution is beyond the scope of the present work. Analytically, we are necessarily limited to rather approximate methods for finding $S(k_y)$. A simple but often reliable method (used in a previous version of this theory[29] and compared with the present version as a rough check) is to estimate of the integrated spectral amplitude in terms of the basic scalings and *rms* type quantities. An improvement over this method, which we now follow, is to Taylor expand $S(k_y')$ about $k_y \simeq k_y'$, which reduces the integral equation to a more tractable differential equation for $S(k_y)$.

Letting $k_y - k'_y = k''_y$, then

$$S(k'_y) \simeq S(k_y) - k''_y \frac{\partial S(k_y)}{\partial k_y} + \frac{k''^2_y}{2} \frac{\partial^2 S(k_y)}{\partial k_y^2}.$$

Since $S(k'_y)$ in narrower than the kernel in k'_y-space, then extracting S from the integration extends the domain over which the kernel is integrated. Therefore, it is necessary to accompany the extraction of S with a normalization of the integral, as $\int_{-\infty}^{\infty} SK dk'_y \rightarrow S \int_{-\Delta_{SK}}^{\Delta_{SK}} K dk'_y \simeq S \frac{\Delta_{SK}}{\Delta_K} \int_{-\infty}^{\infty} K dk'_y$, where S and K represent the spectrum and kernel, respectively, and Δ_{SK} and Δ_K are the widths of SK and K in k'_y-space. While this step is heuristic, one can demonstrate that such a normalization factor is present for S gaussian (Appendix C), and the results produced will be justified a *posteriori*. Also expanding other functions of k'_y as $f(k'_y) \simeq f(k_y) - k''_y \partial f / \partial k_y$ for $f = k'_x, \omega_{k'}$, or $G(b, b')$, then $\gamma^c_{\bar{k}}$ becomes, for $k''_y \ll k_y$,

$$\begin{aligned} \gamma^c_{\bar{k}} = & \sqrt{\frac{\pi}{2}} \frac{r\hat{s}}{q\rho_i} \frac{\Omega_i L_s \Gamma_0}{(1+1/\tau)\omega_{\bar{k}}} \frac{\Delta_{SK}}{\Delta_K} \int_{-\infty}^{\infty} \frac{dx'}{|x'|} \int_{-\infty}^{\infty} dk''_y K(k''_y) \exp\left(-\frac{x'^2}{\Delta_x^2}\right) \\ & \times \left[S(k_y) - k''_y \frac{\partial S(k_y)}{\partial k_y} + \frac{k''^2_y}{2} \frac{\partial^2 S(k_y)}{\partial k_y^2} \right]. \end{aligned} \tag{2.25}$$

where

$$\begin{aligned} K(k''_y) = & (2\rho_i^4 k_x^2 k_y^2) G(b,b) \exp\left[-\left(k''_y \frac{\partial \omega_{\bar{k}}}{\partial k_y} \right)^2 \frac{1}{2s^2 \omega_{*i}} \frac{\rho_i^2}{x'^2} \right] \\ & \times \left\{ -k''_y v_D \left[\left(\frac{1}{2} + \frac{G'(b,b)}{G(b,b)} \right) \eta_i - 1 \right] - \left(k''_y \frac{\partial \omega_{\bar{k}}}{\partial k_y} \right)^3 \frac{\eta_i}{2} \frac{v_D}{s^2 \omega_{*i}} \frac{\rho_i^2}{x'^2} + k''_y \frac{\partial \omega_{\bar{k}}}{\partial k_y} \right\} \end{aligned}$$

It is easy to show that $\Delta_K \simeq \left(\frac{\partial\omega_{\vec{k}}}{\partial k_y}\frac{1}{\sqrt{2}s\omega_{*i}}\frac{\rho_i}{\Delta_x}\right)^{-3}$, and we estimate $\Delta_{SK} \simeq k_y^3$. The integration, first in k_y'' then in x', and using $\omega_{\vec{k}} \ll \omega_{*i}$, produces:

$$\gamma_{\vec{k}}^c \simeq \left(\frac{\pi}{2}\right)^{3/2} \frac{r\hat{s}}{q\rho_i}\frac{\rho_i^4\Omega_i L_s}{(1+1/\tau)}\frac{\omega_{*i}}{\omega_{\vec{k}}}k_x^2k_y^4\Gamma_0(b)G(b,b)\left[\left(2+\frac{G'(b,b)}{G(b,b)}\right)\eta_i - 1\right]\frac{\partial S}{\partial|k_y|}. \tag{2.26}$$

With $S(k_y)$ no longer appearing under an integral sign, the wave kinetic equation has the more tractable form of:

$$\frac{\partial S}{\partial t} - V_{k_y}S\frac{\partial S}{\partial|k_y|} = \gamma_{\vec{k}}^l S, \tag{2.27}$$

where V_{k_y} is the coefficient of $\frac{\partial S}{\partial|k_y|}$ in Eq. (2.26). Equation (2.27) has the form of a transport equation in k_y space, with the linear growth (damping) playing the role of a source (sink) term, and the Compton scattering playing the role of convection. The fact that V_{k_y} is positive definite implies that the transport of spectral energy scatters to lower $|k_y|$.

It is a simple matter to solve Eq. (2.27) for the saturated state ($\partial/\partial t \to 0$). This yields (for $k_y > 0$, with the other half following from symmetry):

$$\begin{aligned} S(k_y) &= -\int_{k_0}^{k_y} dk_y' \frac{\gamma_{\vec{k}'}^l}{V_{\vec{k}_y'}} \\ &= -\int_{k_0}^{k_y} dk_y' \rho_i \frac{4}{\pi^{3/2}}\frac{q\rho_i}{r\hat{s}}(1+1/\tau)\left(\frac{\rho_i}{L_s}\right)^2 \frac{(\Delta_x/\rho_i)}{(\rho_i k_y')^3(\rho_i k_x')^2}\frac{\omega_{\vec{k}'}}{\omega_{*i}'}, \\ &\quad \times \frac{1}{\Gamma_0(b')G(b',b')}\frac{1}{[(2+G'/G)\eta_i - 1]}\frac{\eta_i - \eta_c}{\eta_i\eta_c} \end{aligned} \tag{2.28}$$

where k_0 is the maximum unstable k_y ($\to \infty$ for $\eta_i \geq 1$), and we have applied the boundary condition that $\lim_{k_y\to\infty} S(k_y) = 0$. This integral is straightforward but

algebraicly tedious. To the accuracy of this theory, a simple estimate suffices. The most important k_y dependence of the integrand comes from $\eta_i - \eta_c(b)$, which determines the sign. The essential features of η_c (asymptotics, threshold, etc.) are retained by the approximation:

$$\frac{1}{\eta_c} \simeq \left\{ \begin{array}{ll} \frac{1}{2} + \left(\frac{1}{\eta_{th}} - \frac{1}{2} \right) b & b < 1 \\ 1 + \left(\frac{1}{\eta_{th}} - 1 \right) \frac{1}{b} & b \geq 1 \end{array} \right\},$$

where $\eta_{th} = 0.95$ is the minimum of $\eta_c(b)$, attained for $b \simeq 1$. Also important is the k_y dependence coming from the terms which vary as k_y to a power. Noting that for $b \gtrsim 1$ it is appropriate to expand for Γ_0 and G asymptotically, so that we obtain:

$$\frac{(\Delta_x/\rho_i)}{(\rho_i k_y)^3 (\rho_i k_x)^2} \frac{\omega_{\vec{k}}}{\omega_{*i}} \frac{1}{\Gamma_0(b) G(b,b)} \simeq \frac{2\pi (1 + 1/\tau)}{\eta_i} \left(\frac{L_n}{L_s} \right)^2 \left(\frac{\Delta_x}{\rho_i} \right)^3 \frac{1}{b},$$

where we have taken $k_x \simeq k_y$, $\Gamma_0(b) \simeq (2\pi b)^{-1/2}$ (Ref. 30), and $G(b,b) \propto b^{-1}$ is easily shown. If we use Δ_x as given by Eq. (2.13), then asymptotically we have $\Delta_x^2 \simeq 1/2b$. For all the rest of the k_y dependence, substituting $(k_y \rho_i)_{\rm rms} \simeq 1$ suffices. We now perform the integral in Eq. (2.28), obtaining

$$S(k_y) \simeq \sqrt{\frac{2}{\pi}} \left(\frac{q \rho_i}{r \hat{s}} \right) \frac{(1 + 1/\tau)^2}{\eta_i^2} \left(\frac{L_n}{L_s} \right)^2 \left(\frac{\rho_i}{L_s} \right)^2 I(b). \qquad (2.29)$$

Here, $I(b)$ is a spectral intensity function, defined as follows. If $\eta_i \leq \eta_{th} = 0.95$,

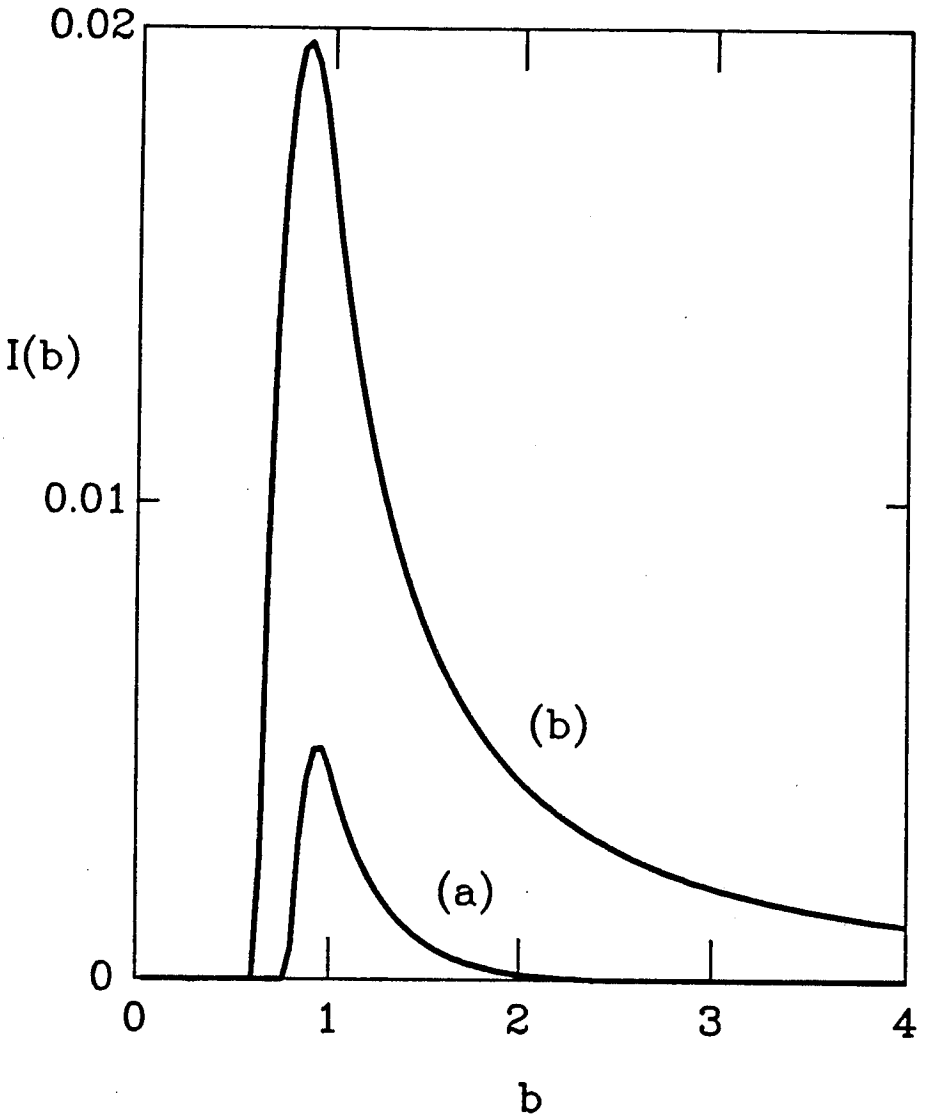

FIGURE 2.2: Form of wavenumber spectrum in Eq. (2.29) (a) for $\eta_i = .98$ and (b) for $\eta_i = 1.02$.

then $I(b) = 0$. If $\eta_i > \eta_{th}$ (within the limits of validity of the theory), then

$$I(b) = \left\{ \begin{array}{ll} \frac{1}{3}\left(1 - \frac{1}{\eta_i}\right)\left(\frac{1}{b^{3/2}} - \frac{1}{b_0^{3/2}}\right) + \frac{1}{5}\left(\frac{1}{\eta_{th}} - 1\right)\left(\frac{1}{b^{5/2}} - \frac{1}{b_0^{5/2}}\right) & b \geq 1 \\ I(1) + \frac{1}{3}\left(\frac{1}{2} - \frac{1}{\eta_i}\right)\left(\frac{1}{b^{3/2}} - 1\right) + \left(\frac{1}{\eta_{th}} - \frac{1}{2}\right)\left(\frac{1}{b^{1/2}} - 1\right) & b < 1 \\ 0 & \text{if } I(b) < 0 \end{array} \right\}$$

The parameter b_0 (*i.e.*, k_0) is the maximum unstable b (given the above approximation for η_c)

$$b_0 = \left\{ \begin{array}{ll} \text{undefined} & \eta_i < \eta_{th} \\ \frac{1 - \eta_{th}}{1 - \eta_i} & \eta_{th} \leq \eta_i < 1 \\ \infty & 1 \leq \eta_i \end{array} \right\}$$

Figure 2.2 shows $I(b)$ for the cases $b_0 < \infty$ and $b_0 \to \infty$. In both cases, the spectrum is concentrated about the region $b \simeq 1$.

The first thing to notice about the spectrum is that the amplitude, $S \sim \frac{L_n^2}{L_s^2}\frac{\rho_i^2}{L_s^2}$ (i. e., the coefficient of $I(b)$ in Eq. (2.29), less the toroidal mode density terms $\frac{q\rho_i}{r\hat{s}}$), is extremely low in comparison to the saturation level in the fluid regime[16] (where $S \sim \frac{\rho_i^2}{L_s^2}$), even when the diminished linear growth rate due to the threshold is taken into consideration. Thus, Compton scattering seems to be much more effective than triad resonances at transferring energy away from unstable modes, thereby holding the turbulent fluctuations to a much lower level. However, as η_i rises from the threshold level to the fluid level, γ becomes greater than ω, and the resonant part of $Z(\zeta)$ becomes zero.[31] Thus, in the fluid regime Compton scattering vanishes, allowing triad resonances to become the saturation mechanism, and $S(k_y)$ rises to the level of Ref. 16.

It is useful to devise a rule of thumb for estimating saturation levels from Compton scattering, although nothing as simple and broadly applicable as the mixing length estimate seems possible. From inspection of Eq. (2.23), it is easy to see that the the Compton scattering rate may be estimated by

$$\gamma_{\vec{k}}^{c} \sim \frac{\Omega_i^2}{\omega}(\rho_i k_\perp)^4 \frac{\omega_{*i}}{k_\parallel v_i}\left(\frac{e\tilde{\phi}}{T}\right)^2,$$

for the present ordering. Balancing $\gamma_{\vec{k}}^{c}$ with the linear growth gives the estimate

$$\sum_{\vec{k}}\left(\frac{e\tilde{\phi}_{\vec{k}}}{T}\right)^2 \sim \frac{\gamma\omega}{\omega_{*i}^2}\frac{\Delta_x/\rho_i}{(k_\perp\rho_i)^4}\frac{\rho_i^2}{L_n L_s}. \tag{2.30}$$

Using γ and ω from Eqs. (2.12) and (2.14), and $\Delta_x \sim k_\perp^{-1} \sim \rho_i$, then Eq. (2.30) recovers the spectral amplitude of Eq. (2.29). This estimate is limited to the present ordering, although one might hope to derive a more general form from balancing the ϵ'' and $\epsilon^{(3)}$ terms in Eq. (2.21).

Considering the approximations leading up to Eq. (2.29), it is essential to justify the main features of our nonlinear theory on physical grounds. First, the amplitude of the spectrum is roughly the same as given by scaling-type estimates[29] based on Eqs. (2.22) and (2.23), with $(k_y\rho_i)_{\rm rms} \simeq 1$, as above. Thus, it appears that the approximations after this equation did not lead to any miscalculation in the basic amplitude of $\tilde{\phi}$. Second, the result that energy scatters to lower k_y is the usual result for ion Compton scattering, *e.g.* as in the case of drift wave turbulence.[28,32] Furthermore, it is reasonable to expect that retaining nonlocal interaction in k_y space (neglected when $S(k_y')$ is expanded)

would only further enhance this flow from the high k_y source to the low k_y sink. Third, our theory suggests that the spectral energy sink occurs for the $k_y\rho_i \simeq 1$, weakly stable ($|\gamma| < |\omega|$) modes. One might ask if the strongly stable $k_y\rho_i \ll 1$ modes might provide a more effective energy sink, and do not appear in our spectrum only as an artifact of neglecting long range interaction in k_y-space. To answer this point, we note that Compton scattering requires that both $S(k_y)$ and $S(k_y')$ be nonzero for transfer from $\vec{k}$ to $\vec{k}'$, while at the same time the strongly stable modes cannot be sufficiently destabilized by nonlinear coupling with weakly unstable modes. Thus, one expects that the weakly stablized modes (which *can* be nonlinearly destabilized to finite amplitude) should provide the dominant energy sink, as this theory shows. Finally, the nonlinear calculation indicates a spectrum that decays as $1/k_y^3$ as $k_y \to \infty$, although the linear theory suggests instability in this limit. This may be due to the fact that Compton scattering produces nonlinear stability at low amplitudes in this limit, but in any event, consideration of ion collisions or electron dissipation would stabilize the high k_y modes, and so a vanishing spectrum is physically correct.

2.5 Transport

Having obtained the saturated spectrum, we next apply this knowledge to finding the saturation level of ion thermal conductivity, χ_i, due to turbulent $\vec{E} \times \vec{B}$ convection. Other transport coefficients are of secondary interest here, since it is the balance of heating and χ_i that determines η_i, and thus the relevance of this threshold regime to experiments. Turbulent transport is described by the guiding center Vlasov equation averaged over fast fluctuations:

$$\frac{\partial \langle F \rangle}{\partial t} + \text{non} - \text{turbulent terms} = \frac{c}{B} \left\langle \tilde{\vec{E}} \times \hat{b} \cdot \nabla \tilde{f} \right\rangle, \tag{2.31}$$

where $F = \langle F \rangle + \tilde{f}$ is the phase space distribution function, and $\langle \ldots \rangle$ represents an average over fast fluctuations. The right hand side of this equation can be written as the divergence of a "flux", $-\nabla_x \Gamma_x(\vec{v})$, where

$$\Gamma_x(\vec{v}) = \frac{c}{B} \sum_{\vec{k}} -ik_y J_0 \left(\frac{k_\perp v_\perp}{\Omega_i} \right) \left\langle \tilde{\phi}_{\vec{k}} \tilde{h}_{-\vec{k}} \right\rangle.$$

Treating $\Gamma_x(\vec{v})$ similarly to the nonlinearity in the gyrokinetic equation yields, after some work,

$$\begin{aligned} \Gamma_x(\vec{v}) = Im \sum_{\vec{k}} k_y \Bigg\{ & - \mu^{(1)}_{\vec{k}}(\vec{v}) \left| \tilde{\phi}_{\vec{k}} \right|^2 + \sum_{\substack{\vec{k}'+\vec{k}''=\vec{k} \\ \omega'+\omega''=\omega}} \frac{2\mu^{(2)}_{\vec{k}',\vec{k}''}(\vec{v}) \epsilon^{(2)}_{-\vec{k}',-\vec{k}''}}{\epsilon^{(1)}_{\vec{k}'+\vec{k}''}} \left| \tilde{\phi}_{\vec{k}'} \right|^2 \left| \tilde{\phi}_{\vec{k}''} \right|^2 \\ & + \sum_{\substack{\vec{k}'+\vec{k}''=\vec{k} \\ \omega'+\omega''=\omega}} \frac{4\mu^{(2)}_{\vec{k}',\vec{k}''}(\vec{v}) \epsilon^{(2)}_{\vec{k},-\vec{k}'}}{\epsilon^{(1)}_{\vec{k}''}} \left| \tilde{\phi}_{\vec{k}'} \right|^2 \left| \tilde{\phi}_{\vec{k}} \right|^2 \\ & - \sum_{\vec{k}'+\vec{k}''=\vec{k}} \mu^{(3)}_{\vec{k}',-\vec{k}',\vec{k}}(\vec{v}) \left| \tilde{\phi}_{\vec{k}'} \right|^2 \left| \tilde{\phi}_{\vec{k}} \right|^2 \Bigg\}, \end{aligned} \tag{2.32}$$

2.5 Transport

Having obtained the saturated spectrum, we next apply this knowledge to finding the saturation level of ion thermal conductivity, χ_i, due to turbulent $\vec{E} \times \vec{B}$ convection. Other transport coefficients are of secondary interest here, since it is the balance of heating and χ_i that determines η_i, and thus the relevance of this threshold regime to experiments. Turbulent transport is described by the guiding center Vlasov equation averaged over fast fluctuations:

$$\frac{\partial \langle F \rangle}{\partial t} + \text{non} - \text{turbulent terms} = \frac{c}{B} \left\langle \tilde{\vec{E}} \times \hat{b} \cdot \nabla \tilde{f} \right\rangle, \tag{2.31}$$

where $F = \langle F \rangle + \tilde{f}$ is the phase space distribution function, and $\langle \ldots \rangle$ represents an average over fast fluctuations. The right hand side of this equation can be written as the divergence of a "flux", $-\nabla_x \Gamma_x(\vec{v})$, where

$$\Gamma_x(\vec{v}) = \frac{c}{B} \sum_{\vec{k}} -ik_y J_0 \left(\frac{k_\perp v_\perp}{\Omega_i} \right) \left\langle \tilde{\phi}_{\vec{k}} \tilde{h}_{-\vec{k}} \right\rangle.$$

Treating $\Gamma_x(\vec{v})$ similarly to the nonlinearity in the gyrokinetic equation yields, after some work,

$$\begin{aligned} \Gamma_x(\vec{v}) = Im \sum_{\vec{k}} k_y \Bigg\{ & - \mu^{(1)}_{\vec{k}}(\vec{v}) \left| \tilde{\phi}_{\vec{k}} \right|^2 + \sum_{\substack{\vec{k}'+\vec{k}''=\vec{k} \\ \omega'+\omega''=\omega}} \frac{2\mu^{(2)}_{\vec{k}',\vec{k}''}(\vec{v}) \epsilon^{(2)}_{-\vec{k}',-\vec{k}''}}{\epsilon^{(1)}_{\vec{k}'+\vec{k}''}} \left| \tilde{\phi}_{\vec{k}'} \right|^2 \left| \tilde{\phi}_{\vec{k}''} \right|^2 \\ & + \sum_{\substack{\vec{k}'+\vec{k}''=\vec{k} \\ \omega'+\omega''=\omega}} \frac{4\mu^{(2)}_{\vec{k}',\vec{k}''}(\vec{v}) \epsilon^{(2)}_{\vec{k},-\vec{k}'}}{\epsilon^{(1)}_{\vec{k}''}} \left| \tilde{\phi}_{\vec{k}'} \right|^2 \left| \tilde{\phi}_{\vec{k}} \right|^2 \\ & - \sum_{\vec{k}'+\vec{k}''=\vec{k}} \mu^{(3)}_{\vec{k}',-\vec{k}',\vec{k}}(\vec{v}) \left| \tilde{\phi}_{\vec{k}'} \right|^2 \left| \tilde{\phi}_{\vec{k}} \right|^2 \Bigg\}, \end{aligned} \tag{2.32}$$

where the $\mu^{(n)}(\vec{v})$ are equal to the corresponding $\epsilon^{(n)}$ without the velocity space integration, and the redundant arguments ω have been omitted from both of these. The similarity of the Eq. (2.32) and the right hand side of Eq. (2.21) is obvious. The $\vec{v}$-moments of $\Gamma_x(\vec{v})$ give the fluxes of the fluid quantities. The particle flux, $\int d^3v\Gamma_x(\vec{v})$, is proportional to the right hand side of the wave kinetic equation, which vanishes at saturation. A phase shift between $\tilde{n}_e$ and $\tilde{\phi}$ (here, adiabatic) would be needed to model particle flux. The ion thermal flux, $q_i = \int d^3v \frac{mv^2}{2}\Gamma_x(\vec{v})$, is a more involved calculation. For the same reasons as in the wave kinetic equation, we retain only the quasilinear and Compton pieces of $\Gamma_x(\vec{v})$ (the first and last terms in Eq. (2.32), respectively), and obtain (after extensive calculation)

$$\begin{aligned} q_i = &-2\sqrt{\pi}v_i n_0 T_i(1+1/\tau)\frac{r\hat{s}}{q\rho_i}\frac{L_n}{L_s} \\ &\times \int_{-\infty}^{\infty} dk_y \rho_i k_y^2 \Delta_x^2 \frac{\omega_{*i}}{\omega_{\vec{k}}}(1-2b+b^2+b\frac{\Gamma_1}{\Gamma_0}-b^2\frac{\Gamma_1^2}{\Gamma_0^2})S(k_y), \end{aligned} \tag{2.33}$$

where we have neglected terms of order γ/ω or less. Inserting the spectrum from Eq. (2.29) and expanding $\Gamma_n(b)$ for $b \gtrsim 1$, we find the ion thermal conductivity:

$$\begin{aligned} \chi_i = &-q_i \Big/ n_0\left(\frac{dT_0}{dx}\right) \\ \simeq &N_{th}\frac{(1+1/\tau)^2}{2\sqrt{\pi}}\left(\frac{L_T}{L_s}\right)^2\frac{\rho_i^2 v_i}{L_s}, \end{aligned} \tag{2.34}$$

where N_{th} is the k_y integrated spectrum, and contains the cutoff of χ_i at thresh-

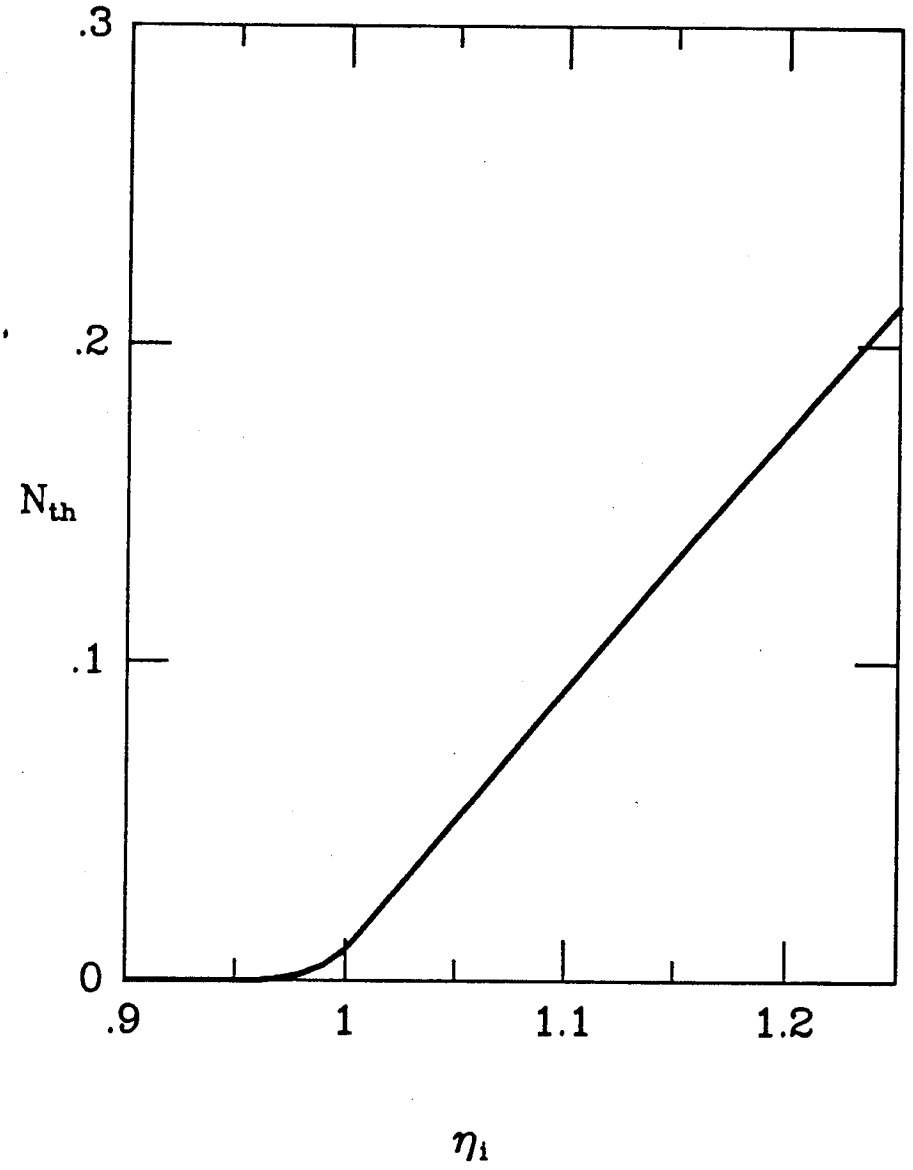

FIGURE 2.3: Integrated spectrum appearing in χ_i, Eq. (2.33) (N_{th} depends only on η_i).

old:

$$N_{th} = \int_0^\infty dbI(b)$$
$$= \left(1 - \frac{1}{\eta_i}\right)\left(1 - \frac{1}{b_0^{1/2}}\right) + \frac{1}{3}\frac{1}{(\eta_{th} - 1)}\left(1 - \frac{1}{b_0^{3/2}}\right)\left(\frac{1}{\eta_{th}} - \frac{1}{\eta_i}\right)\sqrt{2I(1)}, \tag{2.35}$$

where b_0 and $I(1)$ are defined in Section 2.4. The integrated spectrum, N_{th} is a function of η_i only, and is plotted in Figure 2.3. A simple calculation shows that $N_{th} \propto (\eta_i - \eta_{th})^2$ just above threshold, so that the onset of turbulence is gradual as η_i increases above its threshold.

This calculation is valid in the regime $\eta_{th} = 0.95 \leq \eta_i \leq \eta_{th} + (1 + 1/\tau)L_n/L_s$, and $L_n/L_s \ll 1$. When η_i rises above this regime, $\gamma \ll \omega$ no longer holds, and Compton scattering decreases, and is replaced by mode coupling, enhanced by frequency broadening effects. Accompanying this transition is a rise in the saturated level of fluctuation, and χ_i increases to the level predicted by the strong turbulence theory of Ref. 16 (valid when $\eta_i \gg \eta_{th}$).

It is useful to note that the usual $\chi_i \simeq \gamma^l \Delta_x^2$ estimate predicts a χ_i that is too high by a factor of about $(L_s/L_n)^2$, and therefore doesn't apply to the present weak turbulence case. A more appropriate estimate, based on the quasilinear piece of Eq. (2.32), is

$$\chi_i \sim L_T k_y \Delta_x^2 \Omega_i \frac{1}{\eta_i - \eta_{th}} \frac{\gamma}{\omega}\left(\frac{e\tilde{\phi}}{T_i}\right)^2,$$

where the term $\eta_i - \eta_{th}$ cancels the corresponding term in γ (reflecting the fact that χ_i comes from the v^2 moment of $\mu(\vec{v})$, and not the v^0 moment, as does γ).

Using the estimate of $e\tilde{\phi}/T_i$ from Eq. (2.30), we get

$$\chi_i \sim \frac{\gamma^2}{\omega_{*_i}^2} \frac{1}{(k_\perp \rho_i)^6} \frac{\rho_i}{L_s} \Omega_i \rho_i^2.$$

This estimate follows from the orderings of the $\eta_i \sim \eta_{th}$ case, and hence is not as broadly applicable as the $\gamma/k_\perp^2$ estimate from strong turbulence.

2.6 Discussion

This chapter has explored the behaviour of the sheared slab η_i mode near the threshold of instability, applicable to the regime $\eta_{th} \leq \eta_i \lesssim \eta_{th} + (1+1/\tau) L_n/L_s$. Linear stability is determined by the balance of the ion temperature gradient drive and ion Landau damping. The unstable modes have $k_\perp \rho_i \simeq 1$ and $\gamma < \omega$ when η_i is in this regime. Thus, a weak turbulence expansion is applicable. Nonlinearly, the saturation amplitude is determined by the balance of linear growth and ion Compton scattering. This results in a spectrum peaked about $k_\perp \rho_i \simeq 1$ and with an amplitude that is of order $(L_n/L_s)^2$ relative to naïve extrapolation from the fluid regime. The resulting ion thermal conductivity, χ_i, is at a similarly low level. In experimental situations, this low level of χ_i near threshold is probably obscured by competing mechanisms such as neoclassical transport.

The significance of this work is that it gives insight into the regime of η_i turbulence that is applicable to experiments. Since χ_i in the threshold regime, is extremely low, we expect that the strong heating in modern tokamaks should easily drive η_i beyond this. For $\eta_i \gg \eta_{th}$, fluid theory predicts extremely large

χ_i, driving η_i down toward the threshold, even in the presence of strong ion heating.[22] Thus, it appears that the balance of ion heating and ion thermal conductivity results in an η_i in between these two extremes. The linear theory of this study indicates that there is an intermediate regime that differs from either extreme. The linear modes of this middle regime are characterized by a fluid-like interior, ion Landau damping at the edges, and $\gamma \gtrsim \omega$ (prohibiting a weak turbulence expansion). Modes with $l > 0$ become progressively destabilized in this regime, with their growth rate quickly surpassing that of the $l = 0$ mode. With these kinds of complications, developing a satisfactory analytical theory of this intermediate regime is quite a challenge. Short of such an analysis, one might assume on physical grounds that so long as linear ion resonances are important, then nonlinear ion resonances are also present, and the associated nonlinear Landau damping will maintain fluctuations at the low level indicated by this study. In this case, then large χ_i will occur only in the fluid regime, where resonances are negligible. Thus, the fluid predictions should determine the η_i transport relevant to experiments.

Of experimental interest, these results suggest that a steeper ion temperature profile will accompany effects that increase the weak/strong turbulence transition point, $\eta_{\rm th}^{\rm W} \simeq \eta_{\rm th} + (1 + T_i/T_e)L_n/L_s$. This might explain the improved confinement with increased T_i/T_e as observed on TFTR,[33] and with increased current ($\propto 1/L_s$) on many tokamaks.[34] Also, the broadening of the weak turbulence regime with increased L_n might be connected with the observation that

flat density profiles ($L_n \to \infty$) do not seem to worsen H mode confinement (even though a purely fluid η_i-mode theory indicates degraded χ_i, as shown in Chapter IVof this thesis). Of course, a reliable estimate of whether these effects are strong enough to influence observations would require use of a transport code that models χ_i in both the strong and weak turbulence regimes.

The results of this chapter suggest several possible directions for further study. Numerical solution of the integral equations (both linear and nonlinear) would be useful as a check of the analytical theory. Additional effects such as toroidal coupling[6] or trapped particles[35] could greatly alter the characteristics of the threshold regime, perhaps leading to more significant transport. Also, exploration of the regime that exists between the threshold and fluid regimes is clearly interesting. Finally, a weak turbulence analysis for flat density profiles would resolve whether the effects found in this chapter can account η_i transport during H modes.

Acknowledgements

I would like to thank M. N. Rosenbluth, P. W. Terry, and T. S. Hahm for useful conversations on the work in this chapter, and M. E. Glinsky for discussing the possibility of numerical solution of the integral equation.

This work was supported by the United States Department of Energy under Contract No. DE-FG05-80ET-53088, University of Texas, Austin, and under Grant No. DE-FG03-88ER-53275, University of California at San Diego.

CHAPTER III

MOMENTUM AND THERMAL TRANSPORT IN NEUTRAL-BEAM-HEATED TOKAMAKS

3.1 Introduction

For tokamaks to attain ignition, auxiliary heating is probably necessary. The most common means of auxiliary heating is by the tangential injection of an energetic beam of neutrals (NBI heating). Unfortunately, NBI heating generally results in the degradation of energy confinement time (τ_E) which decreases with increasing power so that the heating becomes less efficient the more it is applied.[19] Conventional wisdom explains the heat loss in terms of enhanced electron thermal conduction, but experimental results from D-III indicate that *ion* losses are of comparable importance.[1] Neoclassical predictions of ion conductivity (χ_i) are too low by about an order of magnitude. A good understanding of the ion loss mechanism is at present still developing.

Experimental clues to the nature of the ion conductivity are sparse, since direct ion temperature profile measurements have become possible only recently, with charge exchange spectroscopy. One commonly observed feature is that the confinement times of ion temperature (τ_i) and of the toroidal rotation rate (τ_φ) tend to behave alike, with similar scalings. This suggests that momentum transport arises from the same cause as the anomalous χ_i, and so a unified

description of the two processes is desirable. Further incentive for the study of momentum confinement comes from its inherent ability to isolate ion from electron dynamics less ambiguously than thermal studies, since momentum is carried almost exclusively by the ions.

Attempts to explain momentum loss rates by classical or neoclassical mechanisms appear insufficient to provide a complete description of experimental observations. Classical predictions ($\tau_\varphi^{-1} \sim \nu_{i,i}\rho_i^2/a^2$) are far too slow to agree with observed dissipation rates. The gyroviscous theory of Stacey and Sigmar[36,37] assumes a plasma rotation aligned with the magnetic field, and then argues that the subsequent deviation from solid body motion is damped at a rate governed by the classical *gyro*viscosity ($\tau_\varphi^{-1} \sim v_{th_i}^2/\Omega_i R^2$), which is more consistent with experimental observations. However, it has been noted by Connor et al.[38] that the strong *parallel* damping provided by the gyroviscosity leaves the plasma with a predominantly *toroidal* (rigid rotator) flow. Connor et al. then demonstrate that, excluding up-down asymmetries, etc., collisional damping of this flow is classical, again too slow to agree with experiment. Experimental departure from all *non*local theory predictions has been observed in recent experiments on TFTR,[39] which demonstrate *inward* diffusion of momentum deposited on the tokamak edge. A supplementary description of momentum transport, which accounts for this diffusive anomalous behaviour, is desirable.

The present work examines the possibility that ion temperature gradient driven turbulence (hereafter "η_i-turbulence") plays a substantial role in

determining both momentum and thermal transport in NBI plasmas. This mode is destabilized in plasmas with steep ion temperature profiles and relatively flat density profiles, such that $\eta_i \equiv d\ln T_i/d\ln n_0 > \eta_{ic} \simeq 1.5$. This theory has several distinct advantages. First, we should expect the value of η_i to be greatly affected by the NBI process, since the beam applies heat directly to the ions in a localized region of the plasma. Second, since the mode is essentially a parallel ion sound wave, with fluctuations in ion pressure (heat) and ion parallel velocity (momentum), it offers a good chance to explain a causal connection between the transport of these two quantities. Third, being a localized *micro*instability, the nature of the resulting turbulent momentum transport is inherently diffusive in nature. Fourth, its dependence on the temperature *profile* offers an immediate explanation for the observed decrease of momentum transport in TFTR when the heated region is changed from the plasma core to the edge.[39]

All of these suggest that η_i-turbulence is a good candidate for the cause of the anomalous transport in NBI plasmas. However, current theories of the η_i-instability do not include the effects of a radially sheared toroidal rotation, $dV_{i0}/dr \neq 0$, as introduced by the neutral beam. We find that it has two important effects. First, the sheared velocity field naturally facilitates prediction of the turbulent viscosity required to explain anomalous momentum transport. Second, it acts as an additional free energy source that enhances the existing ion-temperature-gradient turbulence level. Hence, one of our goals here is to improve the current theory of η_i-turbulence by incorporating these two aspects

of toroidal shear flow.

We shall assume the following about present-day NBI regimes. First, the incoming beam of neutrals is rapidly thermalized so that a one-fluid description of the ions is adequate. Second, the value of η_i should be sufficiently above η_{ic} that a fluid theory applies.[25] Finally, we assume that the rotation rate of the plasmas is below the sound speed $\left(V_0/c_s < 1\right)$, so that a shock wave is not excited.

In this chapter we examine the effects of a parallel velocity shear on η_i-turbulence, generalizing the results of Ref. 16. The principal results are the following:

1. The turbulent shear viscosity, calculated from $\chi_\varphi \equiv -\left\langle \tilde{v}_\varphi \tilde{v}_r \right\rangle \left(dV_\varphi/dr\right)^{-1}$, is given by:

$$\chi_\varphi = 3.3 \left[\frac{1+\eta_i}{\tau} + \left(\frac{L_n}{2c_s} \frac{dV_{i0}}{dr} \right)^2 \right]^2 \frac{\langle k_y \rho_s \rangle}{L_s} \rho_s^2 c_s,$$

for $\eta_i > \eta_{ic} \simeq 1$. Here $\langle k_y \rangle$ is the rms spectrum-averaged poloidal wavenumber, and $\langle k_y \rho_s \rangle \simeq 0.4$ may be taken from the non-shear-flow case[16] for the purpose of a rough estimate.

2. The ion thermal conductivity, χ_i, is found to equal the value of χ_φ given above, which is suggestive of experimental observation. This agrees with the basic scaling of Lee and Diamond[16] $\left(\chi_i \simeq \left[\left(1+\eta_i\right)/\tau\right]^2 \langle k_y \rangle / L_s\right)$.

The factor $\left(\frac{L_n}{2c_s}\frac{dV_{i0}}{dr}\right)^2$ (similar to the hydrodynamical Richardson number[40]) represents the role of the shear flow as a free energy source.

3. For dissipative trapped electron dynamics, a simple estimate shows that the electron heat conductivity due to η_i-turbulence is enhanced by the velocity shear:

$$\chi_e \simeq 10\epsilon^{3/2}\left[\frac{1+\eta_i}{\tau}+\left(\frac{L_n}{2c_s}\frac{dV_{i0}}{dr}\right)^2\right]^3\frac{\rho_s^2 c_s^2}{\nu_e L_s^2},$$

where ϵ is the inverse aspect ratio.

4. We demonstrate that the calculation of saturated turbulent diffusivity as an *eigenvalue* of the renormalized equations, as opposed to the more standard mixing-length method, takes far better account of the structure of the eigenmodes. Specifically, it is the *only* available method for accurately determining the saturation levels in the presence of multiple free energy sources, as here. Also, this technique allows resolution of purely numerical factors, like the coefficient of 3.3 above. Furthermore, it allows a prediction of the nonlinear frequency shift, which comes from the imaginary component of the diffusion eigenvalue.

The current theory is relevant in the regime $\eta_i > \eta_{ic} \simeq 1$, $V_0/c_s < 1$,

and $\frac{dV_0}{dr} < \frac{\tau c_s}{L_n}\left(\frac{1+\eta_i}{\tau}\right)^{3/2}$.

The remainder of the chapter is organized as follows. In Sec. II, the basic model is reviewed, and modifications due to the sheared flow are discussed. In Sec. III, the modified linear theory is presented. In Sec. IV, the one-point renormalization is performed, with subsequent solution for saturated turbulence levels. Section V contains calculations of transport coefficients. Section VI contains the summary and comparisons with various experiments.

3.2 Basic Model

To describe the nonlinear ion dynamics of a beam-heated tokamak, we shall adopt a simple one-fluid ion model.[1] In this model, we assume fluid ions and adiabatic electrons, and thereby the phase velocity regime $v_{th_i} \lesssim (\omega/k_\parallel) < v_{th_e}$. Also, we consider a sheared slab configuration, with all inhomogeneities in the radial ($\hat{x}$)-direction, which necessitates the macroscopic gradient ordering of $\eta_i > 1$ for consistency of a fluid treatment. Furthermore, for simplicity we shall take $L_n < L_s$ (i.e. $\eta_i < L_s/L_{T_i}$), although it is possible to construct a similar fluid slab theory with $L_n \gtrsim L_s$.

In sheared slab geometry, the magnetic field is $\vec{B} = B_0\left(\hat{z} + (x/L_s)\,\hat{y}\right)$, and so the parallel wavenumber is given by $k_\parallel = (x - x_s)\,k_y/L_s$ in the neighborhood of a mode rational surface x_s, where $\vec{k}\cdot\vec{B} = 0$. Since the background plasma is inhomogeneous in the x-direction only, perturbations have the form $\tilde{f}(x)\exp\left[-i\omega t + ik_y y + ik_z z\right]$.

Here, the primary modification to previous such models is the inclusion of a radially-dependent toroidal ion velocity, $V_\varphi(x)$ (alternately referred to as rotation velocity, toroidal momentum, and shear flow). We assume that the rotation velocity is subsonic ($V_\varphi/c_s < 1$), apparently consistent with regimes of current experimental interest,[41] but make no assumption yet as to the degree of velocity shear, $(L_V)^{-1} = d\ln V_\varphi/dr$, except that it be consistent with the fluid model, as verified *a posteriori*.

In the sheared slab model of a tokamak, the toroidal direction is given by $\hat{\varphi} = cos\alpha\hat{z} + sin\alpha\hat{y}$, where $\alpha = tan^{-1}(\epsilon_0/q_0)$ (i.e., the angle between $\hat{\varphi}$ and $\hat{b} = \vec{B}/|B|$ at x_s), and ϵ_0 and q_0 are the safety factor and the ratio of minor to major radius, each evaluated at the rational surface. Since $\epsilon_0/q_0 \ll 1$ then $\hat{\varphi}$, $\hat{z}$, and $\hat{b}$ are approximately parallel. The slight deviation between $\hat{b}$ and $\hat{\varphi}$ is crucial to the gyroviscous theory, but in the present case the distinction is much less important, since the primary mechanism of viscosity is temperature gradient driven fluctuations, and is insensitive to this small difference. The difference between the toroidal and parallel components of the velocity is small, since $V_{\|0} = V_\varphi B_\varphi/\sqrt{B_\varphi^2 + B_\theta^2} \simeq V_\varphi\left(1 - \frac{1}{2}\left(\frac{\epsilon_0}{q_0}\right)^2\right)$.

In this fluid model, the ion dynamics are described by the ion density, $n_i = \langle n_0\rangle + \tilde{n}_i(\vec{x},t)$, the ion parallel velocity, $v_{\|i} = \langle V_{\|0}\rangle + \tilde{v}_{\|i}(\vec{x},t)$, and the ion pressure, $P_i = \langle P_{i0}\rangle + \tilde{p}_i(\vec{x},t)$, where $\langle\ \ \rangle$ denotes an ensemble average. These quantities evolve according to the ion continuity equation, the parallel

momentum equation, and the equation of adiabatic pressure evolution

$$\frac{\partial n_i}{\partial t} + \nabla \cdot (n_i \vec{v}_{\perp i}) + \nabla_\parallel \left(n_i v_{\parallel i}\right) = 0 \tag{3.1}$$

$$m_i n_i \left(\frac{\partial v_{\parallel i}}{\partial t} + \left(\vec{v}_E + \vec{v}_{\parallel i}\right) \cdot \nabla v_{\parallel i} \right) = -e n_i \nabla_\parallel \Phi - \nabla_\parallel P_i + \mu_\parallel \nabla_\parallel^2 v_{\parallel i} \tag{3.2}$$

$$\frac{\partial P_i}{\partial t} + \left(\vec{v}_E + \vec{v}_{\parallel i}\right) \cdot \nabla P_i + \Gamma P_i \nabla_\parallel v_{\parallel i} = 0, \tag{3.3}$$

where Φ is the electrostatic potential, Γ is the ratio of specific heats, and $\mu_\parallel$ is the parallel viscosity (due to either Landau damping or collisional viscosity) required for saturation of the turbulence. (One might notice that neither $\nabla_\perp$ nor the gyroviscosity appear in the viscous term of Eq. (3.2), as a result of the gyroviscous cancellation on drift wave time scales.[42] As a result, the viscous term will not in itself be the result of much momentum transport, as noted in the introduction.) The perpendicular ion dynamics are due to $\vec{E} \times \vec{B}$, diamagnetic and, in next order, polarization drifts, where respectively,

$$\vec{v}_E = \frac{c}{B} \hat{b} \times \nabla \Phi$$

$$\vec{v}_{Di} = \frac{c}{e B n_i} \hat{b} \times \nabla P_i$$

$$\vec{v}_p = -\frac{c^2 m_i}{e B^2} \left(\frac{\partial}{\partial t} + \vec{v} \cdot \nabla \right) \nabla \Phi$$

Electron dynamics are assumed adiabatic, and the equations are closed with the quasineutrality condition

$$\tilde{n}_i = \tilde{n}_e = \langle n \rangle \frac{e\tilde{\Phi}}{T_e},$$

where $\Phi = \langle\Phi(x)\rangle + \tilde{\Phi}(\vec{x},t)$. The background radial electric field, generally present in beam-heated tokamaks,[43] is the by-product of a flow which deviates from the direction of $\vec{B}$, and obeys the radial force balance equation. In a slab model, a transformation to the toroidally co-moving frame (below), applied to the electromagnetic field, eliminates E_x from the equations.

To simplify Eqs. (3.1)–(3.3), we eliminate $\tilde{n}_i$ and $\vec{v}_\perp$, and make the assumption that the radial width of the fluctuations is much less than the scale length of any of the macroscopic gradients. To simplify notation, we rescale time and distance to units of Ω_i^{-1} and $\rho_s\ (= c_s/\Omega_i)$ respectively, and undimensionalize the remaining fields as $\tilde{\phi} = e\tilde{\Phi}/T_e$, $\tilde{v}_\parallel = \tilde{v}_{\parallel i}/c_s$, and $\tilde{p} = \left[\tilde{p}_i/\langle P_{i0}\rangle\right](T_i/T_e)$. This yields the following three equations in $\tilde{\phi}$, $\tilde{v}_\parallel$, and $\tilde{p}$

$$\left(\frac{\partial}{\partial t} + \vec{V}_0\cdot\nabla\right)(1-\nabla_\perp^2)\,\tilde{\phi} + v_D\left[1+\left(\frac{1+\eta_i}{\tau}\right)\nabla_\perp^2\right]\nabla_y\tilde{\phi} - \hat{b}\times\nabla\tilde{\phi}\cdot\nabla\left(\nabla_\perp^2\tilde{\phi}\right) + \nabla_\parallel\tilde{v}_\parallel = 0 \tag{3.4}$$

$$\left(\frac{\partial}{\partial t} + \vec{V}_0\cdot\nabla\right)\tilde{v}_\parallel - \frac{V_0}{L_V}\nabla_y\tilde{\phi} + \hat{b}\times\nabla\tilde{\phi}\cdot\nabla\tilde{v}_\parallel = -\nabla_\parallel\tilde{\phi} - \nabla_\parallel\tilde{p} + \mu\nabla_\parallel^2\tilde{v}_\parallel \tag{3.5}$$

$$\left(\frac{\partial}{\partial t} + \vec{V}_0\cdot\nabla\right)\tilde{p} + v_D\left(\frac{1+\eta_i}{\tau}\right)\nabla_y\tilde{\phi} + \hat{b}\times\nabla\tilde{\phi}\cdot\nabla\tilde{p} + \Upsilon\nabla_\parallel\tilde{v}_\parallel = 0, \tag{3.6}$$

where

$$\eta_i = \frac{d\ln T_i}{d\ln n} \qquad v_D = -\frac{d(\ln n_0)}{dx} \qquad L_V = \left(\frac{d\ln V_0}{dx}\right)^{-1}$$

$$V_0 = \langle V_\varphi\rangle/c_s \qquad \mu = \frac{\mu_\parallel\omega_{ci}}{c_s^2} \qquad \Upsilon = \frac{\Gamma}{\tau} \qquad \tau = \frac{T_e}{T_i},$$

and we have retained only the $\vec{E} \times \vec{B}$ nonlinearities, since others are of relative order $k_\parallel / k_y$ ($\ll 1$).

The shear flow V_0 has two effects on the η_i equations. First, it introduces a toroidal Doppler shift in all time derivatives, which we eliminate by performing a Galilean transformation in the $\hat{\varphi}$ direction to the co-moving frame. More importantly, the radial $\vec{E} \times \vec{B}$ convection of ion momentum, represented by the second term in Eq. (3.5), determines radial momentum transport. The fact that $\vec{E} \times \vec{B}$ motion also determines ion thermal transport, represented by the second term in Eq. (3.6), is the underlying reason for the eventual result that $\chi_i = \chi_\varphi$.

Finally, we note that the inclusion of toroidal ion momentum does not modify the nonlinear structure of Ref. 16, and so the energetics, renormalization, etc., are all quite similar. However, the fact that the shear flow provides an additional free energy source underlies our result that the inclusion of dV_0/dx effects *enhances* transport.

3.3 Linear Theory

The linear theory of the η_i-instability has been addressed by many authors, and we do not repeat all the basic details here. However, no one has considered the effects of a sheared toriodal ion flow on the η_i-mode, so we find it necessary to modify the basic linear theory to include this effect. Also, we shall consider the possibility that the sheared velocity field, acting as the *dominant* free energy source, might drive a pure shear-flow instability, as described in Ref. 44.

Linearizing Eqs. (3.4)–(3.6), Fourier transforming in the y and z directions, neglecting Υ (which gives corrections of order $(k_\parallel/k_y)^4$), and taking $k_\parallel = k_y x/L_s$, we obtain the following eigenmode equation

$$\frac{d^2\tilde{\phi}_{\vec{k}}}{dx^2} + Q(x,\Omega)\tilde{\phi}_{\vec{k}} = 0, \tag{3.7}$$

where the "potential" function is given by

$$Q(x,\Omega) = \left\{ -k_y^2 + \frac{1-\Omega}{\Omega+K} - \frac{J^{1/2}}{\Omega(\Omega+K)}sx + \frac{s^2x^2}{\Omega^2} \right\}, \tag{3.8}$$

and we have used the notation

$$\Omega = \frac{\omega}{k_y v_D}, \qquad s = \frac{L_n}{L_s} \ll 1, \qquad K = \frac{1+\eta_i}{\tau}, \qquad \text{and} \qquad J = \left(\frac{V_0 L_n}{L_V}\right)^2.$$

As will become apparent, K and J serve to parameterize the free energy content of the ion temperature gradient and the ion shear flow, respectively. The parameter J is analogous to the Richardson number, used to describe shear flows in classical fluid dynamics, here inverted for convenience. The difference is

that the bouyancy terms due to the gravitational effect on the density gradient (g/L_n) are replaced by drift frequency terms $(k_y^2 v_D^2)$, and adjusted to fit into the present scheme of parameter de-dimensionalization.

Equation (3.7) is a simple Weber's equation, and the lowest mode is given by

$$\tilde{\phi}_{\tilde{k}}(x) = \phi_0 \exp\left[-\frac{is}{\Omega}(x - x_0)^2\right], \tag{3.9}$$

where

$$x_0 = \frac{J^{1/2}}{2s}\frac{\Omega}{\Omega + K}, \tag{3.10}$$

with the dispersion relation:

$$\left(1 + k_y^2\right)\Omega^2 + \left[Kk_y^2 + is - 1\right]\Omega + isK = -\frac{J}{4}\frac{\Omega}{\Omega + K}. \tag{3.11}$$

The left-hand side of Eq. (3.11) is the standard dispersion relation for the slab η_i-mode,[6,10] and the right-hand side represents the modification due to shear flow. This equation describes three modes: the usual Pearlstein-Berk electron drift mode, the shear-flow modified η_i-mode, and also a shear-flow-driven instability. The drift mode is stable everywhere for adiabatic electrons; however, the last two of these are potentially more important, and hence are the focus of the rest of this section.

We first consider the η_i-instability. For the regime where the present fluid theory is applicable (discussed below) it suffices to solve for Ω by iteration,

assuming that the right-hand side of Eq. (3.11) is small. Neglecting the drift-wave root, a first order iteration gives the unstable η_i-root as

$$\Omega_{\eta_i} \cong \frac{isK}{1 - J/4K} \simeq is\left(K + \frac{J}{4}\right) \tag{3.12}$$

in the low-k_y regime (i.e., $k_y^2 \ll 1/K$).

From this simple analysis, we see that the shear flow has two effects on the η_i-mode. First, it enhances the growth rate at low k_y, with leading correction of order $J \sim \left(V_0/L_V\right)^2$. This enhancement is without regard to the sign of either V_0 or L_V. Second, we see from Eqs. (3.9)–(3.10) that the shear flow shifts the center of the mode away from the $x = 0$ rational surface. While this latter effect is not too important for regimes of current interest, it underlies a third effect that is not described by our simple fluid equations.

This third effect, which is apparent in the kinetic analogue of Eq. (3.7), is a cross term combining effects of shear flow and magnetic shear damping, and varies as $J^{1/2}x^3$ (see Appendix D). This effect is not represented in the fluid mode equation, Eq. (3.7), although it sets an upper limit on J for the model to be valid. We find that the best way to describe this limit involves a gyrokinetic analysis. Since this analysis is not germane to our central purpose, it is outlined in Appendix D. The upshot of this analysis is that in order for the cross-term to be unimportant, we must require

$$J^{1/2} \ll \left|\frac{\tau\Omega(\Omega + K)}{3sx_{\max}}\right|.$$

Using $\Omega \simeq isK$ and $x_{\max} \simeq x_T \simeq K^{1/2}$ (the WKB turning point), we find that $J^{1/2} \ll \frac{\tau}{3} K^{3/2}$. Beyond this limit, the simple quadratic well structure embodied by the fluid approximation is no longer valid, due to the disappearance of one of the WKB turning points. While the mode may still be *locally* unstable, the *eigenfunction* characteristics are drastically altered and require a more detailed description than that given here. Shooting code comparisons of Eqs. (3.7) and (D4) verify this result. Comparison of the above limit with the measurements of Isler et al.,[41] reveals that this restriction does not exclude present-day parameter regimes, where typically $J < 1$ and $K \sim 3 - 5$.

We next consider the question of whether or not there is a pure shear-flow-driven instability described by our equations. This is the mode which persists in the limit where the η_i driving force is turned off in Eq. (3.11). This mode is somewhat different from the classical Kelvin-Helmholtz instability, even though the free energy source is the same. The latter is essentially a two-dimensional mode and is restricted by the Rayleigh inflection point theorem to be localized about radii where $d^2V/dr^2 = 0$.[45] The present case has two significant differences. First, the line bending term, $\nabla_\parallel J_\parallel$, is present, which tends to stabilize the mode except at the outer edge of the torus. Second, parallel sound wave coupling (with magnetic shear) is retained, thereby localizing the mode and allowing it to be unstable on any rational surface. In this form, the shear-flow-driven instability is a more plausible explanation of microturbulence than the classical Kelvin-Helmholtz instability, since the former modes, if unstable,

are able to span the entire radial profile with small scale fluctuations without relying on the existence of inflection points.

A similar type of mode has been studied previously by Catto, Rosenbluth, and Liu,[44] who used the term "Kelvin-Helmholtz", although their analysis differs from the classical case in the same sense mentioned above. In their work unstable modes were found, which in various limits ($\eta_i \to 0$, $\tau \gg 1$, $L_n \to \infty \ldots$) seem to agree with the solution of Eq. (3.11). However, their study only addresses the limits $L_s \to \infty$ and then $L_n \to \infty$ individually, so that in both cases the potential is approximated as a simple quadratic in x. The more realistic case of a shear damped mode with moderate Richardson number is never addressed. Since a consistent treatment of this situation involves solution of a Schrödinger-like equation with a relatively complicated cubic potential (coming from the same effect that limits the validity of the η_i mode above), analytical results are difficult to obtain; however, it is possible to examine the situation numerically using a shooting code with the full kinetic potential, Eq. (D4). Our preliminary studies indicate no regime where the unstable shear-flow-driven modes predicted by the fluid theory persist in the more detailed kinetic analysis. The reason appears to be that if the Richardson number is above the threshold of instability predicted by the fluid theory ($J > 1$), the subsequent shift of the mode center is so large that the potential is drastically altered by terms of order x^3 and higher. However, we must stress that the above only implies that the pure shear-flow-driven instability is not well described by the fluid equations and the

particular geometry of the present simplified model. It is possible that toroidal effects, FLR effects, and so forth are present in a more realistic situation to give a strong shear flow instability.

3.4 Nonlinear Theory

Approximation of the one-point nonlinear η_i equations has been performed in Ref. 16, using DIA renormalization of the nonlinearities. Then, an augmented mixing-length scheme was used to estimate the saturated turbulence levels. In the following, we adopt a similar approach, but differ in two significant ways. First, the vorticity nonlinearity in the continuity equation is renormalized so as to include qualitatively the effects of the nonlinearly driven potential fluctuations, which are generally neglected. Second and more importantly, we improve upon the arguments used in Ref. 16 by following a method whereby the renormalized diffusivity is treated as an eigenvalue necessary for turbulent saturation.[46]

The following calculations are also valid in the zero-flow limit ($J \to 0$) and hence supercede the one-point results of Ref. 16.

a. Renormalization

Fourier transforming Eqs. (3.4)–(3).6 in y and z yields

$$\frac{\partial}{\partial t}\left(1-\nabla_\perp^2\right)\tilde{\phi}_{\vec{k}} + i\omega_{*e}\left(1+K\nabla_\perp^2\right)\tilde{\phi}_{\vec{k}} + ik_\parallel \tilde{v}_{\parallel\vec{k}} = -N_{\vec{k}}\left(\tilde{\phi}, \nabla_\perp^2\tilde{\phi}\right) \quad (3.13)$$

$$\frac{\partial}{\partial t}\tilde{v}_{\parallel\vec{k}} - \frac{V_0}{L_V}ik_y\tilde{\phi}_{\vec{k}} + ik_\parallel\tilde{\phi}_{\vec{k}} + ik_\parallel\tilde{p}_{\vec{k}} + \mu k_\parallel^2\tilde{v}_{\parallel\vec{k}} = N_{\vec{k}}\left(\tilde{\phi}, \tilde{v}_\parallel\right) \quad (3.14)$$

$$\frac{\partial}{\partial t}\tilde{p}_{\vec{k}} + iK\omega_{*e}\tilde{\phi}_{\vec{k}} + ik_\parallel\Upsilon\tilde{v}_{\vec{k}} = N_{\vec{k}}\left(\tilde{\phi}, \tilde{p}\right), \quad (3.15)$$

where the symmetrized nonlinear convolutions have the form

$$N_{\vec{k}}\left(\tilde{\phi},\tilde{f}\right) \equiv \left\{\frac{\partial}{\partial x}\left[\sum_{\vec{k}'}\left(-ik_y'\right)\tilde{\phi}_{-\vec{k}'}\tilde{f}_{\vec{k}''}\right] - ik_y\sum_{\vec{k}'}\frac{\partial\tilde{\phi}_{-\vec{k}'}}{\partial x'}\tilde{f}_{\vec{k}''}\right\} - \left\{\tilde{f}\leftrightarrow\tilde{\phi}\right\}, \tag{3.16}$$

where $\vec{k}$, $\vec{k}'$, and $\vec{k}''$ denote the "test," "background," and "driven" modes, respectively, such that $\vec{k}+\vec{k}'=\vec{k}''$. Using the standard weak coupling closure approximation to renormalize the nonlinearities, we iteratively substitute the nonlinearly driven fields $\tilde{\phi}^{(2)}_{\vec{k}''}$, $\left(\nabla_\perp^2\tilde{\phi}_{\vec{k}''}\right)^{(2)}$, $\tilde{v}^{(2)}_{\parallel\vec{k}''}$, and $\tilde{p}^{(2)}_{\vec{k}''}$ for the corresponding modal $\left(\vec{k}''\right)$ fluctuations. The superscript (2) denotes the "driven" fluctuation resulting from the direct beating of test and background modes. Hence,

$$\Delta\omega_{\vec{k}''}\left(1-\nabla_\perp^2\right)\tilde{\phi}^{(2)}_{\vec{k}''} + i\omega''_{*e}\left(1+K\nabla_\perp^2\right)\tilde{\phi}^{(2)}_{\vec{k}''} + ik''_\parallel\tilde{v}^{(2)}_{\parallel\vec{k}''} = -S\left(\nabla_\perp^2\tilde{\phi}\right) \tag{3.17}$$

$$\Delta\omega_{\vec{k}''}\tilde{v}^{(2)}_{\parallel\vec{k}''} - \frac{V_0}{L_V}ik''_y\tilde{\phi}^{(2)}_{\vec{k}''} + ik''_\parallel\tilde{\phi}^{(2)}_{\vec{k}''} + ik''_\parallel\tilde{v}^{(2)}_{\parallel\vec{k}''} = S(\tilde{v}) \tag{3.18}$$

$$\Delta\omega_{\vec{k}''}\tilde{p}^{(2)}_{\vec{k}''} + iK\omega''_{*e}\tilde{\phi}^{(2)}_{\vec{k}''} + ik''_\parallel\Upsilon\tilde{v}^{(2)}_{\vec{k}''} = S(\tilde{p}), \tag{3.19}$$

where the nonlinear sources are given by

$$S(\tilde{f}) = \left\{ik_y'\tilde{\phi}_{\vec{k}'}\frac{\partial}{\partial x}\tilde{f}_{\vec{k}} - ik_y\frac{\partial\tilde{\phi}_{\vec{k}}}{\partial x'}\tilde{f}_{\vec{k}} + ik_y\tilde{\phi}_{\vec{k}}\frac{\partial}{\partial x'}\tilde{f}_{\vec{k}'} - ik_y'\frac{\partial\tilde{\phi}_{\vec{k}}}{\partial x}\tilde{f}_{\vec{k}'}\right\}, \tag{3.20}$$

which will yield phase coherent terms when substituted into the nonlinearities. Here, $\Delta\omega_{\vec{k}''}$ may be regarded as the rate of decorrelation for three wave resonance.

At this point, we depart slightly from the previous renormalization of the η_i equations.[16,46] The standard procedure is to neglect the driven potential, $\tilde{\phi}^{(2)}_{\vec{k}''}$, completely, based on its smoothness relative to the other driven fields, and the fact that its direct inclusion renders the equations intractable. While this is probably adequate for the $\tilde{v}_{\|}$ and $\tilde{p}$ equations, the convective quantity of the continuity equation, $\nabla^2_{\perp}\tilde{\phi}$, has a simple and direct (linear) relation to the field that convects it, $\tilde{\phi}$. Therefore, it is not clear that the convection and the subsequent back-reaction of the convecting velocity are independent effects, as in the other equations.

Due to the mathematical difficulty of explicitly including the driven potential, $\tilde{\phi}^{(2)}_{\vec{k}''}$, it is better to express it in terms of $\left(\nabla^2_{\perp}\tilde{\phi}_{\vec{k}''}\right)^{(2)}$, which may be done via an "integration by parts" in the vorticity nonlinearity (i.e., Eq. (3.16) with $\tilde{f} \rightarrow \nabla^2_{\perp}\tilde{\phi}$) with respect to x. This latter operation is performed by noting that near the mode rational surface of $\vec{k}$, $k'_{\|} \simeq k''_{\|}$, and hence

$$\frac{\partial}{\partial x'} \simeq \frac{k'_y}{k''_y}\frac{\partial}{\partial x''},$$

which allows us to rewrite the vorticity nonlinearity as

$$N_{\vec{k}}\left(\tilde{\phi}, \nabla^2_{\perp}\tilde{\phi}\right) = \left[\frac{\partial}{\partial x}\sum_{\vec{k}'}(-ik_y)\,\frac{k_y^2 + 2k_y k'_y}{k''^2_y}\,\tilde{\phi}_{-\vec{k}'}\nabla^2_{\perp}\tilde{\phi}_{\vec{k}''}\right.$$
$$\left. -ik_y\sum_{\vec{k}'}\left(\frac{k_y^2 + 2k_y k'_y}{k''^2_y}\right)\frac{\partial\tilde{\phi}_{-\vec{k}'}}{\partial x'}\nabla^2_{\perp}\tilde{\phi}_{\vec{k}''}\right]. \tag{3.21}$$

However, since the η_i-mode has, to lowest order, incompressible mass flow ($\nabla\cdot(n\vec{v}) \simeq 0$), this amended renormalization of the vorticity nonlinearity will have only secondary importance relative to the final results.

Now that $N_{\vec{k}}\left(\tilde{\phi}, \nabla_\perp^2 \tilde{\phi}\right)$ can be expressed in terms of $\left(\nabla_\perp^2 \tilde{\phi}_{\vec{k}''}\right)^{(2)}$ alone, we can neglect $\tilde{\phi}^{(2)}_{\vec{k}''}$ in the remaining two nonlinearities, as usual. Furthermore, we neglect the terms in Eqs. (3.17)–(3.19) which vary as k_y''. Hence

$$\left(\nabla_\perp^2 \tilde{\phi}_{\vec{k}''}\right)^{(2)} \simeq \frac{S\left(\nabla_\perp^2 \tilde{\phi}\right)}{\Delta\omega_{\vec{k}''}} \tag{3.22}$$

$$\tilde{v}^{(2)}_{\parallel \vec{k}''} \simeq \frac{S\left(\tilde{v}_\parallel\right)}{\Delta\omega_{\vec{k}''}} \tag{3.23}$$

$$\tilde{p}^{(2)}_{\vec{k}''} \simeq \frac{S(\tilde{p})}{\Delta\omega_{\vec{k}''}}. \tag{3.24}$$

Substituting these for the $\tilde{f}_{\vec{k}''}$ in the nonlinearities yields

$$N_{\vec{k}}\left(\tilde{\phi}, \nabla_\perp^2 \tilde{\phi}\right) = \frac{\partial}{\partial x}\mu^{xx}_{\vec{k}}\frac{\partial}{\partial x}\nabla_\perp^2\tilde{\phi}_{\vec{k}} - k_y^2\mu^{yy}_{\vec{k}}\nabla_\perp^2\tilde{\phi}_{\vec{k}} + \frac{\partial}{\partial x}\beta^{xx}_{\vec{k}}\frac{\partial}{\partial x}\tilde{\phi}_{\vec{k}} - k_y^2\beta^{yy}_{\vec{k}}\tilde{\phi}_{\vec{k}} \tag{3.25}$$

$$N_{\vec{k}}\left(\tilde{\phi}, \tilde{v}_\parallel\right) = \frac{\partial}{\partial x}D^{xx}_{\vec{k}}\frac{\partial}{\partial x}\tilde{v}_{\parallel\vec{k}} - k_y^2 D^{yy}_{\vec{k}}\tilde{v}_{\parallel\vec{k}} \tag{3.26}$$

$$N_{\vec{k}}(\tilde{\phi}, \tilde{p}) = \frac{\partial}{\partial x}D^{xx}_{\vec{k}}\frac{\partial}{\partial x}\tilde{p}_{\vec{k}} - k_y^2 D^{yy}_{\vec{k}}\tilde{p}_{\vec{k}}, \tag{3.27}$$

where the various diffusion coefficients are given by

$$\mu^{xx}_{\vec{k}} \equiv \sum_{\vec{k}'} \frac{k_y^2}{\left(k_y''\right)^2}\frac{k_y'^2\left|\tilde{\phi}_{\vec{k}'}\right|^2}{\Delta\omega_{\vec{k}''}}$$

$$\mu^{yy}_{\vec{k}} \equiv \sum_{\vec{k}'} \frac{k_y^2}{\left(k_y''\right)^2}\frac{\left|\partial\tilde{\phi}_{\vec{k}'}/\partial x'\right|^2}{\Delta\omega_{\vec{k}''}}$$

$$\beta^{xx}_{\vec{k}} \equiv \sum_{\vec{k}'} \frac{k_y^2}{\left(k_y''\right)^2}\frac{k_y'^2\left|\nabla'_\perp\tilde{\phi}_{\vec{k}'}\right|^2}{\Delta\omega_{\vec{k}''}}$$

$$\beta_{\vec{k}}^{yy} \equiv \sum_{\vec{k}'} \frac{k_y^2}{\left(k_y''\right)^2} \frac{\left|\nabla_\perp' \partial \tilde{\phi}_{\vec{k}'}/\partial x'\right|^2}{\Delta\omega_{\vec{k}''}}$$

$$D_{\vec{k}}^{xx} \equiv \sum_{\vec{k}'} \frac{k_y'^2 \left|\tilde{\phi}_{\vec{k}'}\right|^2}{\Delta\omega_{\vec{k}''}}$$

$$D_{\vec{k}}^{yy} \equiv \sum_{\vec{k}'} \frac{\left|\partial \tilde{\phi}_{\vec{k}'}/\partial x'\right|^2}{\Delta\omega_{\vec{k}''}}.$$

We propose the following physical interpretations for the above renormalized nonlinearities. First, $D_{\vec{k}}^{xx}$ and $D_{\vec{k}}^{yy}$, which appear in both the momentum and pressure equations, act as non-Markovian turbulent diffusivities that scatter the $\tilde{v}$ and $\tilde{p}$ fluctuations radially, away from the rational surface. This is directly reflects the property that the unrenormalized nonlinearities couple incoming fluctuation energy from the low-k_y modes (bound and growing) to high k_y (which couple to radially outgoing waves), so that fluctuation energy is transported away from the mode rational surfaces in a diffusive manner (Appendix E).

In a similar way, $\mu_{\vec{k}}^{xx}$ and $\mu_{\vec{k}}^{yy}$ serve as nonlinear eddy diffusivities acting on the vorticity, $\nabla_\perp^2 \tilde{\phi}$, while $\beta_{\vec{k}}^{xx}$ and $\beta_{\vec{k}}^{yy}$ act as a turbulent back-reaction to $\mu_{\vec{k}}^{xx}$ and $\mu_{\vec{k}}^{yy}$, maintaining the property that $\tilde{\phi}$ ($\sim \tilde{n}$) not be convected by the $\vec{E} \times \vec{B}$ motion. The fact that μ and β vanish as $k_y \to 0$ may be readily demonstrated from the unrenormalized equation. This does not pose a problem for determining the low-k_y mode saturation level however, since energy cascading may proceed by linear coupling of $\tilde{\phi}$ to $\tilde{v}_\parallel$, which can then cascade via the mode coupling

represented by $D_{\vec{k}}$.

Finally, it is useful to estimate the relative magnitude of the various diffusivities in the $k_y^2 \ll \langle k_y^2 \rangle_{\rm rms}$ limit as

$$\mu_{\vec{k}}^{xx} \simeq \frac{k_y^2}{\langle k_y^2 \rangle_{\rm rms}} D_{\vec{k}}^{xx} \tag{3.28}$$

$$\beta_{\vec{k}}^{xx} \simeq \frac{k_y^2}{\langle k_y^2 \rangle_{\rm rms}} \frac{1}{(\Delta x)_{\rm rms}^2} D_{\vec{k}}^{xx} \tag{3.29}$$

with similar relations for $\mu_{\vec{k}}^{yy}$ and $\beta_{\vec{k}}^{yy}$. Here,

$$\langle k_y^2 \rangle_{\rm rms} \equiv \frac{\sum_{\vec{k}} k_y^2 \left| \tilde{\phi}_{\vec{k}} \right|^2}{\sum_{\vec{k}} \left| \tilde{\phi}_{\vec{k}} \right|^2} \qquad \text{and} \qquad \frac{1}{(\Delta x)_{\rm rms}^2} \equiv \frac{\sum_{\vec{k}} \left(\partial \tilde{\phi}_{\vec{k}} / \partial x \right)^2}{\sum_{\vec{k}} \left| \tilde{\phi}_{\vec{k}} \right|^2}.$$

Thus, while μ and β are small relative to D, and have little influence on thermal and momentum transport, we retain them because of their physical significance for the model used here. The rms quantities must remain as free parameters, since their evaluation requires a two-point, spectrum theory. However, for the purpose of estimation, we can use the result from Ref. 16 that $\langle k_y \rho_s \rangle_{\rm rms} \simeq 0.4$.

b. Solution at Saturated Turbulence

The renormalized equations may now be regarded as analagous to the linear equations, and the renormalized nonlinearities play the role of $\vec{k}$-dependent free parameters that account for transport of energy to and from various parts of $\vec{k}$-space. A one-point "closure" calculation may now be completed by considering only the lowest k_y part of the spectrum, which is almost purely growing, and

asking how large the renormalization quantities D, μ, and β must be in order to couple energy to smaller scales as fast as it is fed in by the instability mechanism.

The standard method for calculating saturation is the "mixing-length" scheme. While this method is useful for obtaining the correct scalings with certain key parameters, it is deficient in several regards. First, the condition for saturation is derived from "asymptotic balance" of certain parameters, while ignoring others. Such a procedure is inherently insensitive to the detailed phase and amplitude structure of the various modes at different $\vec{k}$, which may be important. Specifically, while some basic parameter scalings are determined, others are ignored completely. It is difficult or impossible to devise a more elaborate mixing-length scheme to incorporate the more subtle scalings. For example, in the present case of a system driven by two free energy sources (gradients), it is not clear how to use asymptotic balance of source and sink for an accurate determination of the relative contributions of η_i and the shear flow to the turbulent excitation. Second, the differential operators are approximated asymptotically using the turbulent mixing length, $\Delta_{\vec{k}}$, and the subsequent approximation of a differential equation as an algebraic equation leaves potentially large numerical factors unresolved. Finally, a consistent picture of turbulent saturation, one based on steady-state energetics, is never established. Using the current approach, such a picture is outlined in Appendix E. All of these deficiencies are corrected in the following "diffusion as eigenvalue" calculation. This technique makes no further assumption on the dynamics of the system, and applies

everywhere the fluid equations are valid.

Considering only the low-k_y portion of the spectrum (dominantly growing), we set $\partial/\partial t$ to zero in Eqs. (3.13)–(3.15). In this regime, we can also neglect $k_y^2 D_{\vec{k}}^{yy}$, $k_y^2 \mu_{\vec{k}}^{yy}$, $k_y^2 \beta_{\vec{k}}^{yy}$, $k_\parallel^2 \mu$, and $\Upsilon k_\parallel$, and let $\nabla_\perp^2 \simeq \partial^2/\partial x^2$. Then, Fourier transforming Eqs. (3.13)–(3.15) (with Eqs. (3.25)–(3.27) as the $N_{\vec{k}}$) in x and solving for $\tilde{\phi}_{\vec{k}}$ yields

$$\frac{1}{k_x^2}\frac{\partial}{\partial k_x}\frac{1}{k_x^2}\frac{\partial}{\partial k_x}\psi + \frac{D^{xx}L_s}{k_y}\frac{J^{1/2}}{K}\frac{1}{k_x^2}\frac{\partial}{\partial k_x}\left(\frac{\psi}{1+iD^{xx}k_x^2/K\omega_{*e}}\right) + \frac{\left(D^{xx}\right)^2 L_s^2}{k_y^2}\frac{1}{K}\left(\frac{1-\left(K-i\beta^{xx}/\omega_{*e}\right)k_x^2 - i\mu^{xx}k_x^4/\omega_{*e}}{1+iD^{xx}k_x^2/K\omega_{*e}}\right)\psi = 0, \tag{3.30}$$

where for convenience we have defined

$$\psi \equiv \left(1 - iK\omega_{*e}/D^{xx}k_x^2\right)\tilde{\phi}_{\vec{k}}.$$

We can reduce the number of parameters, and extract the basic mixing-length scalings of diffusion and mode width by defining $N = \left(L_s/K^2 k_y\right) D_{\vec{k}}^{xx}$, $M = \left(L_s/K^2 k_y\right)\mu_{\vec{k}}^{xx}$, $B = \left(L_s/K k_y\right)\beta_{\vec{k}}^{xx}$, $u = \sqrt{K}k_x$. This yields

$$\frac{1}{u^2}\frac{\partial}{\partial u}\frac{1}{u^2}\frac{\partial}{\partial u}\psi + N\left(\frac{J}{K}\right)^{1/2}\frac{1}{u^2}\frac{\partial}{\partial u}\left(\frac{\psi}{1-isNu^2}\right) + N^2\frac{1-(1+isB)u^2+isMu^4}{1-isNu^2}\psi = 0. \tag{3.31}$$

Cast in this form, it is clear that the resulting dispersion relation for N, M, and B will depend only on $s = L_n/L_s$ and J/K, so the mixing-length results somewhat succeed in resolving basic scalings.

Equation (3.31) may be manipulated into "Schrödinger form" as

$$\frac{\partial^2}{\partial z^2}\varphi + Q(z;N,M,B)\varphi = 0 \tag{3.32}$$

with

$$Q = \frac{N^2}{9}\left[\frac{1-(1+isB)|z|^{2/3}+isM|z|^{4/3}}{1-isN|z|^{2/3}} - \frac{J}{4K}\frac{1}{\left(1-isN|z|^{2/3}\right)^2}\right], \tag{3.33}$$

where

$$z \equiv u^3, \qquad \varphi \equiv \exp\left[\frac{NJ}{6K}\left(\frac{z}{1-isN|z|^{2/3}}\right)\right]\psi,$$

and we have noted that small mode width ($\Delta z \lesssim 1$, shown *a posteriori*) implies that

$$\frac{\partial}{\partial z}\left(\frac{\psi}{1-isN|z|^{2/3}}\right) \simeq \frac{1}{1-iNs|z|^{2/3}}\frac{\partial\psi}{\partial z}.$$

This approximation is only applied to the term which is dependent on J, so this "Schrödinger approximation" is exact in the limit of no shear flow, $J \to 0$.

The dispersion relation for Eq. (3.33) may be obtained by a WKB approximation, with the $z_T \simeq 1$ turning point (since $\Delta Z \lesssim 1$ implies a potential smooth relative to the mode). Using $s \ll 1$ as an ordering parameter, we find to order s

$$\int_{-z_T}^{z_T}[Q(z;N,M,B)]^{1/2}\,dz = N\left(1-\frac{J}{4K}\right)^2\frac{\pi}{8}\left[1+\frac{is}{4}(N+5M-6B)\right] = \frac{\pi}{2}. \tag{3.34}$$

That is,

$$N^2 is\left(1+\frac{5M}{N}-\frac{6B}{N}\right)+4N-\frac{16}{(1-J/4K)^2} = 0. \tag{3.35}$$

If we assume that M/N and B/N are independent of N, as with Eqs. (3.28) and (3.29), then we can solve Eq. (3.35) as a quadratic equation in N. The root that is dominantly *real* is, to order s,

$$N = \frac{4}{(1 - J/4K)^2}\left[1 - is\left(1 + \frac{5M}{N} - \frac{6B}{N}\right)\right]. \tag{3.36}$$

Restoring the parameter scalings and using the estimates in Eqs. (3.28) and (3.29) yields, for $J/4K \ll 1$,

$$D_{\vec{k}}^{xx} = 4\left(K + \frac{J}{4}\right)^2 \frac{k_y}{L_s}\left[1 - is\left(1 - \frac{k_y^2}{\langle k_y^2 \rangle_{\text{rms}}}\right)\right]. \tag{3.37}$$

This is the principal result of this nonlinear analysis.

The first thing to notice is that $D_{\vec{k}}^{xx}$ is dominantly *real*, the imaginary component being of order s. In the $J \to 0$ limit, the scaling agrees with the results of Ref. 16 (i.e., $D \sim K^2 k_y/L_s$) and importantly, we find that this result is enhanced by a numerical factor of 4 in this more accurate calculation. The shear flow, represented by J, further enhances the diffusion rate.

The imaginary part of D^{xx} is a nonlinearly induced frequency shift, and does not affect overall transport. It is interesting because it lends itself to a simple physical interpretation, as follows. From inspection of Eq. (3.37), one can see that this shift comes from two physical processes. First, nonlinear coupling to modes of different frequency produces the portion of $\text{Im}\,(D^{xx})$ that is independent of μ and β, i.e., which remains in the $k_y^2 \ll \langle k_y^2 \rangle_{\text{rms}}$ limit. Second, there is a part induced by nonzero eddy diffusivity, which contributes *only* to the imaginary part of D^{xx}. This is because transport of vorticity, which represents

momentum fluctuation with no net momentum content, will only affect the fluctuation frequency of the momentum, not its overall rate of diffusion. The latter is a good example of a process that may only be resolved by an *eigenvalue* solution for the turbulent diffusivity, in which the details of the *linear* energy exchange processes are accounted for.

Numerical analysis of Eq. (3.32) (shooting code) qualitatively confirm the WKB solution. Quantitatively, they show a factor of 3.3 in place of 4, which is constant for $s \lesssim 0.2$.

Finally, we should note that in Ref. 16 it was shown that consideration of spectrum broadening reveals that $D_{\vec{k}}^{xx}$ is enhanced by a factor of about $\left(\frac{\pi}{4} ln(R_e)\right)^2$, where R_e is the η_i-turbulence analogue of the Reynolds number. We expect that a spectrum analysis applied to the present case would show a similar enhancement. However, since this requires a two-point theory, we shall not address this issue here.

3.5 Transport

Having obtained the saturation level of turbulent diffusivity at long wavelength, where most of the turbulent transport takes place, we next apply this knowledge to finding the levels of turbulent viscosity χ_φ, the particle convection velocity, V_r, and the ion and electron thermal conductivities, χ_i and χ_e. This we do by replacing the nonlinear convection, $\hat{b} \times \nabla\tilde{\phi} \cdot \nabla$ in Eqs. (3.5)–(3).6, with the nonlinear decorrelation rate, $\Delta\omega_{\vec{k}''}$, taking $\partial/\partial t \to 0$ and solving. Neglecting Γ, which gives contributions of order s^2 (where $s = L_n/L_s$), we obtain:

$$\tilde{v}_{\parallel\vec{k}} = \left[\frac{V_\varphi}{L_V v_D}\frac{i\omega_{*e}}{\Delta\omega_{\vec{k}''}} + i\omega_{*e}\left(1 - \frac{iK\omega_{*e}}{\Delta\omega_{\vec{k}''}}\right)\frac{sx}{\Delta\omega_{\vec{k}''}}\right]\tilde{\phi}_{\vec{k}} \tag{3.38}$$

$$\tilde{p}_{\parallel\vec{k}} = -\frac{i\omega_{*e}}{\Delta\omega_{\vec{k}''}}K\tilde{\phi}_{\vec{k}}, \tag{3.39}$$

which allow various turbulent correlations to be placed in terms of $D_{\vec{k}}$.

The turbulent viscosity is calculated from the appropriate Reynolds stress:

$$\chi_\varphi\frac{dV_\varphi}{dr} = -\left\langle\tilde{v}_r\tilde{v}_\varphi\right\rangle \simeq -\sum_{\vec{k}'}\left\langle -ik'_y\tilde{\phi}_{\vec{k}'}\tilde{v}_{\parallel_{-\vec{k}'}}\right\rangle, \tag{3.40}$$

where the departure of $\tilde{v}_\varphi$ from $\tilde{v}_\parallel$ is of order $(\epsilon/q)^2$. Substituting Eq. (3.38) we note that the terms which vary as x average to terms proportional to the radial mode shift in Eqs. (3.9)-(3.10). Since the real part of this varies as s, these terms give a total contribution of relative order s^2 and we neglect them, obtaining:

$$\chi_\varphi\frac{dV_\varphi}{dr} = \frac{V_\varphi}{L_V}\sum_{\vec{k}'}\left\langle\frac{k'^2_y\left|\tilde{\phi}_{\vec{k}'}\right|^2}{\Delta\omega_{\vec{k}''}}\right\rangle + O\left(s^2\right) \simeq \frac{V_\varphi}{L_V}\left\langle D^{xx}_{\vec{k}}\right\rangle, \tag{3.41}$$

and hence the turbulent viscosity is

$$\chi_\varphi = 4\left(K + \frac{J}{4}\right)^2 \frac{\langle k_y \rangle_{\rm rms}}{L_s}, \tag{3.42}$$

where we have neglected $\mathrm{Im}\,(D^{xx})$, which does not contribute to transport. Redimensionalizing Eq. (3.42), using the numerical coefficient of 3.3 from the shooting code analysis, and taking $\langle k_y \rho_s \rangle_{\rm rms} \simeq 0.4$ from Ref. 16, we find

$$\chi_\varphi = 1.3\left[\frac{1+\eta_i}{\tau} + \left(\frac{V_\varphi L_n}{2c_s L_V}\right)^2\right]^2 \frac{\rho_s^2 c_s}{L_s}. \tag{3.43}$$

The above value of the rms wavenumber was derived in the $V_\varphi \to 0$ limit, and is probably slightly modified by the shear flow. Although calculation of this effect is beyond the scope of the present study, we expect that, as in Ref. 16, the dependence on the free energy strength will be weak.

For particle flux in the central region, the necessary phase shift between $\tilde{v}_{E_r}$ and $\tilde{n}_e$ (here adiabatic) is provided by dissipative trapped electron dynamics.[16] In this case, the perturbed trapped electron distribution is given by:[47]

$$\tilde{f}_e^T = \frac{eF_{Me}}{T_e}\left(\tilde{\Phi} - \frac{\omega - \omega_{*e}\left[1 + \eta_e\left(E/T_e - \frac{3}{2}\right)\right]}{\omega - \overline{\omega}_{De} + i\nu_{\mathrm{eff,e}}}\overline{\Phi}\right), \tag{3.44}$$

where $E = \frac{1}{2}mv^2$, $\overline{\omega}_{De}$ is the bounce average of the electron curvature drift frequency, $\nu_{\mathrm{eff,e}} = \nu_e/\epsilon$ is the effective electron collision frequency, and $\overline{\Phi}$ is the bounce average of the fluctuating potential. For the purpose of a simple estimate, we shall ignore the bounce average in the following. The particle flux

is then given by:

$$\Gamma_r^T = \langle \tilde{v}_r \tilde{n} \rangle \simeq n_0 \epsilon^{3/2} \frac{1 + \frac{3}{2}\eta_e}{L_n \nu_e} \sum_{\vec{k}'} \left\langle k_y'^2 \left| \tilde{\phi}_{\vec{k}'} \right|^2 \right\rangle \tag{3.45}$$

in the high-collisionality limit of the banana regime where $\nu_{\mathrm{eff,e}} \gg \omega, \overline{\omega}_{De}$. Using the approximation $\sum_{\vec{k}'} k_y'^2 \left| \tilde{\phi}_{\vec{k}'} \right|^2 \simeq \langle \gamma_{\vec{k}} D_{\vec{k}} \rangle \simeq 3.3 \left(K + \frac{J}{4}\right)^3 \langle k_y^2 \rho_s^2 \rangle / L_s^2$, and redimensionalizing, we find that the particle convection velocity is given by:

$$V_r = \Gamma_r^T / n_0 \simeq 0.5 \frac{\epsilon^{3/2}}{\nu_e L_n L_s^2} \left(1 + \frac{3}{2}\eta_e\right) \left(\frac{1 + \eta_i}{\tau} + \left(\frac{V_\varphi L_n}{2 c_s L_V} \right)^2 \right)^3 \rho_s^2 c_s^2. \tag{3.46}$$

The reader is cautioned that the approximations in this paragraph make the scalings and numerical coefficients for particle transport, as well as the electron thermal transport below, somewhat less quantitatively reliable than the χ_φ and χ_i calculations. For example, a full resolution of the ϵ dependence in Eq. (3.46) would require a theory that includes a treatment of toroidal effects on the η_i-turbulence level, which is not presented here. For low collisionality plasmas, the collisionless trapped electron response should be used in place of Eq. (3.44).

The radial flux of toriodal momentum is given by:

$$\begin{aligned} q_\varphi &= m_i \left\langle \tilde{v}_r \left(n_0 \tilde{v}_\varphi + \tilde{n} V_\varphi \right) \right\rangle \\ &= m_i n_0 \left(-\chi_\varphi \frac{dV_\varphi}{dr} + V_r V_\varphi \right), \end{aligned} \tag{3.47}$$

where χ_φ and V_r are given by Eqs. (3.42) and (46). The ratio of the viscous to convective terms is of order $\frac{\nu_{\mathrm{eff,e}}}{\epsilon^{1/2}\omega}$ ($\gg 1$), so we expect χ_φ, not V_r, to determine the momentum flux.

The ion thermal flux is calculated similarly to the viscosity[25], and using Eq. (3.39) we obtain:

$$q_i \equiv \langle \tilde{v}_r \tilde{p}_i \rangle = -(1+\eta_i) \sum_{\vec{k}'} \left\langle \frac{k_y'^2 \left| \tilde{\phi}_{\vec{k}'} \right|^2}{\Delta\omega_{\vec{k}''}} \right\rangle \tag{3.48}$$

with resulting ion thermal conductivity

$$\chi_i = 4 \left(K + \frac{J}{4} \right)^2 \frac{\langle k_y \rangle_{\rm rms}}{L_s} = \chi_\varphi, \tag{3.49}$$

and the redimensionalized form is given by Eq. (3.43).

The result that $\chi_i = \chi_\varphi$ is an important property of η_i-turbulence in the presence of a shear flow, and suggests a plausible explanation of experimental observations on TFTR[39], ISX-B[41], PDX[48], D-III[49], and other beam-heated tokamaks.

Following Ref. 16, we can crudely estimate the electron thermal conductivity (χ_e) associated with the trapped electron response to the turbulent potential fluctuations.[47] In the dissipative trapped electron regime ($\omega_{*e} < \nu_{\rm eff,e}$), we may estimate χ_e as:

$$\chi_e = \left\langle \frac{1}{2} m v^2 \left[\tilde{f}_e^T \tilde{v}_{Er} \right] \right\rangle^T \simeq 15\sqrt{2}\epsilon^{3/2} \frac{\rho_s^2 c_s^2}{\nu_e} \sum_{\vec{k}'} k_y'^2 \left| \frac{e\tilde{\phi}_{\vec{k}}}{T_e} \right|^2 . \tag{3.50}$$

The notation $\langle \ldots \rangle^T$ represents the velocity space average over trapped electrons. In the second part of Eq. (3.50), in addition to using the same approximations that led to Eq. (3.45), we have retained only the diffusive portion of the flux. Applying the same approximations that led to Eq. (3.46), we find:

$$\chi_e \simeq 10 \frac{\epsilon^{3/2}}{\nu_e L_s^2} \left[\frac{1+\eta_i}{\tau} + \left(\frac{V_\varphi L_n}{2 c_s L_V} \right)^2 \right]^3 \rho_s^2 c_s^2, \tag{3.51}$$

and thus χ_e is also enhanced by the sheared toroidal flow. The same caveats mentioned after Eq. (3.46) apply to the χ_e calculation.

3.6 Discussion

In this work, the effects of a subsonic, radially sheared toroidal ion flow on η_i-turbulence have been examined, in an effort to assess its role in neutral-beam-heated tokamaks. We have shown that the levels of fluctuation and turbulent transport increase with (an analogue of) the Richardson number, $J \equiv \left(\frac{L_n}{c_s}\frac{dV_{i0}}{dr}\right)^2$. We have demonstrated that there is significant diffusive momentum transport (viscosity) in the presence of η_i-turbulence, and that the momentum diffusivity and ion thermal diffusivity are the same, thereby providing a plausible explanation for the observation that momentum and thermal transport tend to behave similarly.

There is a striking correlation in the experimental literature, albeit mostly qualitative, between the application of stimuli which alter η_i and/or J, and the concomitant observation of a like change in momentum and/or thermal diffusivity. The well known degradation of χ_i with increasing beam power[19] is one example. As a possible explanation for this, it has been proposed[50,51] that the beam injection increases η_i, thus degrading χ_E via the anomalous χ_i, as well as the increased χ_e due to the dissipative trapped electron response to the enhanced potential fluctuations. As a second example, recent experiments on TFTR[39] compare beam center-heating with edge-heating (which reduces η_i).

During edge-heating, both χ_φ and the energy diffusivity are reduced by a factor of about 2. As a third example, a substantial decrease of χ_φ following beam turn-off is observed in TFTR,[39] PDX,[47] and ISX-B.[41] This might be explicable as the result of $T_i(r)$ and $V_\varphi(r)$ flattening (thereby reducing η_i and J) as the direct ion heating and shear flow excitation are terminated. Finally, the decrease of χ_i in TFTR "supershots"[52] accompanying balanced injection may possibly be connected with the concomitantly observed peaked density profiles, as well as the $V_\varphi \to 0$ turnoff of the Richardson number enhancement. However, care is required in interpreting supershot results, since the large density of high energy in this regime makes the applicability of our one-fluid ion model questionable.

The results of this chapter have indicated that shear flow enhanced η_i-turbulence is quite possibly an important factor in beam-heated tokamaks. However, the present model is a crude one, and there are several possible directions for further study. Among these are consideration of the effects of toroidicity, neoclassical damping of ion flows, the effects of an unthermalized beam, and further investigation into the possibility of the shear flow dominating the temperature gradient drive, and hence destabilizing a predominantly shear-flow-driven rather than η_i mode.

Acknowledgements

I would like to thank T. S. Hahm for improvements in the eigenvalue calculation, and M. Zarnstorff, R. J. Goldston, and F. W. Perkins for stimulating conversations regarding the work in this chapter. One of us (N. M.) would like to thank G. S. Lee for helpful advice during the initial stages of this work.

This research was supported by the United States Department of Energy under Contract No. DE-FG05-80ET-53088.

CHAPTER IV

ION TEMPERATURE GRADIENT DRIVEN TURBULENCE IN TOKAMAKS WITH FLAT DENSITY PROFILES

4.1 Introduction

One observation that seems to contradict the theory of ion temperature gradient driven turbulence ("η_i-turbulence" for short) as currently invoked is that D-III shows improved energy confinement ("H-modes") accompanying (among other changes) density profiles that are flat at the center of the tokamak, while the temperature profile apparently remains peaked.[34] Naïve application of the usual fluid η_i model[16] (for which the ion thermal diffusivity, χ_i, is proportional to $L_n \equiv \left(\frac{1}{n}\frac{dn}{dr}\right)^{-1}$), shows a trend toward *worse* confinement as the density profile is flattened (although the model is restricted to the regime $L_n < \sqrt{L_s L_T}$). Thus, there arises the question of why η_i mode transport doesn't destroy H-mode energy confinement for flat density plasmas.

A recent study[15] shows that when $L_n \to \infty$ the critical temperature scale length (proportional to L_n for peaked density profiles) becomes fixed at $L_T = \alpha R$, where R is the major radius and $\alpha \sim 0.1 - 0.4$. (We note that this is not a feature unique to the toroidal branch, and also occurs in the slab limit with L_s replacing R.) Qualitatively, this allows nonzero T_i gradients for flat density profiles, indicating that ITGDT might not be excited for these plasmas.

However, while it is not impossible that complete stabilization is the reason why the energy confinement doesn't degrade, it is not clear that the temperature scale length for these plasmas is on the order of the major radius, as required by the threshold. Therefore, it is desirable to know χ_i for the excited flat density gradient mode.

This study examines the strong turbulence and transport that comes from ITGDT in the flat density limit. For simplicity, we consider the slab limit, valid for a tokamak when $\hat{s}/q > 1$, where q is the tokamak safety factor and $\hat{s} = d\ln q/d\ln r$. In the slab limit, the mode is basically a parallel ion sound wave, and for $L_n < \sqrt{L_s L_T}$ radial convection along the density gradient balances sound wave compression (so that the the dynamics are characterized by incompressible mass flow to lowest order, *i.e.*, $\nabla \cdot (n\vec{v}) \simeq 0$). When the density profile becomes flat, mass compressibility becomes important as ω rises above ω_{*e}. This study addresses the changes in the nonlinear dynamics that result from this effect.

4.2 Basic Model and Linear Theory

The renormalized nonlinear equations below, Eqs. (4.1)-(4.3), are taken directly from Chapter III. They represent the ion continuity, ion parallel velocity, and ion pressure evolution equations:

$$\frac{\partial n_i}{\partial t} + \nabla \cdot (n_i \vec{v}_{\perp i}) + \nabla_\parallel (n_i v_{\parallel i}) = 0$$

$$m_i n_i \left(\frac{\partial v_{\parallel i}}{\partial t} + (\vec{v}_E + \vec{v}_{\parallel i}) \cdot \nabla v_{\parallel i} \right) = -e n_i \nabla_\parallel \Phi - \nabla_\parallel P_i + \mu_\parallel \nabla_\parallel^2 v_{\parallel i}$$

$$\frac{\partial P_i}{\partial t} + (\vec{v}_E + \vec{v}_{\parallel i}) \cdot \nabla P_i + \Gamma P_i \nabla_\parallel v_{\parallel i} = 0,$$

where Φ is the electrostatic potential, and Γ is the ratio of specific heats. Electrons are assumed adiabatic, $\tilde{n}_e = n_0 \frac{e\tilde{\phi}}{T_e}$, and the quasineutrality condition, $n_i = n_e$, is assumed. The perpendicular dynamics are due to $\vec{E} \times \vec{B}$, ion diamagnetic, and polarization drifts. Temporal and spatial scales are normalized to units of Ω_i^{-1} (inverse gyrofrequency) and $\rho_s = c_s/\Omega_i$, where c_s is the sound speed. A sheared slab model of the magnetic field is used, with $\vec{B} = B_0 (\hat{z} + (x/L_s)\, \hat{y})$, so that the parallel wave number is given by $k_\parallel = (x - x_s)\, k_y/L_s$ in the neighborhood of a rational surface, x_s. The dominant nonlinearities are $\vec{E} \times \vec{B}$ convection of parallel velocity, and pressure fluctuations, and are given in renormalized form on the right hand side of Eqs. (4.2)-(4.3), respectively. The vorticity nonlinearity in the continuity equation is small (of order $k_y^2/\langle k_y^2 \rangle$) for the low k_y regime considered here, as a result of a slight variation in the usual DIA renormalization procedure in which the back reaction of $\tilde{\phi}$ to $\vec{E} \times \vec{B}$ vorticity diffusion is

included. A derivation of these equations may be found in Chapter III, and the renormalization procedure is detailed in Ref. 46.

$$\frac{\partial}{\partial t}\left(1-\nabla_{\perp}^{2}\right)\tilde{\phi}+v_{D}\nabla_{y}\tilde{\phi}+v_{D}\left(\frac{1+\eta_{i}}{\tau}\right)\nabla_{\perp}^{2}\nabla_{y}\tilde{\phi}+\nabla_{\parallel}\tilde{v}_{\parallel}=0, \tag{4.1}$$

$$\frac{\partial}{\partial t}\tilde{v}_{\parallel}+\nabla_{\parallel}\tilde{\phi}+\nabla_{\parallel}\tilde{p}-\mu\nabla_{\parallel}^{2}\tilde{v}_{\parallel}=\frac{\partial}{\partial x}D_{\vec{k}}^{xx}\frac{\partial}{\partial x}\tilde{v}_{\parallel\vec{k}}-k_{y}^{2}D_{\vec{k}}^{yy}\tilde{v}_{\parallel\vec{k}}, \tag{4.2}$$

$$\frac{\partial}{\partial t}\tilde{p}+v_{D}\left(\frac{1+\eta_{i}}{\tau}\right)\nabla_{y}\tilde{\phi}+\frac{\Gamma}{\tau}\nabla_{\parallel}\tilde{v}_{\parallel}=\frac{\partial}{\partial x}D_{\vec{k}}^{xx}\frac{\partial}{\partial x}\tilde{p}_{\vec{k}}-k_{y}^{2}D_{\vec{k}}^{yy}\tilde{p}_{\vec{k}}, \tag{4.3}$$

where $\tilde{\phi}=e\tilde{\Phi}/T_{e}$, $\tilde{p}=\tilde{p}_{i}/\tau P_{i0}$, and

$$\eta_{i}=\frac{d\left(\ln T_{i}\right)}{d\left(\ln n_{0}\right)} \qquad v_{D}=-\frac{d\left(\ln n_{0}\right)}{dx} \qquad \mu=\frac{\mu_{\parallel}\Omega_{i}}{c_{s}^{2}} \qquad \tau=\frac{T_{e}}{T_{i}}.$$

The turbulent diffusion coefficients are given by

$$D_{\vec{k}}^{xx}\equiv\sum_{\vec{k}'}\frac{k_{y}'^{2}\left|\tilde{\phi}_{\vec{k}'}\right|^{2}}{-i\omega_{\vec{k}''}+\Delta\omega_{\vec{k}''}}, \tag{4.4}$$

$$D_{\vec{k}}^{yy}\equiv\sum_{\vec{k}'}\frac{\left|\partial\tilde{\phi}_{\vec{k}'}/\partial x'\right|^{2}}{-i\omega_{\vec{k}''}+\Delta\omega_{\vec{k}''}}. \tag{4.5}$$

The linear beat frequency, $\omega_{\vec{k}''}$, has been written explicitly in Eqs. (4.4) and (4.5) because in the flat density regime the real part of the frequency is comparable to the growth rate, as shown below.

There is only one change in all the above for the flat density limit, which is the vanishing of the drift term, $v_D \nabla_y \tilde{\phi}$, in Eq. (4.1). This term represents $\vec{E} \times \vec{B}$ convection along the density gradient, and is important in the lowest order dynamics of the (finite L_n) η_i-mode since it allows $\nabla_\parallel \tilde{v}_\parallel$ to be nonzero while maintaining incompressible mass flow (i. e., $\nabla \cdot (n\vec{v}) \simeq 0$). Without the density gradient, $\partial \tilde{n}/\partial t$ assumes this role, mass incompressibility no longer holds, and the theory must be reformulated.

Linearizing Eqs. (4.1)-(4.3), Fourier transforming in y, z, and t, with $k_\parallel = k_y x/L_s$, taking the drift term in Eq. (4.1) to zero, and solving for $\tilde{\phi}$, we obtain the following mode equation:

$$\frac{d^2 \tilde{\phi}_{\vec{k}}}{dx^2} + Q(x,\omega)\tilde{\phi}_{\vec{k}} = 0, \tag{4.6}$$

where the "potential" function is given by

$$Q(x,\omega) = \left\{ -k_y^2 - \frac{\omega}{\omega + \omega_*^T} + \frac{k_y^2 x^2}{L_s^2 \left(\omega^2 - \frac{\Gamma}{\tau} \frac{k_y^2 x^2}{L_s^2} \right)} \right\}, \tag{4.7}$$

where $\omega_*^T = -k_y/\tau L_T$ (in dimensionless units).

Neglecting the term that varies as Γ (which gives corrections of order $\sqrt{L_T/L_s}$), then Eq. (4.6) is the usual Weber's equation, with solution given by the Hermite functions, and yields the following dispersion relation:

$$(1 + k_y^2) \left(\frac{\omega}{\omega_*^T} \right)^2 + \left(k_y^2 + i\,(2l+1)\,\frac{\tau L_T}{L_s} \right) \left(\frac{\omega}{\omega_*^T} \right) + i\,(2l+1)\,\frac{\tau L_T}{L_s} = 0, \tag{4.8}$$

where l is a positive integer. For the regime $k_y^2 \lesssim \tau L_T/L_s$ ($\ll 1$) and $l < L_s/\tau L_T$, the roots are, approximately,

$$\omega \simeq \pm \left(\frac{1-i}{\sqrt{2}}\right)(2l+1)^{\frac{1}{2}}\left(\frac{\tau L_T}{L_s}\right)^{\frac{1}{2}}\omega_*^T, \tag{4.9}$$

of which one root is unstable. It is important to notice that here $Re(\omega) \simeq Im(\omega)$, whereas for the finite density gradient case, a purely growing portion of the spectrum exists at low k_y, where $\omega \simeq i\frac{L_n}{L_s}\frac{1+\eta_i}{\tau}\omega_{*e}$. Physically this difference is due to the introduction of mass compression into the basic dynamics, an effect also present in the turbulent regime, which influences construction of the nonlinear theory.

The width of the mode may be found by taking the x^2 moment of the Hermite functions, and is, in the low l and low k_y-regime,

$$(\Delta x)^2 \simeq \frac{1+i}{\sqrt{2}}(2l+1)^{3/2}\left(\frac{L_s}{\tau L_T}\right)^{1/2}. \tag{4.10}$$

Despite the imaginary component of Δx, the mode remains a bound state since $Im(\Delta x) < Re(\Delta x)$.

We have numerically compared the above fluid results with the more complete kinetic theory by using a shooting code with a potential derived from the ion gyrokinetic equation, similar to that used in Appendix D. This analysis is tedious, and not presented here, but the basic result is that fluid and kinetic theory agree at least as well in the flat density limit as in the usual finite L_n regime. The neglect of ion resonances requires that

$$\frac{k_\parallel v_i}{\omega} \simeq (2l+1)^{1/4}\left(\frac{L_T}{L_s}\right)^{1/4} \ll 1,$$

or $\frac{L_s}{L_T} \gg 2l+1$, which may be interpreted to mean that the temperature gradient must be well above threshold for a fluid theory to apply.

In Ref. 15 it was demonstrated that compression of the ion diamagnetic drift (where $\nabla \cdot \vec{v}_D \simeq [\hat{b} \times (\hat{b} \cdot \nabla)\hat{b}] \cdot \vec{k}_\perp \tilde{p} \simeq k_y \tilde{p}/R$, in undimensional units, where R is the major radius), which is neglected here, can have a stabilizing effect on the mode. However, this study also neglected the parallel sound wave dynamics, which is clearly the destabilization mechanism in the slab limit. A comparison of these terms in the present ordering shows:

$$\frac{\nabla_\perp \cdot \tilde{v}_D}{\nabla_\parallel \tilde{v}_\parallel} \simeq \left(\frac{L_s}{R}\right)^{\frac{1}{2}} = \frac{q}{\hat{s}}.$$

Thus, perpendicular compression is important in the weak shear limit where $q/\hat{s} > 1$ (*i.e.*, the toroidal limit), whereas for strong shear (the slab limit) it is replaced by parallel compression.

A mixing length estimate of the turbulent diffusion rate produces:

$$D^{xx}_{\vec{k}} \simeq \gamma_{\vec{k}} (\Delta x)^2_{\vec{k}} \simeq (2l+1)^2 \frac{\omega^T_*}{2}. \tag{4.11}$$

The absence of L_s in this estimate is a result of the dual role of the shear, which both destabilizes the mode (which enhances D^{xx}), and localizes it (which decreases D^{xx}), with net cancellation.

4.3 Nonlinear Theory

In this section, we seek to improve upon the mixing length estimate given above by use of a technique of solving for the renormalized diffusions as an *eigenvalue* of the system of differential equations, as explained in Chapter III. This has the advantage of being a fully analytical method, capable in principle of taking account of the full dynamics of the system. By comparison, the usual mixing length scheme, which employs such heuristic concepts as "asymptotic balance" to estimate scalings with various key terms, is inherently limited in its ability to resolve the more subtle details. The basic scheme here is to set the linear growth rate, $Im(\omega)$, to zero at saturation, and solve in its place an eigenvalue problem for D (henceforth D will denote $D_{\vec{k}}^{xx}$). This yields the level of turbulent energy diffusion (which in k_y space is a cascade) necessary to shut off the growth. In this study, we use this technique to analyze whether the renormalized nonlinear dynamics produce any modification over the mixing length estimate, as can occur in other cases.[9]

This approach was carried out successfully for the case of finite density gradient η_i-turbulence. In that work, it was possible to drop all of the time derivative at saturation, since in the low k_y regime considered it represents growth only. However, in the flat density case $Re(\omega)$ assumes the important role of balancing parallel compression in the continuity equation. This compression (which vanishes as k_y) will persist in the saturated state, and cannot be balanced by any of the nonlinearities in Eq. (4.1) (which vanish as k_y^2 or faster, which is

also a property of the *un*renormalized $\vec{E} \times \vec{B}$ vorticity nonlinearity), in the $k_y \rightarrow 0$ limit. Thus, for large wavelength (the limit of interest in this one-point, transport theory), it is essential to retain $Re\,(\omega)$ to balance compression in the continuity equation.

Thus, the analytical method proceeds as follows: restricting consideration to the low k_y portion of the spectrum (which is responsible both for energy feed and for transport), we solve Eqs. (4.1)-(4.3) for $\tilde{\phi}$ retaining both ω *and* the renormalized diffusivities. The resulting differential equation is then manipulated into "Schrödinger" form, and a WKB approximation produces a complex dispersion relation for D. The other "eigenvalue" $Re\,(\omega)$, remains at its linear value, since any nonlinear frequency modifications are contained in $Im\,(D)$.

Proceeding along these lines, we Fourier transform Eqs. (4.1)-(4.3) in t, y, z, *and* x and solve for $\tilde{\phi}$, neglecting terms which vary as k_y^2 and higher. This results in the following second order differential equation:

$$\left(\frac{1}{\omega + iDk_x^2}\frac{\partial}{\partial k_x}\right)^2 \psi + \frac{L_s^2}{k_y^2}\frac{\omega + \left(\omega_*^T + \omega\right)k_x^2}{\omega_*^T + \omega + iDk_x^2}\psi = 0 \qquad (4.12)$$

where,

$$\psi = \frac{\omega_*^T + \omega + iDk_x^2}{\omega + iDk_x^2}\tilde{\phi}.$$

Applying the WKB phase quantization approximation to this equation produces:

$$i\left(\omega_*^T + \omega\right)^{\frac{1}{2}}\frac{L_s}{k_y}\int_{-k_T}^{k_T}\frac{\omega + iDk_x^2}{\left(\omega_*^T + \omega + iDk_x^2\right)^{\frac{1}{2}}}\left(k_T^2 - k_x^2\right)^{\frac{1}{2}}dk_x = \frac{\pi}{2}\left(2l+1\right), \quad (4.13)$$

where,

$$k_T^2 = -\frac{\omega}{\omega_*^T + \omega}.$$

The choice of k_T as the turning point recovers all the characteristics of the linear mode in the $D \to 0$ limit, which demonstrates that this branch is the nonlinear extension of the linear theory. Expanding the denominator of the integrand to order k_x^2 and integrating, yields the following dispersion relation:

$$-i\left(\omega_*^T+\omega\right)+\frac{D}{4}\left(1-\frac{1}{2}\frac{\omega}{\omega_*^T+\omega}\right)=(2l+1)\,\frac{k_y}{L_s}\left(\frac{\omega_*^T+\omega}{\omega}\right)^2. \qquad (4.14)$$

In the saturated state, the growth is shut off, so only the real part of ω remains, which is given by Eq. (4.9). Solution of Eq. (4.14) then yields:

$$D=8\omega_*^T\frac{\left(1-s_l^{\frac{1}{2}}\right)^3}{1-s_l^{\frac{1}{2}}}\left(1-\frac{i}{2}\frac{1}{1-s_l^{\frac{1}{2}}}\right), \qquad (4.15)$$

where $s_l=(l+1/2)\,\frac{\tau L_T}{L_s}$, and $\frac{\tau L_T}{L_s}\ll 1$. The basic scaling, $D\sim\omega_*^T$, agrees with the mixing length estimate, Eq. (4.11). However, there is a discrepancy of $(2l+1)^2$, missing in Eq. (4.15). Possibly, this is a consequence of Eq. (4.15) being calculated in k_x space (which leads to $D_{\rm eig}\simeq\Delta\omega_{\vec{k}''}/\left(\Delta k_x\right)^2$), while the linear estimate uses a mode width calculated in x-space (so that $D_{\rm ML}\simeq\Delta\omega_{\vec{k}''}\left(\Delta x\right)^2$). While it is true that $\Delta x\simeq 1/\Delta k_x$ for the $l=0$ mode, one can easily show that for the higher l Hermite functions this must be generalized to $\Delta k\simeq(l+1/2)/\Delta x$. This could account for the discrepancy between Eq. (4.11) and Eq. (4.15). Physically, one might expect that it is the mode width in x-space that determines the step length in the random walk, and hence the radial diffusion. On this basis, one would expect the mixing length estimate of Eq. (4.11) to yield the correct l scaling. However, in light of the ambiguity, we shall consider only the diffusivity

of the $l = 0$ mode, using this for rough comparison with the transport of the finite L_n case as described in Ref. 16 (which also considers only the $l = 0$ case).

4.4 Transport

Having obtained the saturation level of turbulent diffusivity at long wavelength, where most of the turbulent transport takes place, we next apply this knowledge to finding the saturation levels of ion and electron thermal conductivities, χ_i and χ_e, and the particle convection velocity, V_r. This is best done using the unrenormalized equations, and the basic technique and formulas are given in Ref. 16 and Chapter III. Since these formulas do not change in the $L_n \to \infty$ limit, here we only apply, and do not rederive, them.

The ion thermal flux is calculated from the correlation between ion pressure fluctuations and radial velocity fluctuations, which yields:

$$q_i = -\frac{T_i}{L_T} \left\langle D_{\vec{k}} \right\rangle ,$$

with resulting ion thermal conductivity:

$$\chi_i = \left\langle D_{\vec{k}} \right\rangle \simeq 2 \frac{\langle k_y \rho_s \rangle_{\rm rms}}{\tau L_T} \rho_s^2 c_s . \tag{4.16}$$

Evaluation of $\langle k_y \rho_s \rangle_{\rm rms}$ would require solving a two-point spectrum equation, which is beyond the scope of the present study.

The electron thermal conductivity (χ_e) is derived from the trapped electron response to the turbulent potential fluctuations in the dissipative trapped

electron regime[47] ($\omega_{*e} < \nu_{\mathrm{eff,e}}$). Here, χ_e is estimated as:

$$\chi_e = 15\sqrt{2}\epsilon^{3/2}\frac{\rho_s^2 c_s^2}{\nu_e}\sum_{\vec{k}'}\left\langle k_y'^2\left|\frac{e\tilde{\phi}_{\vec{k}'}}{T_e}\right|^2\right\rangle.$$

Using the approximation $\sum_{\vec{k}'} k_y'^2\left|\frac{e\tilde{\phi}_{\vec{k}'}}{T_e}\right|^2 \simeq \langle\Delta\omega_{\vec{k}'}D_{\vec{k}'}\rangle \simeq \left\langle D_{\vec{k}'}^2/\Delta x_{\vec{k}'}^2\right\rangle$, we find:

$$\chi_e \simeq 85\frac{\epsilon^{3/2}}{\nu_e}\left(\frac{\tau L_T}{L_s}\right)^{\frac{1}{2}}\frac{\langle k_y^2\rho_s^2\rangle}{(\tau L_{T_i})^2}\rho_s^2 c_s^2, \tag{4.17}$$

where ϵ is the inverse aspect ratio and ν_e is the electron collisionality.

For particle flux in the central region, the necessary phase shift between $\tilde{v}_{E_r}$ and $\tilde{n}_e$ (here adiabatic) is also provided by dissipative trapped electron dynamics.[47] In the flat density limit, the flux is:

$$\Gamma_r = \langle\tilde{v}_r\tilde{n}\rangle \simeq \frac{3}{2}\frac{n_0\epsilon^{3/2}}{\nu_e L_{T_e}}\sum_{\vec{k}'}\left\langle k_y'^2\left|\frac{e\tilde{\phi}_{\vec{k}'}}{T_e}\right|^2\right\rangle$$

in the high-collisionality limit of the banana regime where $\nu_{\mathrm{eff,e}} \gg \omega, \overline{\omega}_{De}$. Redimensionalizing, and applying the same approximation that led to Eq. (4.17), we find that the particle convection velocity is given by:

$$V_r = \Gamma_r/n_0 \simeq 6\frac{\epsilon^{3/2}}{\nu_e}\left(\frac{\tau L_T}{L_s}\right)^{\frac{1}{2}}\frac{\langle k_y^2\rho_s^2\rangle}{L_{T_e}(\tau L_{T_i})^2}\rho_s^3 c_s^2. \tag{4.18)}$$

This represents a purely outward particle flux, although for different collisionality regimes the flux can be inward.[53]

4.5 Discussion

This chapter has examined the behaviour of ion temperature gradient driven turbulence in the presence of a flat density profile. This has entailed the development of a renormalized one-point turbulence theory applicable to the case where $\gamma \sim \omega_r$. The turbulence level and subsequent transport reach a plateau for $L_n > \sqrt{L_T L_s}$, and roughly speaking, the present results may be obtained from the finite density gradient results by replacing L_n with $\sqrt{L_s L_T}$. The thermal transport of this regime is larger than that for finite density gradients (which is already large enough to yield greatly degraded confinement), and hence we conclude that straightforward application of the usual fluid η_i transport does not explain why the energy confinement of H-modes on D-III is not degraded. The threshold effects invoked in Ref. 15 show that the critical temperature scale length is comparable to the major radius, but it is not clear that the degree of temperature flatness necesary for full stabilization is actually obtained.

A possible alternative explanation for H-mode behaviour might be based on two results from the examination in Chapter II of the weak turbulence regime which exists near the threshold. First, in the regime $\eta_i \lesssim \eta_{\rm th} + (1+T_i/T_e)L_n/L_s$ then $\gamma \ll \omega_r$ and the instability saturates at a weak turbulence level. Second, χ_i in this regime is greatly reduced from a naïve extrapolation of the strong turbulence level. Thus, the limit of large L_n can extend the regime of weak turbulence, and one might expect an increased distance between the allowable temperature gradient and the threshold value. However, this weak turbulence

work is restricted to the regime $L_n \ll L_s$, so that the broadening of the weak turbulence regime with L_n is only a trend. A study of weak turbulence in the flat density limit will be undertaken in the future.

Acknowledgements

I would like to thank Paul Terry for several useful discussions. This research was supported by the United States Department of Energy under Grant No. DE-FG05-80ET-53088, University of Texas, Austin, and under Grant No. DE-FG03-88ER-53275, University of California, San Diego. One of us (P. H. D.) would like to acknowledge support from an Alfred P. Sloan Fellowship.

CHAPTER V

CONCLUSIONS

In this section, I will summarize the impact of this work in a broader sense than in the preceding chapters, and give my own thoughts on directions for future study. Many of the comments made in this section are quite speculative, and reflect the opinions of myself alone.

5.1 Summary

This thesis has been a compilation of three studies of ion temperature gradient driven turbulence ("η_i-turbulence" for short) in limits not considered previously, and as a result have furthered understanding of anomalous transport in plasmas. Further than this, however, some of the techniques employed in this paper have been rather innovative, and I hope that this work has helped advance the understanding of plasma turbulence theory in general.

The direct relevance of this thesis to magnetic fusion experiments may be summarized as follows. First, Chapter III has shown that the ion thermal confinement and momentum transport due to η_i turbulence are the same. This fact lends itself to a number of useful inferences. For example, recent divertor experiments on D-III have indicated that the momentum confinement time equals the *total energy* confinement time;[5] this implies that electron thermal losses are small in those discharges. Second, Chapter II has shown that the *transport*

threshold (i.e., where χ_i becomes relevant to experiments) is the point where wave-ion resonances become negligible, which is not the same as the linear instability threshold. This validates the applicability of fluid-like η_i-mode theory[16] to experiments (by allowing the ion temperature profile to steepen into the fluid regime). Furthermore, one might expect a steeper ion temperature gradient accompanying effects that broaden the weak turbulence zone, which may appear as an enhanced energy confinement time. The boundary between weak and strong turbulence occurs for $\eta_i \simeq \eta_{th} + (1 + T_i/T_e)\frac{L_n}{L_s}$, which could possibly account for the observations of improved confinement in the cases of increasing T_i/T_e,[54] flatter densities[34] and higher current[55] (which decreases L_s). As it happens, none of these effects are explained by the usual theory that considers only the $l = 0$ radial eigenmodes in the fluid limit.[16]

The main theoretical contributions to knowledge of η_i turbulence are as follows. Chapter II is the first analytical study of the linear and nonlinear behaviour of the instability near threshold. Here, the most important insight is that nonlinear Landau damping becomes the dominant saturation mechanism in this limit, and holds the turbulence level and transport to low levels. Chapter III has shown that the temperature gradient can "combine" with a toroidal momentum gradient, each contributing free energy to the instability, and transporting both quantities at the same rate. Chapter IV has shown that a fluid theory will predict large transport when the density becomes flattened. It has also explored the effects of compressibility on the saturated turbulent state, and

demonstrated the proper way of accounting for this effect.

Several techniques developed in this thesis may be useful beyond their application to η_i modes. The most significant of these has been the development of the eigenvalue technique of calculating one-point diffusion coefficients for strong turbulence (in the nonlinear theory sections of Chapters III and IV). Although this technique was originally introduced by Carreras *et al.*[46] in order to resolve numerical coefficients, in this work we have clearly demonstrated that it has uses beyond this. It is clearly superior to the other available analytical methods, which are asymptotic balance[7,16] (which are inherently unable to consider more than the grossest details of the dynamics) and dimensional analysis techniques[56,57,58] (which are limited to simple situations, and also do nothing to resolve dynamics). The diffusion-as-eigenvalue calculations in this work have provided several results that could not have been resolved by either of these. First, when there are two free energy sources feeding the instability, as in Chapter III, the eigenvelue calculation is the only way to take both of them into account properly. Second, this method can be applied when there are multiple renormalized turbulent diffusivities appearing (although these must be reduced in approximate fashion to only one diffusivity), as in the case of μ, β, and D used in the calculation of Chapter III. Finally, this method can yield an expression for the nonlinear frequency shift, (appearing as the imaginary part of D), which can be quite important in the basic dynamics of the saturated state, as in Chapter IV. Certainly, there are further uses for this diffusion-as-eigenvalue

technique, which in principle is capable of accounting for any effect described by the renormalized one-point equations.

Other techniques introduced here may also be useful beyond this study. Section 4.3 introduced a technique of incorporating the real part of the frequency, ω_r, into the nonlinearly saturated dynamics. (Previous theories, generally applied to cases where $\omega_r \ll \gamma$, neglect all of $\omega_r + i\gamma$ for the saturated state.) Finally, Section 2.3 has introduced a method of calculating the linear growth rate locally and averaging over a normal mode to find the growth of the mode. This can lend great simplification to calculating the linear growth rate, and applies to cases where $\gamma \ll \omega_r$.

5.2 Further Directions

As is the case when any progress is made, this work has produced as many questions as it has answers, and here I will list some problems that I feel would make useful future study.

The results of the threshold study in Chapter II suggest that the true "threshold" for transport is the point where nonlinear Landau damping becomes negligible. However, there is no good way to estimate where this point is, beyond a loose connection with the vanishing of linear Landau damping when $\eta_i \gg 1$. What is needed for better resolution of this is a kinetic strong turbulence theory (*i.e.*, one that can describe resonances). Short of this, it may be possible to use existing particle codes, which give good agreement with the fluid regime results

for $\eta_i \gg 1$.[59] By tracing η_i downward toward the threshold, one could find where there is significant departure from the strong turbulence mixing length estimate, and nonlinear wave-ion resonances become important. This point could be taken as the value of η_i where the *transport threshold* occurs.

There is still no definitive explanation as to why tokamaks show improved energy confinement with increased current. The basic slab model, which retains only the $l = 0$ radial eigenmode, shows $\chi_i \propto L_s^{-1}$, which apparently contradicts this experimental result. Several schemes have been proposed to remedy this, including global transport models, finite-β effects on electron thermal conductivity, $q(a)$ dependence of L_{T_i},[60] and effects due to higher l eigenmodes.[13] Of these, all but the last call into question the premise that anomalous η_i transport comes from enhanced χ_i over some "confinement zone" by invoking secondary effects such as nonlocality of transport, interdependence of plasma parameters, or an energy confinement that depends on χ_i for some scalings and χ_e for others. Although it may turn out that these kinds of secondary effects are inevitable, they greatly diminish the predictive power of any theoretical transport model which relies on them, since such arguments can lead ambiguously in a number of directions. (Indeed, if the presence of such effects means that one is not to believe the L_s scaling of χ_i, how much faith can one have in the L_T or L_n?) Before invoking a more ambiguous model, one should exhaust the possibility of finding a local transport model with the correct current scaling for χ_i, and several indications make it seem too early to preclude this. First, the work of

Ref. 13 indicates that simply considering the $l > 0$ modes could produce the correct current scaling. These results are promising, but more work is required for a complete model. Among the important effects that need to be considered are Landau damping (which gives a maximally unstable l differing markedly from the fluid prediction, as noted in Ref. 13 and described analytically in Appendix A here) and nonlinear coupling of the radial eigenmodes. Second, the weak turbulence theory indicates that with higher current (*i.e.*, decreased L_s), the steady state T_i profile (from the balance of heating and transport) can steepen further above the threshold level. I feel it is possible to construct a theory that accounts both for this effect and for Landau damping of the $l > 0$ modes, which are closely related. Although these are rather difficult to handle analytically in an exact way, simplification could be gained from $\gamma\Delta_x^2$ estimates that use the stable radius derived from local kinetic theory[23] for the mixing length (since this width will be closely related to the maximally instable l), or from a continuous l approximation (similar to the continuous m and n approximations of Section 2.4). Finally, a valuable experimental clue could be gleaned from measuring the current scaling of the frequency of the broadband turbulence observed in infrared scattering experiments[3] This measurement, combined with $\chi_i \simeq \gamma\Delta_x^2$ and the crude estimate that γ has L_s dependence similar to ω_r, would indicate how much of the disparity of current scaling comes from frequency effects and how much comes from mode width effects.

The question remains of what is happening with η_i turbulence during

H-modes on D-III-D with flat density profiles. It is becoming clear that the improved confinement has more to do with edge effects than η_i modes[60,61] but the question remains of why the η_i confinement doesn't degrade enormously for flat density profiles. One possible solution worthy of investigation is the broadening of the weak turbulence zone accompanying increased L_n. This trend is observed for the $L_n < L_s$ regime examined in Chapter II, but a detailed analysis of the linear and weak turbulence behaviour of the flat density regime is necessary.

At present, there is no clearcut way to distinguish experimentally between the toroidal and slab limits of the instability. Theoretically, the former transforms into the latter for higher shear,[11] so that either limit is possible on any given tokamak, but the magnetic shear profile is not known accurately enough to determine which regime is appropriate. One approach is to look for predictive differences arising from the fact that the toroidal limit has a ballooning mode structure, while the slab limit is a sound wave. One such possibility is the momentum/energy confinement similarity shown for the slab branch in Chapter III here. Since this results from the correlation of momentum and heat fluctuations inherent to sound waves, then one might expect this property to be altered in the toroidal limit, where sonic character vanishes. A theoretical analysis of momentum transport for the toroidal branch would be useful.

Further experimental verification that momentum is transported by the η_i mode could be provided by combining tangential beam heating with some

non-directional ion heating source, such as ICRH. An experimental correlation between rotation velocity and nondirectional power level would strengthen the case for temperature profiles being the cause of momentum transport.

I believe that it is possible to devise a more complete derivation of the eigenvalue calculation, based on the transport and nonlinear fluctuation equations. As it stands, the calculation is based on the intuitive physical notion that the ultimate sink of the turbulence energy is related to transport. That the various nonlinear diffusions are combined as one term is justifiable by noting that they all have the same net effect of carrying energy from the linear source to the sink at a different radius, and that the details of the intermediate processes are not important so long as the rate determining step is the linear instability; that is, the level of turbulent diffusion will adjust itself so that it carries away energy as fast as it is supplied. A consistently ordered formulation of this intuitive argument would lend it better credence.

In astrophysical accretion disks the question of turbulent angular momentum transport is central to understanding disk luminosity, and the approach of Chapter III has shown promise[62] One possible scenario is that unstable vertical convection instability couples to the angular momentum gradient, providing symmetry breaking and transport similar to that of η_i modes. Preliminary findings from local theory indicate that the convection instability can couple with the shear flow, modifying the growth rate so as to favor waves with positive angular momentum content relative to the disk. This gives turbulent spectrum

with a favored sense of angular momentum, and thus providing transport and an effective turbulent viscosity. Further investigation of the linear modes and the nonlinear coupling mechanism is needed before the viscosity can be resolved.

APPENDICES

Appendix A: Stability of Higher Radial Eigenmodes

In Section 2.3, we obtained the growth rate of the $l = 0$ mode by averaging the local growth rate over the normal mode. Here, we apply this technique to the $l > 0$ modes. These are broader, and experience more Landau damping away from the rational surface; this underlies the result that the stability threshold increases sharply with l.

Averaging the local growth rate in Eq. (2.9), with $k_\parallel = k_y x/L_s$, over the modes given by Eq. (2.11), and using the mode width given by Eq. (2.13), we find

$$\gamma_{k_y,l} = \sqrt{2}\,\omega_{*i} s(2l+1)\frac{\Delta_x^{l=0}}{\rho_i} \times \left[I_l^{[3/2]} \frac{1}{\eta_i}\left(\frac{\eta_i}{\eta_c} - 1\right) - \frac{3}{2} I_l^{[5/2]} (2l+1)^2 \left(\frac{\Delta_x^{l=0}}{\rho_i}\right)^2 \frac{p(p-1)}{\eta_i^2} s^2 \right] \quad \text{(A1)}$$

where

$$I_l^{[r]} = \frac{\sqrt{\pi}\, 2^l\, F(-l,-l;-l+r;\frac{1}{2})}{2\, l!\, \Gamma(-l+r)}, \qquad p = \frac{1+1/\tau}{\Gamma_0},$$

$$\Delta_x^{l=0} = (1-\Gamma_1/\Gamma_0)^{1/2}\rho_i, \qquad s = \frac{L_n}{L_s}, \qquad \Gamma_n = e^{-b} I_n(b),$$

F is a hypergoemetric function, and Γ is the gamma function (not to be confused with Γ_n). The first several $I_l^{[r]}$ are listed in Table 1. In deriving Eq. (A1), we have assumed that $2l + 1 < \eta_i/s$, so that the exponential in $\gamma_{\bar{k}}(k_\parallel)$ may be

neglected relative to the exponential in Eq. (2.11). For $l = 0$, Eq. (A1) reduces to Eq. (2.14).

Setting $\gamma_{k_y,l}$ to zero and solving for the $\eta_i > 0$ branch yields the stability threshold for the higher radial eigenmodes

$$\eta_c^l = \eta_c \left[\frac{1}{2} + \left(\frac{1}{4} + C_l \frac{(1 - \Gamma_1/\Gamma_0)p(p-1)}{\eta_c} s^2 \right)^{1/2} \right], \tag{A2}$$

where $C_l = \frac{3}{2}(2l+1)^2 I_l^{[5/2]}/I_l^{[3/2]}$. The basic threshold, η_c, is modified by the term which varies as C_l. The modification is of order $s^2 \ll 1$, and is extremely small for the $l = 0$ mode; however, the coefficient is a rapidly increasing function of l, which raises the threshold significantly for $l > 0$ (see Table 1 and Fig. A1). This higher threshold agrees with the shooting code results of Ref. 13. They are also consistent with the kinetic shooting code result[16] that for weaker shear (*i.e.*, smaller s) a larger number of eigenmodes are unstable.

Once η_i rises above the threshold for the higher l modes, the growth rate increases rapidly, so that above the threshold regime these modes dominate the transport.[16] However, it should be noted that η_i must be significantly greater than 1 for a large number of the higher l modes to be in the fluid regime. This is unlikely in light of the strong thermal transport they cause. Thus, we can expect that at most, only the first few radial eigenmodes are relevant to tokamak regimes.

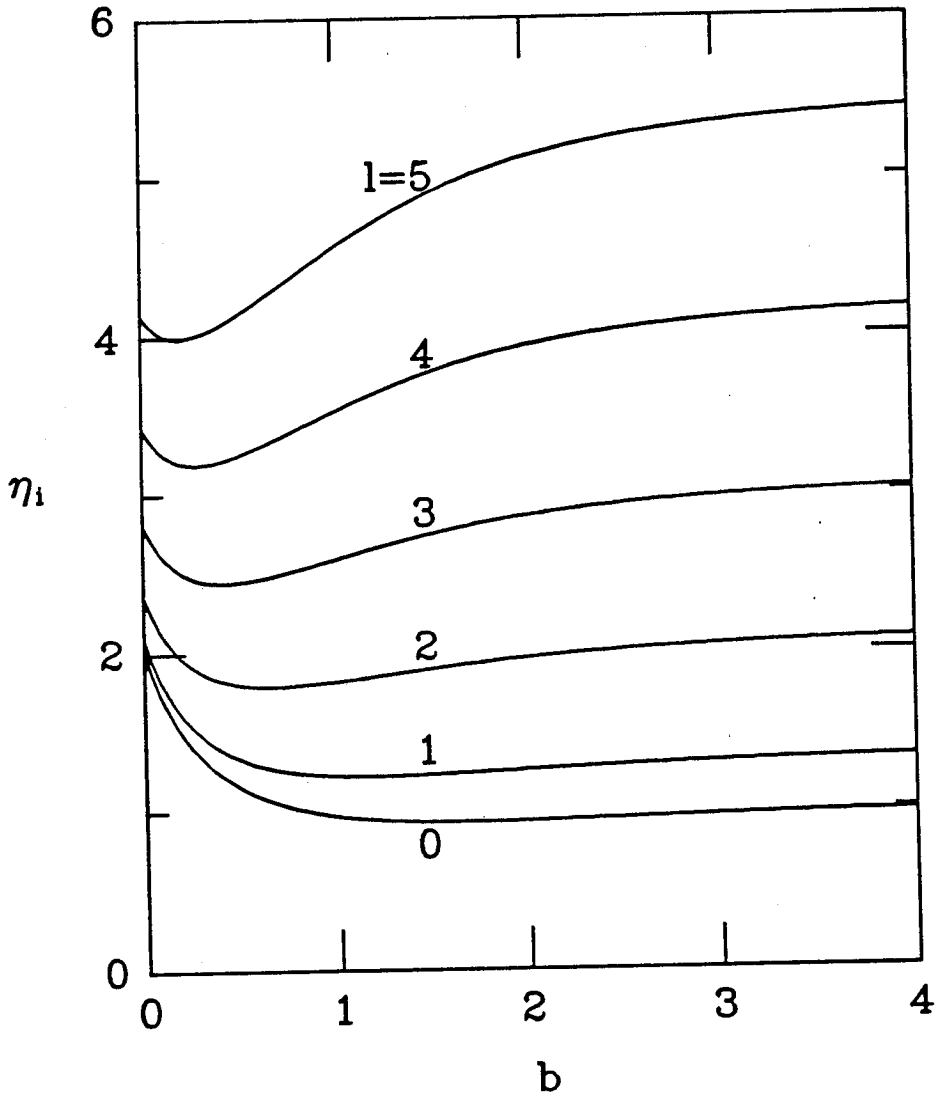

FIGURE A1: Stability threshold for higher radial eigenmodes, with $L_n/L_s = 0.05$ and $\tau = 1$.

l	$I_l^{[3/2]}$	$I_l^{[5/2]}$	C_l
0	1	2/3	1
1	2	8/3	18
2	5/2	17/3	85
3	3	28/3	228.7
4	27/8	163/12	489
5	15/4	55/3	887.3
6	65/16	565/24	1469

Table 1: Functions used in Eqs. (A1) and (A2).

Appendix B: Stability of Flat Density Modes

Here, we use the technique of Section 2.3 to calculate stability in the limit $1 \ll L_n/L_s \to \infty$ (formerly assumed small). This may be considered either as the limit of flat density, or as stabilization coming from increased shear. In this limit, the dielectric function of Eq. (2.5) becomes

$$\epsilon_{\tilde{k}}(\omega) = 1 + 1/\tau - \frac{\omega_*^T}{\omega}\Gamma_0\zeta^2 + \frac{\omega_*^T}{\omega}\left(\frac{1}{\eta_c} - \zeta^2 + \frac{\omega}{\omega_*^T}\right)\Gamma_0\zeta Z(\zeta), \qquad \text{(B1)}$$

where $\omega_*^T = k_y\rho_i^2\Omega_i/L_{T_i}$. Treated locally using the $\gamma = \frac{-\epsilon''}{(\partial\epsilon'/\partial\omega)}$ approximation as before, with $k_\parallel$, this yields

$$\gamma_{\tilde{k}}(x) = \sqrt{2\pi}\omega_*^T\frac{L_T}{L_s}\frac{|x|}{\rho_i}\left[\frac{1}{\eta_c} - 2p(p-1)\left(\frac{L_T}{L_s}\right)^2\left(\frac{x}{\rho_i}\right)^2\right]\exp\left[-2\left(\frac{L_T}{L_s}\frac{x}{\rho_i}\right)^2\right]. \qquad \text{(B2)}$$

Arguing as after Eq. (2.9) gives the result that only for $(L_s/L_T)^2 \to 0$ is $\gamma(x)$ stable for all x. Thus, locally there is instability for all values of L_T. However, from our quasi-local point of view, $\gamma(x)$ must be positive over a wide enough

region to give a net positive energy input to the mode. The normal modes in this regime are described, as in the $L_n/L_s \ll 1$ theory, by Eqs. (2.11)-(2.13) (the first three terms of Eqs. (2.5) and (B1) are the same, and the rest are subdominant in both threshold regimes). Averaging $\gamma(x)$ over the $l = 0$ mode produces

$$\gamma_{\vec{k}} = \sqrt{2}\frac{L_T}{L_s}\omega_*^T \frac{\Delta_x}{(\rho_i^2 + (\Delta_x p L_T/L_s)^2)^{1/2}} \left[\frac{1}{\eta_c} - \frac{2p(p-1)}{\Delta_x^2/\rho_i^2}\frac{L_T^2}{L_s^2} - 2p^3(p-1)\frac{L_T^4}{L_s^4}\right]. \tag{B3}$$

This shows that the threshold for ∇T_i is given by

$$\left(\frac{L_s}{L_T}\right)_c^2 = \eta_c \frac{p(p-1)}{\Delta_x^2/\rho_i^2}\left[1 + \left(1 + \frac{2(\Delta_x/\rho_i)^4 p}{\eta_c(p-1)}\right)^{1/2}\right]. \tag{B4}$$

For $b = 0$, then $(L_s/L_T)_c$ is about $\sqrt{2(1+\tau)/\tau^2}$, and increases rapidly with b, as show in Figure A2. Thus, it appears that modes with $b \ll 1$ are the most relevant to the flat density regime.

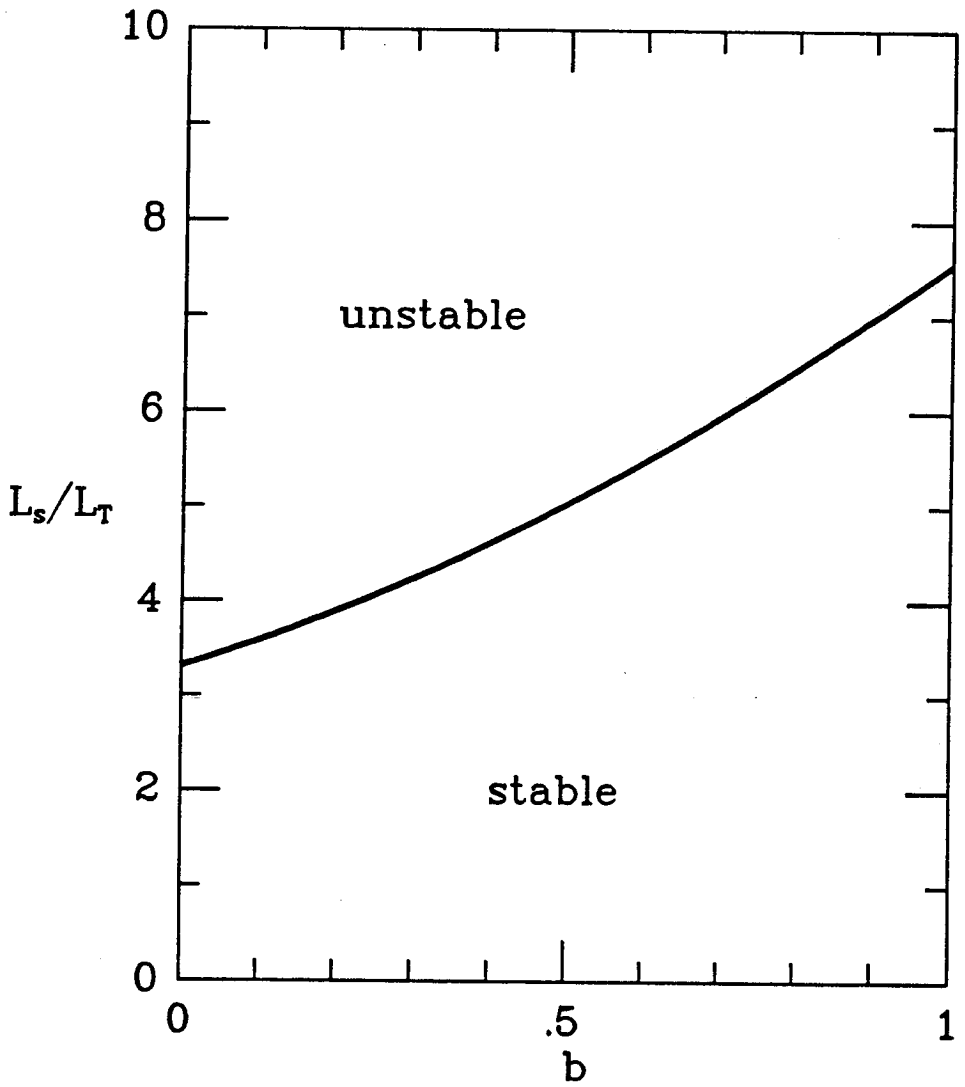

FIGURE A2: Stability threshold for flat density profiles, with $\tau = 1$

Appendix C: Normalization of the Expanded Spectrum

This Appendix demonstrates that the step of expanding $S(k'_y)$ under the integral (as in going from Eq. (2.24) to Eq. (2.25)) must be accompanied by a normalization of the integral. Here, we show this when $S(k'_y)$ is a gaussian, and assume on intuitive grounds that this holds for more general shapes of S.

Letting $S(k') = e^{-k'^2/\Delta_S^2}$ and $K(k'') = k'' e^{-k''^2/\Delta_K^2}$ (which is the form of the kernel in Eq. (2.25)), then it is easy to show that the exact integral is

$$\int_{-\infty}^{\infty} S(k')K(k'')dk' = \frac{\Delta_S \Delta_K^3}{(\Delta_S^2 + \Delta_K^2}\sqrt{\pi}k \exp\left[-k^2/(\Delta_S^2 + \Delta_K^2)\right]. \qquad \text{(C1)}$$

Now, if $S(k')$ is Taylor expanded about k, where $k = k' + k''$, then the integral is

$$\int_{-\infty}^{\infty} \left[S(k) - k''\frac{dS}{dk} + \frac{k''^2}{2}\frac{d^2S}{dk^2}\right] K(k'')dk' = \frac{\Delta_K^3}{\Delta_S^2}\sqrt{\pi}k \exp\left[-k^2/\Delta_S^2\right]. \qquad \text{(C2)}$$

In the limit where $\Delta_K \ll \Delta_S$, for which such an expansion is fully consistent, then Eqs. (C1) and (C2) are the same. However, in our case, $\Delta_K \gg \Delta_S$, so that Eq. (C2) must be multiplied by $(\Delta_S/\Delta_K)^3 \exp\left[-k^2\left(\frac{\Delta_K^2 - \Delta_S^2}{\Delta_K^2 \Delta_S^2}\right)\right]$ to agree with the correct answer. The exponential part of this normalization is of order 1 for modes in the spectrum (*i.e.*, those for which $k \lesssim \Delta_S$), as well as an artifact of the gaussian shape of S, so we ignore it. (In comparing this derivation with the normalization used in Section 2.4, one should keep in mind that the width of $k''K$ varies as Δ_K^3, and the width of SK varies as Δ_S^3.)

Appendix D: Kinetic Limit of the Linear Fluid Equations

Here, we explore the limit of validity of the fluid equations by examining the ion gyrokinetic theory[24] for geometry and gradients similar to the preceding fluid model. A Maxwellian velocity distribution shifted by $V_{\varphi 0}(x)$ in the $\hat{\varphi}$-direction is assumed. This yields the following perturbed phase space ion distribution:

$$\tilde{f}_i(\vec{k};v_\perp,v_\parallel) = F_M\left(\vec{v}-V_{\parallel 0}\hat{b}\right)\left\{1-\frac{J_0^2\left(k_\perp v_\perp/\Omega_i\right)}{\omega-k_\perp V_{\perp 0}-k_\parallel v_\parallel}\times\left[\omega-k_\perp V_{\perp 0}-k_\parallel V_{\parallel 0}\right.\right.$$
$$\left.\left.-\frac{\omega_{*e}}{\tau}\left[1+\frac{\eta_i}{2}\left(\frac{v_\perp^2+\left(v_\parallel-V_{\parallel 0}\right)^2}{v_i^2}-3\right)+\frac{L_n V_{\parallel 0}\left(v_\parallel-V_{\parallel 0}\right)}{L_v v_i^2}\right]\right]\right\}$$
$$\times\frac{e\tilde{\phi}}{T_i}, \tag{D1}$$

where F_M is the Maxwellian, J_0 is the zeroth Bessel function, and $v_i^2 = T_i/m_i$. Integrating away the $\vec{v}$-dependence and undimensionalizing time and distance to Ω_i^{-1} and ρ_s, we find that

$$\tilde{n}_i = G(\vec{k})\frac{e\tilde{\phi}}{T_i}, \tag{D2}$$

where

$$G(\vec{k}) = -\left[1+\frac{1}{2\Omega'}Z_p'(\zeta)\Gamma_0\left(\left(\frac{2J}{\tau}\right)^{1/2}\zeta-\frac{\eta_i}{\tau}\zeta^2\right)\right.$$
$$\left.+\frac{1}{\Omega'}\zeta Z_p(\zeta)\left(\left(\Omega'+\frac{1}{\tau}-\frac{\eta_i}{2\tau}\right)\Gamma_0+\frac{\eta_i}{\tau^2}k_\perp^2\left(\Gamma_0-\Gamma_1\right)\right)\right], \tag{D3}$$

where Z_p and Z_p' are the plasma dispersion function and its derivative, $\zeta = \sqrt{\tau/2}\left(\Omega' k_y/L_n k_\parallel\right)$, $\Omega' = \left(\omega-\vec{V}_\varphi\cdot\vec{k}\right)/\omega_{*e}$, and $\Gamma_n = I_n\left(k_\perp^2/\tau\right)\exp\left(-k_\perp^2/\tau\right)$, where I_n is a modified Bessel function. Applying the quasineutrality equation

with adiabatic electrons, $\tilde{n}_i = e\tilde{\phi}/T_e$, expanding in k_x^2 to first order, and then taking $k_x^2 = -\partial^2/\partial x^2$ and $k_\parallel = k_y x/L_s$, we obtain the following differential equation in x:

$$\frac{\partial^2 \tilde{\phi}_{\vec{k}}}{\partial x^2} + Q(x;\Omega)\tilde{\phi}_{\vec{k}} = 0, \qquad (D4)$$

where

$$Q(x;\Omega) = \frac{1/\tau - G\left(k_y^2\right)}{G'\left(k_y^2\right)}. \qquad (D5)$$

This equation reduces to the fluid eigenmode equation, Eq. (3.7), when expanded to order x^2 and k_y^2 in the limit $|\zeta| \gg 1$ and $k_y^2 \ll 1$. As with the fluid version, the potential is even in x *except* for the terms induced by V_0 through the Richardson number, J. The terms which vary as x shift the fluid potential, but do not alter the quadratic structure; however this is not true of the odd terms which vary as x^3 or higher, which tend to destroy the quadratic structure at large x. Physically, these terms represent the effects of higher shear damping when the velocity shear causes the mode to stray too far from the mode rational surface. Analytically, we can derive a crude but adequate estimate of the regime of fluid validity by requiring that the term cubic in x which is not in the fluid theory, be less than the quadratic term, which *is* in the fluid theory. Upon expanding, we find

$$J^{1/2} \ll \left|\frac{\tau\Omega(\Omega + K)}{3s x_{\max}}\right|. \qquad (D6)$$

This is the principal result of this appendix.

The shooting code analysis of Eq. (D4) may also be used to find the effect of $\frac{dV_\varphi}{dr}$ on the instability threshold, η_{ic}, in the spirit of Ref. 7. Although

we have not done a detailed analysis, preliminary studies show that η_{ic} is *lowered* as $\frac{dV_\varphi}{dr}$ is increased, but not by more than about 15% before the limiting effects mentioned in the above paragraphs become important. This result is interesting in light of recent results from transport simulations by Goldston et al.,[25] which indicate that η_i tends to maintain itself at marginal stability, even when strong central ion heating is applied. If this is the case, then in the presence of a shear flow the allowable ion temperature gradient is even lower.

Appendix E: Energy Saturation

Here, we propose a criterion for turbulent saturation based on the ensemble-averaged turbulence energies, and then translate this criterion into a mathematical method for accurately solving for the diffusion in the low-k_y regime of the spectrum, which is responsible for most of the transport.

We may define the following energy-like integrals,[8] which represent the degree of turbulence excited in the various fields:

$$E^W = \frac{1}{2}\int d^3x \left(\left|\tilde{\phi}\right|^2 + \left(\nabla_\perp \tilde{\phi}\right|^2 \right) \qquad (E1)$$

$$E^K = \frac{1}{2}\int d^3x \left|\tilde{v}_\parallel\right|^2 \qquad (E2)$$

$$E^I = \frac{1}{2}\frac{1}{\Upsilon}\int d^3x \left|\tilde{p}\right|^2 . \qquad (E3)$$

Energy evolution equations are obtained by integrating Eqs. ((3.4))–(()3.6), with the conservative property of convective nonlinearities, $\int d^3x \tilde{A}\left(\nabla\tilde{\phi}\times\hat{b}\right)\cdot\nabla\tilde{A} = 0$

for any $\tilde{A}$. This yields

$$\frac{\partial}{\partial t}E^W = -\int d^3x \tilde{\phi}\nabla_\parallel \tilde{v}_\parallel \tag{E4}$$

$$\frac{\partial}{\partial t}E^K = -\int d^3x \left[\tilde{v}_\parallel \nabla_\parallel \tilde{\phi} + \tilde{v}_\parallel \nabla_\parallel p + \frac{V_0}{L_V}\tilde{v}_\parallel \nabla_y \tilde{\phi} + \mu \left|\nabla_\parallel v_\parallel\right|^2\right] \tag{E5}$$

$$\frac{\partial}{\partial t}E^I = -\int d^3x \left[\tilde{p}\nabla_\parallel \tilde{v}_\parallel + \frac{1}{\Gamma}\left(\frac{1+\eta_i}{\tau}\right) v_D \tilde{p}\nabla_y \tilde{\phi}\right]. \tag{E6}$$

Hence, the total energy of the system evolves by

$$\frac{\partial}{\partial t}E = -\int d^3x \left[\frac{1}{\Gamma}\left(\frac{1+\eta_i}{\tau}\right) v_D \left\langle \tilde{p}\nabla_y \tilde{\phi}\right\rangle + \frac{V_0}{L_V}\left\langle \tilde{v}_\parallel \nabla_y \tilde{\phi}\right\rangle + \mu \left|\nabla_\parallel v_\parallel\right|^2\right]. \tag{E7}$$

This energy evolution equations state that turbulence energy so defined enters the spectrum at low k_y through the η_i and dV_0/dr free energy sources, and leaves the spectrum at high k_y through viscous (Landau or collisional) damping. In order for the energy to move from low to high k_y, nonlinear mode coupling must occur, here modelled as triad resonance coupling of $\vec{k}$ and $\vec{k}'$ modes to $\vec{k}''$ over a time of $\left(\Delta\omega_{\vec{k}''}\right)^{-1}$.

In $\vec{k}$-space, this transfer of energy must go in the direction of source (low k_y) to sink (high k_y). Meanwhile, back in configuration space, the transfer to higher k_y translates to energy going out away from the mode rational surface, where turbulent fluctuations can damp through the higher $k_\parallel$.

For the renormalized equations, which replace the nonlinear equations by linear equations with energy sink $D_{\vec{k}}$, saturation occurs when $D_{\vec{k}}$ has become

large enough that all the energy fed into the system by instability are carried off to higher k_y, thus turning off the growth of all parts of the spectrum.

Analytically, $D_{\vec{k}}$ may be treated as an eigenvalue of the renormalized equations that regulates energy transfer between various parts of the spectrum. By restricting ourselves to the low-k_y part of the spectrum, where most of the radial transport occurs, all diffusivities except $D_{\vec{k}}^{xx}$ are of small relative importance in Eqs. (3.25)–(3.27), and hence we may neglect them.

REFERENCES

1. R. J. Groebner, W. W. Pfeiffer, F. P. Blau and K. H. Burrell, Nuclear Fusion **26**, 543 (1986).
2. M. Greenwald, D. Gwinn, S. Milora, J. Parker, R. Parker, and S. Wolfe *10th International Conference on Plasma Physics and Controlles Nuclear Fusion Research*, London (IAEA, Vienna, 1984) Vol. 1, p.45.
3. D. L. Brower, W. A. Peebles, S. K. Kim, N. C. Luhmann Jr., W. M. Tang, and P. E. Phillips, Phys. Rev. Lett. **59**, 49 (1987).
4. R. J. Fonck, Bull. Am. Phys. Soc. **32**, 1846 (1987).
5. K. H. Burrell, R. J. Groebner, H. St. John, and R. P. Seraydarian, Nucl. Fusion **28**, 3 (1988).
6. P. N. Guzdar, L. Chen, W. M. Tang, and P. N. Rutherford, Princeton Plasma Physics Laboratory Report 1601, (1980).
7. B. B. Kadomtsev, **Plasma Turbulence**, translated by L. C. Ronson, edited by M. G. Rusbridge (Academic Press, New York, 1965).
8. R. H. Kraichnan, J. Fluid Mech., **5**, 497 (1959).
9. L. Garcia, P. H. Diamond, B. A. Carreras, and J. D. Callen, Phys. Fluids **28**, 2147 (1988).
10. B. Coppi, M. N. Rosenbluth, and R. Z. Sagdeev, Phys. Fluids **10**, 582, (1967).
11. C. W. Horton, Jr., Duk-In Choi, and W. M. Tang, Phys. Fluids **24**, 1077 (1981).

12. A. A. Galeev , V. N. Oraevskiĭ, and R. Z. Sagdeev, Sov. Phys. JETP **17**, 615 (1963).

13. P. W. Terry, J. N. Leboeuf, P. H. Diamond, D. R. Thayer, and G. S. Lee, Phys. Fluids **31** (1988).

14. O. J. Kwon, P. H. Diamond, in preparation.

15. R. R. Dominguez and R. E. Waltz, Phys. Fluids **31** 3147 (1988).

16. G. S. Lee and P. H. Diamond, Phys. Fluids **29**, 3291 (1986).

17. R. J. Groebner, W. W.Pfeiffer, F. P. Blau, and K. H. Burrell, Nuclear Fusion **26**, 543 (1986).

18. A. A. Galeev, V. N. Oraevskiĭ, and R. Z. Sagdeev, Sov. Phys. JETP **17**, 615 (1963).

19. D. O. Overskei, C. J. Armentrout, J. F. Baur, F. P. Blau, G. Bramson, K. H. Burrell, R. P. Chase, J. C. DeBoo, S. Ejima, E. S. Fairbanks, R. Groebner, C. L. Hsieh, G. L. Jahns, C. L. Kahn, D. H. Kellman, D. Knowles, J. Lieber, J. M. Lohr, N. Ohyabu, T. W. Petrie, L. C. Rottler, D. P. Schissel, R. P. Seraydarian, J. R. Smith, R. T. Snyder, R. D. Stambaugh, R. E. Stockdale, H. St. John, E. J. Strait, C. S. Tucker, D. Vaslow, S. S. Wojtowicz, and S. K. Wong, in *Proceedings of the 4th International Symposium on Heating in Toroidal Plasmas* (International School of Plasma Physics, Varenna, 1984), p. 21.

20. N. Mattor and P. H. Diamond, Phys. Fluids **31**, 1180 (1988).

21. R. J. Fonck, Bull. Am. Phys. Soc. **32**, 1846 (1987)

22. R. J. Goldston, Y. Takase, D. C. McCune, M. G. Bell, M. Bitter, C. E. Bush, P. H. Diamond, P. C. Efthimion, E. D. Fredrickson, B. Grek, H. Hendel, K. W. Hill, D. W. Johnson, D. Mansfield, K. McGuire, E. Nieschmidt, H. Park, M. H. Redi, J. Schivell, S. Sesnic, and G. Taylor, in *14th European Conference on Controlled Fusion and Plasma Physics* (European Physical Society, Budapest, 1987), p. 140.

23. B. B. Kadomtsev and O. P. Pogutse in *Reviews of Plasma Physics* (Leontovitch, M. A., ed.), Vol. 5, pg. 249 (Consultants Bureau, New York, 1970).

24. T. Antonsen, B. Coppi, and R. Englade, Nucl. Fusion **19** 641 (1979).

25. R. E. Waltz, W. Pfeiffer, and R. R. Dominguez, Nucl. Fusion **20**, 43 (1980).

26. F. Romanelli, submitted for publication in Phys. Fluids.

27. E. A. Frieman and Liu Chen, Phys. Fluids **25**, 502 (1982).

28. R. Z. Sagdeev and A. A. Galeev, **Nonlinear Plasma Theory**, edited by T. M. O'Neil and D. L. Book (Benjamin, New York, 1969).

29. N. Mattor and P. H. Diamond, *Proceedings of the 1988 Sherwood Controlled Theory Conference* (Oak Ridge National Laboratory, Oak Ridge, 1988) p. 2C09.

30. F. W. J. Olver, Chapter 9 of **Handbook of Mathematical Functions**, edited by M. A. Abramowitz and I. A. Stegun (National Bureau of Standards Applied Mathematics Series 55, 1972).

31. B. Fried and S. Conte, **The Plasma Dispersion Function** (Academic Press, New York, 1961).

32. P. H. Diamond and M. N. Rosenbluth, Phys. Fluids **24**, 1641 (1981).

33. M. C Zarnstorff, M. G. Bell, M. Bitter, C. Bush, R. J. Fonck, R. J. Goldston, B. Grek, K. W. Hill, R. B. Howell, H. Hsuan, K. P. Jaehnig, D. W. Johnson, R. Knize, D. Mansfield, H. Park, A. Ramsey, J. Schivell, and G. Taylor, Bull. Am. Phys. Soc.**33**, 1882 (1988).

34. Stanley M. Kaye, Phys. Fluids **28**, 2327 (1985).

35. M. Tagger, G. Laval, and R. Pellat Nucl. Fusion **17**, 109.

36. W. M. Stacey and D. J. Sigmar, Phys. Fluids **27**, 2076 (1984).

37. W. M. Stacey and D. J. Sigmar, Phys. Fluids **28**, 2800 (1985).

38. J. W. Connor, S. C. Cowley, R. J. Hastie, and L. R. Pan, Plasma Physics and Controlled Fusion, **29**, 919 (1987).

39. S. D. Scott, M. Bitter, H. Hsuan, K. W. Hill, R. J. Goldston, S. von Goeler, and M. Zarnstorff, in *14th European Conference on Controlled Fusion and Plasma Physics* (European Physical Society, Budapest, 19-87), p. 65.

40. S. Chandrasekhar, **Hydrodynamic and Hydromagnetic Stability** (Oxford U.P., Oxford, 1961).

41. R. C. Isler, A. J. Wootton, L. E. Murray, R. A. Langley, J. D. Bell, C. E. Bush, A. Carnevali, P. H. Edmonds, D. P. Hutchinson, R. R. Kindsfather, E. A. Lazarus, C. H. Ma, J. K. Munro, M. Murakami,

G. H. Neilson, S. D. Scott, and C. E. Thomas, Nucl. Fusion **26**, 391 (1986).

42. A. B. Mikhailovski, Soviet Physics JETP, **25**, 623 (1967).

43. M. Murakami, P. H. Edmonds, G. A. Hallock, R. C. Isler, E. A. Lazarus, G. H. Nielson, A. J. Wooton, J. D. Bell, A. Carnevali, B. A. Carreras, J. L. Dunlap, A. C. England, W. L. Gardner, R. L. Hickok, H. C. Howe, D. P. Hutchinson, W. C. Jennings, R. R. Kindsfather, R. A. Langley, C. H. Ma, J. Mathew, P. K. Mioduszewski, J. K. Munro, V. K. Paré, M. J. Saltmarsh, S. D. Scott, D. J. Sigmar, M. L. Simpson, C. E. Thomas, R. M. Wieland, W. R. Wing, and K. E. Yokoyama, in *Plasma Physics and Controlled Nuclear Fusion Research 1984, 10th International Conference, London* (IAEA, Vienna, 1985), Vol. 1, p. 87.

44. P. J. Catto, M. N. Rosenbluth, and C. S. Liu, Phys. Fluids **16**, 1719 (1973).

45. P. G. Drazin and W. H. Reid, **Hydrodynamic Stability** (Cambridge U.P., Cambridge, 1981).

46. B. A. Carreras, L. Garcia, and P. H. Diamond, Phys. Fluids, **30**, 1388 (1987).

47. J. C. Adam, W. M. Tang, and P. H. Rutherford, Phys. Fluids **19**, 561 (1976).

48. K. Brau, M. Bitter, R. J. Goldston, D. Manos, K. McGuire, and S. Suckewer, Nucl. Fusion **23**, 1643 (1983).

49. K. H. Burrell and R. D. Stambaugh, private communication.

50. W. M. Tang, Nucl. Fusion **26**, 1605 (1986).

51. R. R. Dominguez and R. E. Waltz, Nucl. Fusion 27, 65 (1987).

52. R. J. Hawryluk, V. Arunasalam, M. G. Bell, M. Bitter, W. R. Blanchard, N. L. Bretz, R. Budny, C. E. Bush, J. D. Callen, S. A. Cohen, S. K. Combs, S. L. Davis, D. L. Dimock, H. F. Dylla, P. C. Efthimion, L. C. Emerson, A. C. England, H. P. Eubank, R. J. Fonck, E. Fredrickson, H. P. Furth, G. Gammel, R. J. Goldston, B. Grek, L. R. Grisham, G. Hammett, W. W. Heidbrink, H. W. Hendel, K. W. Hill, E. Hinnov, S. Hiroe, R. A. Hulse, H. Hsuan, K. P. Jaehnig, D. Jassby, D. W. Johnson, L. C. Johnson, R. Kaita, R. Kamperschroer, S. M. Kaye, S. J. Kilpatrick, R. J. Knize, H. Kugel, P. H. LaMarche, B. LeBlanc, R. Little, C. H. Ma, D. M. Manos, D. K. Mansfield, M. P. McCarthy, R. T. McCann, D. C. McCune, K. McGuire, D. H. McNeill, D. M. Meade, S. S. Medley, D. R. Mikkelsen, S. L. Milora, W. Morris, D. Mueller, V. Mukhovatov, E. B. Nieschmidt, J. O'Rourke, D. K. Owens, H. Park, N. Pomphrey, B. Prichard, A. T. Ramsey, M. H. Redi, A. L. Roquemore, P. H. Rutherford, N. R. Sauthoff, G. Schilling, J. Schivell, G. L. Schmidt, S. D. Scott, S. Sesnic, J. C. Sinnis, F. J. Stauffer, B. C. Stratton, G. D. Tait, G. Taylor, J. R. Timberlake, H. H. Towner, M. Ulrickson, V. Vershkov, S. Von Goeler, F. Wagner, R. Wieland, J. B. Wilgen, M. Williams, K. L. Wong, S. Yoshikawa, R. Yoshino, K. M. Young, M. C.

Zarnstorff, V. S. Zaveriaev, and S. J. Zweben, in *Plasma Physics and Controlled Nuclear Fusion Research 1986, 11th International Conference Kyoto* (IAEA, Vienna, 1987), Vol. 1, p. 51.

53. P. W. Terry, Bull. Am. Phys. Soc. **33**, 2020 (1988).
54. M. Zarnstorff *et al.*, in *Plasma Physics and Controlled Nuclear Fusion Research 1988, 12th International Conference Kyoto* (IAEA, Vienna, 1989) (to be published).
55. R. J. Groebner *et al.*, Bull. Am. Phys. Soc. **33**, 1964 (1988).
56. A. N. Kolmogorov, Compt. Rend. Acad. Sci. USSR **30**, 301 (1941).
57. J. W. Connor and J. B. Taylor, Phys. Fluids **27**, 2676 (1984).
58. J. W. Connor, Nucl. Fusion **26**, 193 (1986).
59. R. D. Sydora, T. S. Hahm, W. W. Lee, and J. M. Dawson (preprint, 1988).
60. H. Biglari *et al.*, in *Plasma Physics and Controlled Nuclear Fusion Research 1988, 12th International Conference Kyoto* (IAEA, Vienna, 1989) (to be published).
61. John Lohr, B. W. Stallard, R. Prater, R. T. Snider, *et al.*, Phys. Rev. Lett. **60**, 2630 (1988).
62. N. Mattor, P. H. Diamond, and E. T. Vishniac, Bull. Am. Phys. Soc. **32**, 1726 (1987).

63. P. H. Rutherford and E. A. Frieman, Phys. Fluids **11**, 569 (1968).